Lene Christin Olsen

miRNA and mRNA expression in the hippocampal region during postnatal development in rats

Doctoral thesis

Lene Christin Olsen

NTNU
Norwegian University of Science and Technology
Thesis for the Degree of
Philosophiae Doctor
Faculty of Medicine and Health Sciences
Department of Clinical and Molecular Medicine

NTNU
Norwegian University of
Science and Technology

NTNU
Norwegian University of
Science and Technology

NTNU

Lene Christin Olsen

miRNA and mRNA expression in the hippocampal region during postnatal development in rats

Thesis for the Degree of Philosophiae Doctor

Trondheim, February 2018

Norwegian University of Science and Technology
Faculty of Medicine and Health Sciences
Department of Clinical and Molecular Medicine

NTNU
Norwegian University of
Science and Technology

NORGES TEKNISK-NATURVITENSKAPELIGE UNIVERSITET

FAKULTET FOR MEDISIN OG HELSEVITENSKAP

Lene Christin Olsen

SAMMENDRAG

Hjernestrukturene entorhinal cortex og hippocampus er viktige for minnefunksjon og navigering. Innenfor hver av disse strukturene finnes underregioner som har forskjellige celletyper og forbindelser i hjernen. Noen av celletypene og forbindelsene dannes før fødsel, mens andre kommer til etter fødsel. I tillegg spesialiseres alle celletypene etter fødsel. Alle disse begivenhetene kommer av en blanding av gener og miljøpåvirkning. Hovedmålet med dette arbeidet var å karakterisere genuttrykket i underregionene mens disse spesialiseres etter fødsel hos rotter, og finne potensiell molekylær basis for forskjellene som sees mellom underregionene.

Artikkel 1 tar for seg to underregioner i hippocampus, den dorsale og ventrale delen. Flere egenskaper viser forskjeller langs denne aksen, inkludert elektrofysiologi, genuttrykk, og forbindelser til andre deler av hjernen. I tillegg er dorsal hippocampus viktig for minne og navigering, mens ventral hippocampus er mer involvert i følelser og angst-relatert oppførsel. Vi undersøkte når denne forskjellen var til stede etter fødsel basert på anatomi og genuttrykk. Anatomisk sett så vi ingen forskyvninger mellom den dorsale og ventrale delen, og forskjellene i hjerneforbindelser var til stede allerede den første uken etter fødsel. Vi fant også forskjeller i genuttrykk mellom dorsal og ventral hippocampus allerede ved fødsel, og mange av genene var fortsatt forskjellig uttrykt hos voksne dyr. Vi konkluderte derfor at forskjellene mellom dorsal og ventral hippocampus allerede er til stede den første uka etter fødsel.

I artikkel 2 undersøkte vi forskjellene i uttrykket av mikroRNA og proteinkodende gener mellom lag II og de dypere lagene i medial entorhinal cortex ved fire tidspunkt etter fødsel. Lag II i entorhinal cortex inneholder en høy prosentandel av stellat nevroner, som har unikt utseende og elektrofysiologi, og påvirkes særlig i Alzheimer's sykdom. Vi fant at forskjellene i uttrykk av både mikroRNA og protein-kodende gener var større mellom alder enn mellom lag. MikroRNA er små RNA molekyler som regulerer proteinsyntesen fra protein-kodende gener, og som har viktige funksjoner i hjerneutvikling og funksjon. For å finne hvilke gener som var regulert av mikroRNA molekyler med forskjellig uttrykk, fant vi gener som hadde konservert bindingssted for mikroRNA samt hadde motsatt uttrykksprofil. Når genene er kjent, kan en også finne ut potensielle funksjoner for mikroRNA. Vi fant at mikroRNA sannsynligvis bidrar til cellespesialisering i medial entorhinal cortex. Flere av mikroRNAene som hadde forskjeller i uttrykk mellom lag er også involvert i Alzheimer's sykdom, som åpner for muligheten at disse bidrar til de molekylære sykdomsmekanismene. Vi sammenlignet også mikroRNA uttrykk mellom stellat nevroner og resten av cellene i medial entorhinal cortex. Et av mikroRNAene som var oppregulert i lag II, miR-143, var også høyere uttrykt i stellat nevronene. Analysen vår viste at miR-143 mest sannsynlig regulerer Lmo4 genet, som er viktig for navigeringsminnet samt utvikling av entorhinal cortex på fosterstadiet.

I tillegg til forskjellene som finnes mellom lag i entorhinal cortex, ser man også forskjeller i celletyper, elektrofysiologi, og hjerneforbindelser mellom den laterale og den mediale delen av strukturen. Det finnes også forskjeller i minnefunksjon, da medial entorhinal cortex er mer involvert i navigering, mens lateral entorhinal cortex er involvert i minne for fysiske objekter og lukter. I artikkel 3 karakteriserte vi forskjellene i uttrykket av protein-kodende og ikke-kodende gener mellom de to regionene ved fire forskjellige tidspunkt etter fødsel. Forskjellene mellom lag II og de dypere lagene i hver region ble også undersøkt. Vi fant at forskjellene i genuttrykk mellom de mediale og laterale delene var størst i lag II sammenliknet med de dypere lagene, og at mange av disse genene kodet for neuropeptidreseptorer, som er viktige for minnefunksjon. Forskjellene mellom lag II og de dypere lagene besto i strukturen som omgir cellene, blodkardannelse, nevronspesialisering og funksjon, samt myelindannelse. Basert på ulike genkategorier fant vi kandidatgener som kan forklare forskjellene i funksjon mellom ulike lag og mellom medial og lateral entorhinal cortex, inkludert gener involvert i nevronenes elektriske egenskaper, minnefunksjon, og sykdomssensitivitet.

Dette arbeidet represeter det første molekylære overblikket av forskjeller i underregioner av hippocampus og entorhinal cortex under utvikling etter fødsel. Dataene er gjort tilgjengelige for videre studier av den molekylære bakgrunnen for utvikling av minne- og navigeringsfunksjonene i disse regionene.

Kandidat: Lene Christin Olsen
Institutt: Institutt for klinisk og molekylærmedisin
Hovedveileder: Pål Sætrom
Biveiledere: Menno P. Witter, Kally C. O'Reilly, og Finn Drabløs
Finansiering: FUGE (Norsk Forskningsråd)

Ovennevnte avhandling er funnet verdig til å forsvares offentlig for graden PhD i molekylærmedisin. Disputas finner sted i MTA, Medisinsk Teknisk Forskningssenter, torsdag 22. februar 2018 kl. 12.15.

ACKNOWLEDGEMENTS

TABLE OF CONTENTS

LIST OF PAPERS

Paper I

Identification of dorsal-ventral hippocampal differentiation in neonatal rats
Kally C. O'Reilly, Arnar Flatberg, Sobia Islam, **Lene C. Olsen**, Ingvild U. Kruge, Menno P. Witter
Brain Struct Funct. 2015 Sep;220(5):2873-93

Paper II

MicroRNAs contribute to postnatal development of laminar differences and neuronal subtypes in the rat medial entorhinal cortex
Lene C. Olsen, Kally C. O'Reilly, Nina B. Liabakk, Menno P. Witter, Pål Sætrom
Brain Struct Funct. 2017 doi:10.1007/s00429-017-1389-z

Paper III

Molecular signatures of regional and laminar differences in medial and lateral entorhinal cortex during postnatal development in rats
Lene C. Olsen, Laurent F. Thomas, Kally C. O'Reilly, Endre B. Stovner, Menno P. Witter, Pål Sætrom
Manuscript

ADDITIONAL CONTRIBUTIONS DURING PHD

Pathway Analysis of Skin from Psoriasis Patients after Adalimumab Treatment Reveals New Early Events in the Anti-Inflammatory Mechanism of Anti-TNF-α.
Langkilde A; **Olsen, L.C.**; Sætrom, P.; Drabløs, F; Besenbacher, S; Raaby, L.; Johansen, C.; Iversen, L.
PLoS ONE 2016 11(12): e0167437. doi:10.1371/journal. pone.0167437

Level of basal autophagy and LC3BII correlate with DHA-induced cytotoxicity in human colorectal cancer cell lines.
Samdal, H.; Sandmoe, M.; **Olsen L. C.;** Chen D.; Schønberg, S. A.; Pettersen, C. H. H.
Submitted to FEBS, August 2017

ABBREVIATIONS

ANOVA	Analysis of variance
BMP	Bone morphogenic protein
CA1-3	Cornus ammoni regions 1-3
CCK	Cholecystokinin
DG	Dentate gyrus
dl	Dorso-lateral
EC	Entorhinal cortex
GO	Gene Ontology
Hcn	Hyperpolarization-activated cyclic nucleotide-gated
HF	Hippocampal formation
ISH	*In situ* hybridization
KEGG	Kyoto Encyclopedia of Genes and Genomes
LEC	Lateral entorhinal cortex
L	Layer
LDeep	Deep layers of the EC (LIII-LVI)
LNA	Locked nucleic acid
lncRNA	Long non-coding RNA
LTP	Long term potentiation
MEC	Medial entorhinal cortex
miRISC	miRNA-mediated silencing complex
miRNA	Micro RNA
mRNA	Messenger RNA
ncRNA	Non-coding RNA
P	Postnatal day
PaS	Parasubiculum
piRNA	PIWI-interacting RNA
PNN	Perineuronal net
POR	Postrhinal cortex
Pri-miRNA	Primary miRNA
Pre-miRNA	Precursor miRNA
PrS	Presubiculum
PV+	Parvalbumin positive
qRT-PCR	Quantitative reverse transcription polymerase chain reaction
rRNA	Ribosomal RNA
siRNA	Short interfering RNA
snRNA	Small nuclear RNA
snoRNA	Small nucleolar RNA
Sub	Subiculum
tRNA	Transfer RNA
UTR	Untranslated region
VIP	Vasoactive intestinal polypeptide
vm	Ventro-medial

x

INTRODUCTION

The structures in the medial temporal lobe of the brain are important for the formation and consolidation of memory as well as spatial navigation. The following sections describe the anatomy, functions, and development of this brain region, with a special focus on the hippocampus and the entorhinal cortex (EC). I then present an overview of the contributions of the transcriptome for brain development and function, and the methods used to study the state and dynamics of the brain transcriptome.

1. The medial temporal lobe system - history and discovery of functions

The hippocampal formation (HF) has attracted people studying the brain for centuries. The Alexandrians likened the distinct structure of the hippocampus to the horns of the ram, and the remnants of this is found today in the names of the subregions of the hippocampus, cornus ammoni regions 1-3 (CA1-CA3) (Andersen, Morris et al. 2007). The current name of the hippocampus was coined around 1564 by Italian anatomist Giulio Cesare Aranzi, who noted its resemblance to the seahorse.

The role of the HF in memory became evident in 1957 with Scoville and Milner's work on brain-damaged patients, one of whom would become the most famous patient in neuroscience, patient H.M. (Scoville and Milner 1957). In an effort to cure H.M.'s debilitating epilepsy, Scoville removed the medial temporal lobes of both brain hemispheres. The surgery impaired H.M.'s ability to form new long-term declarative memories, which is the memory for facts, events, people, places, and objects (Thompson and Kim 1996; Kandel, Dudai et al. 2014). However, he was still able to learn new skills, maintained his above average IQ, and was able to memorize things over a short period of time (Annese, Schenker-Ahmed et al. 2014).

The findings from the study of patient H.M. inspired an array of research into the medial temporal lobe, which led to the discovery that multiple memory systems exist (Sweatt 2016). It now seems clear that all the structures included in this part of the brain (the HF and the parahippocampal region) are indeed involved in the formation and consolidation of declarative memories (Squire, Stark et al. 2004). To form long-term memories, the hippocampal region is thought to work together with the neocortex in encoding them, and eventually allowing the memory recall to become largely independent of the hippocampal region (Knierim 2015).

A few years before H.M.'s surgery, Hebb introduced his "cell assembly" hypothesis of what memories could represent on a cellular level (Hebb 1949). When learning occurs, a discrete group of excitatory neurons will fire together as a response to the input, and as a result, the synapses between the co-firing neurons will strengthen. With repetition, the wiring strengthens further, forming a cell assembly. The firing of such combinations of neurons is thought to be the basis of operations in the brain, including memory (Buzsaki 2010; Huyck and Passmore 2013).

In 1973, Bliss and Lømo discovered a phenomenon in the hippocampus that correlated with Hebb's hypothesis of synapse strengthening (Bliss and Lomo 1973). Their electrical stimulation of neurons led to an increase in responsiveness for the same type of input for

1

some time afterwards, and they named the phenomenon Long Term Potentiation (LTP). The opposite phenomenon, Long Term Depression, causes a weakening of the synapse after the un-correlated activity between the post and presynaptic neurons (Ito and Kano 1982; Luscher and Malenka 2012). These processes require extensive cellular signaling, which includes induction of gene expression. Today, learning is viewed as the rewiring of the nervous system, and this change in wiring represents the actual memory formed. However, whether LTP is the mechanism for memory storage is still highly debated (Gallistel and Matzel 2013).

Another phenomenon discovered in the hippocampus in the 70's was theta frequency firing. Electroencephalographic recordings revealed rhythmic firing in the 5Hz range arising from hippocampal neuronal populations when an animal moved around and explored a new environment (Winson 1978; Sweatt 2016), as is necessary for spatial navigation. More evidence for the role of the hippocampus in spatial learning came with the discovery of hippocampal neurons whose firing corresponded to the animal's location in its environment (place cells) by John O'Keefe and colleagues in 1971 (O'Keefe and Dostrovsky 1971). The involvement of the medial temporal lobe system in spatial navigation became further strengthened with the discovery of other spatially and speed tuned cells in the entorhinal cortex (EC) by May-Britt and Edvard Moser between 2004 and 2015 (Hafting, Fyhn et al. 2005; Savelli, Yoganarasimha et al. 2008; Solstad, Boccara et al. 2008; Kropff, Carmichael et al. 2015). It is still not clear whether navigation and memory form one common system or two separate systems that exist side by side, but some have hypothesized that certain memory types could have evolved from the brain's system for navigation (Buzsaki and Moser 2013).

Other roles demonstrated for the hippocampus are in emotional memory (Kim and Fanselow 1992) and temporal aspects of memory as encoded by time cells, neurons that fire at successive time points (Eichenbaum 2014). However, despite all the investigations into the medial temporal lobe structures, the functions of the structures within are still debated, and linking the known neuropsychology and physiology of this brain area remains a challenge (Strange, Witter et al. 2014; Kesner and Rolls 2015; Shapiro 2015). The main working hypothesis is that the hippocampus works together with other brain areas in memory storage and retrieval, integrating the spatial input it receives via the medial entorhinal cortex, and the object-related input it receives via the lateral entorhinal cortex (Derdikman and Knierim 2014).

2. Anatomy of the medial temporal lobe system
The medial temporal lobe system is generally divided into the HF and the parahippocampal region. The HF consists of a group of structures that are located in the medial temporal lobe of mammals (Figure 1, (Amaral and Lavenex 2007; van Strien, Cappaert et al. 2009; Cappaert, Strien et al. 2015)). It includes the hippocampus proper (CA1-CA3), the dentate gyrus, and the subiculum. Some also include the presubiculum, parasubiculum, and the EC in the HF, while others group these three structures together with the perirhinal and postrhinal cortices under the term parahippocampal region (Amaral and Lavenex 2007). This thesis will use the latter definition.
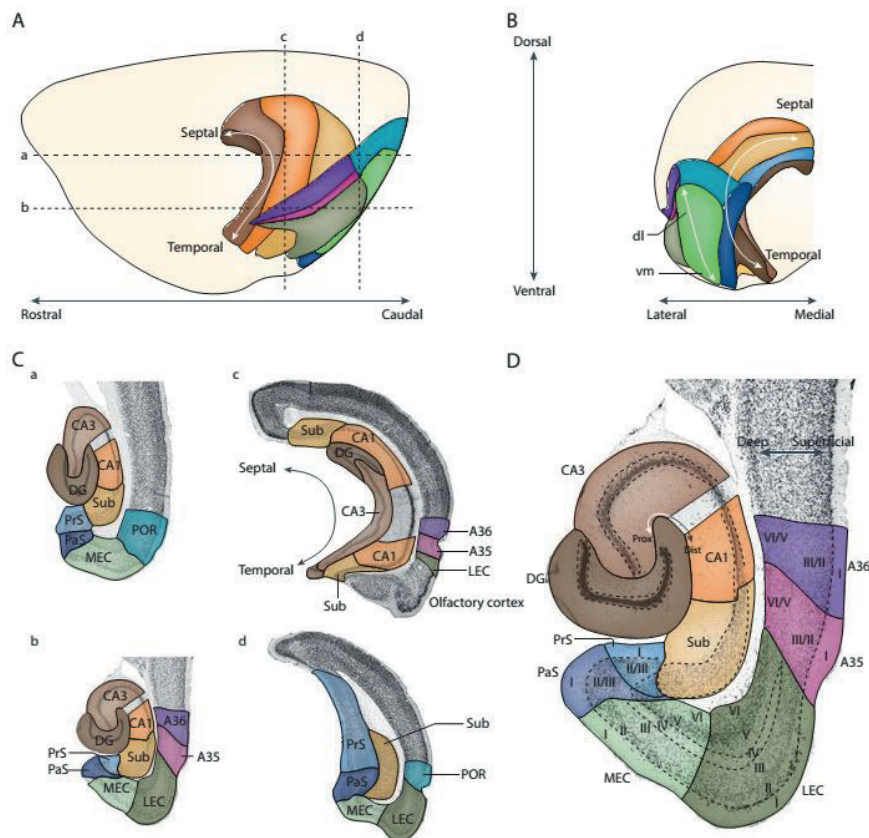
Figure 1 Representations of the anatomy of the HF and the parahippocampal region in rats. Adapted with permission from (van Strien, Cappaert et al. 2009). A lateral A) and B) caudal view, with axes indicating orientation (rostro-caudal, dorso-ventral, lateral-medial). In addition, the septo-temporal (also known as dorso-ventral) axis of the hippocampus proper is shown, as is the dorsolateral (dl) and ventromedial (vm) extent of the medial EC. Color coded substructures in the hippocampal formation: Dentate gyrus (DG, dark brown), CA3 (medium brown), CA1 (orange), subiculum (Sub, yellow). Color coding for substructures in the parahippocampal region: Presubiculum (PrS, medium blue), parasubiculum (PaS, dark blue), lateral entorhinal cortex (LEC, dark green), medial entorhinal cortex (MEC, light green), perirhinal cortex (Brodmann areas A35 (pink) and A36 (purple)), and the postrhinal cortex (POR, blue-green). The dashed lines show locations of the horizontal (a,b) and coronal sections (c,d) shown in Ca-d). d) Nissl stained horizontal section (enlargement of b in panel C). The roman numerals denote cortical layers.

The HF and the parahippocampal region are strongly interconnected (Figure 2). It was the father of the neuron theory, Santiago Ramón y Cajal, who first described the dense connections between the HF and what is now known as the EC, and postulated that the two brain regions might have related physiological roles (Canto, Wouterlood et al. 2008). This tight connection from the upper layers of the EC to the dentate gyrus and the CA3 is today known as the perforant path, and it is through the perforant path that the entorhinal cortex funnels input received from numerous cortical areas to the hippocampus (Kerr, Agster et al. 2007; van Strien, Cappaert et al. 2009; Khalaf-Nazzal and Francis 2013; Witter, Canto et al. 2014). The perforant path forms the start of the trisynaptic pathway, which continues from the dentate gyrus to the CA3 through the mossy fibers and from the CA3 to the CA1 through the Schaffer collaterals (Cappaert, Strien et al. 2015). Finally, the CA1 cells project to the subiculum and the deep layers of the entorhinal cortex, which in turn projects back to the cortical areas that originally projected to EC layer II (LII).
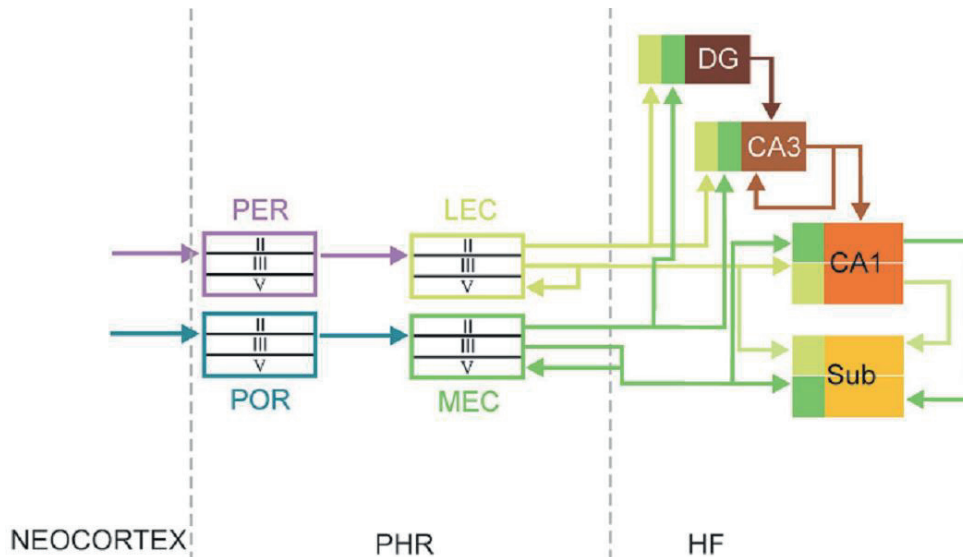
Figure 2 Wiring diagram of the entorhinal-hippocampal network, showing the main features of the trisynaptic pathway. Processed sensory input from the neocortex is funneled through the perirhinal cortex to the LEC, and through the postrhinal cortex to the MEC. MEC and LEC in turn project to all major subfields of the hippocampus. The major input comes from the axons of the perforant path, originating in EC LII, projecting to the dendrites of granule cells in the dentate gyrus (DG). The axons of dentate granule cells (mossy fibers) project to pyramidal cells in CA3, which in turn project to pyramidal cells in CA1 through the Schaffer collaterals. EC LIII also provides input to CA1 pyramidal neurons and the subiculum (Sub). The CA1 and Sub projects back to the deeper layers of the EC. Reprinted from (Witter et al. 2010) with permission from Springer.

Together with the other structures in the parahippocampal region, the entorhinal cortex is believed to function somewhat akin to a hub, relaying signals from the rest of the cortex to the HF (Canto, Wouterlood et al. 2008).

3. The hippocampal formation

The HF has a C-shaped structure extending along a dorsal to ventral axis, also known as the septotemporal axis. The subregions include the dentate gyrus, the subiculum and the cornus ammoni regions (CA1-CA3), each with three main differentiated layers based on morphology (van Strien, Cappaert et al. 2009). The different hippocampal fields and layers contain neurons with distinct morphological, connective, gene expression and physiological properties (Khalaf-Nazzal and Francis 2013). The majority of the neurons of the pyramidal cell layer in the CA regions are place cells, neurons which fire action potentials when an animal is in a certain location (Figure 3; (Henriksen, Colgin et al. 2010; Langston, Ainge et al. 2010; Lu, Igarashi et al. 2015)). Some place cells appear to be adult-like already at postnatal day 16 (P16), but display a gradually increased level of stability in their firing fields until P45 (Wills and Cacucci 2014). The proportion of hippocampal neurons with place field firing also increases until P28/30 (Langston, Ainge et al. 2010).

4
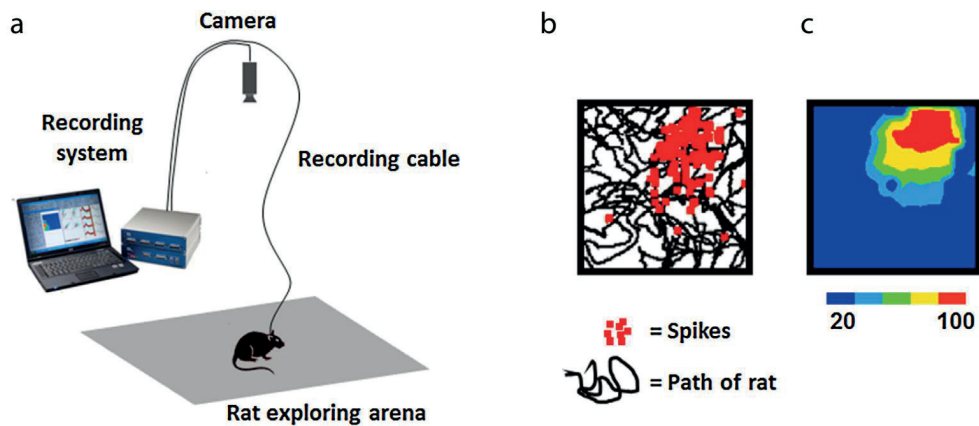
Figure 3 Firing of a place cell. a) A typical experimental set-up for recording of single neurons, with the rat freely roaming in the available arena. b) Plot showing the path of the rat (black line) and action potentials ("spikes", red squares). The spikes mostly occurred in the upper right corner of the arena. c) Heat plot representing binned, smoothened and divided action potential data from b). The patch of localized firing is known as the place field. Adapted from (Grieves and Jeffery 2017) with permission from Elsevier.

In addition to the traditionally differentiated hippocampal subregions, there is increasing evidence for differences in functions along the dorsal-ventral axis of the hippocampus based on findings from connectivity, gene expression, and behavioral studies (Strange, Witter et al. 2014). Gene expression studies have revealed both expression gradients and discretized areas across the axis, and that the boundaries of differential gene expression coincide with the connectional gradients (Thompson, Pathak et al. 2008). The sizes of the place fields vary along the dorsoventral axis of the hippocampus (Gallistel and Matzel 2013), and there are also gradual differences in excitability and theta dynamics along this axis (Strange, Witter et al. 2014). For the hippocampal-entorhinal connections, the dorsolateral-to-ventromedial projections from the EC gradually terminate along the hippocampal longitudinal axis (van Strien, Cappaert et al. 2009). Cortical input to the EC is also topographically organized, so that cortical areas involved in spatial processing project through the dorsolateral EC onto the dorsal part of the hippocampus, and cortical areas involved in emotional regulation through the ventromedial EC onto the ventral part of the hippocampus (Strange, Witter et al. 2014). Also supporting the role of the ventral hippocampus in emotional processing is its dense connections to the amygdala (Kishi, Tsumori et al. 2006). Together with the findings from lesional behavioral studies in rodents, this has led to a hypothesis of a functional organization along the dorsoventral axis (Moser and Moser 1998; Bannerman, Rawlins et al. 2004; Fanselow and Dong 2010; Strange, Witter et al. 2014). The dorsal part is proposed to support spatial learning and cognition, and the ventral part emotional response (Strange, Witter et al. 2014). However, as several of the properties display multiple discretized or gradual changes along the axis, it is likely that multiple functional domains exist along the dorsal-ventral axis of the hippocampus.

4. The entorhinal cortex

This section presents the subdivisions of the EC, describing the cell types and the known properties of each subdivision, including their susceptibility in diseases affecting the region.

4.1. Subdivisions within the entorhinal cortex

Based on its cytoarchitecture, the EC is divided into a lateral and a medial part (LEC and MEC; Brodmann areas 28a and 28b, respectively, Figure 1d), each with a 6-layered structure (Insausti, Herrero et al. 1997; Canto, Wouterlood et al. 2008). The layers are often grouped into superficial (II-III) and deep layers (V-VI), where the superficial layers project to the dentate gyrus of the hippocampus through the perforant path, and the deep layers receive reciprocal hippocampal projections (Tahvildari and Alonso 2005). This separation between superficial and deep layers also applies to physiological, molecular, and morphological differences (Canto and Witter 2012; Canto and Witter 2012; Ramsden, Surmeli et al. 2015).

To a lesser extent, such differences are also seen between MEC and LEC. MEC receives input from brain areas related to space and movement, like the presubiculum, parasubiculum, retrosplenial cortex and the postrhinal cortex, while LEC receives input from areas likely involved in object information processing, such as the perirhinal cortex, insular and orbitofrontal cortices (Eichenbaum, Amaral et al. 2016). The parts of the CA1 region proximal to the dentate gyrus receive MEC projections, while the distal parts receive LEC projections (Witter, Doan et al. 2017). Also, LEC projects to the proximal and MEC to the distal subiculum (van Strien, Cappaert et al. 2009). For the projections to the dentate gyrus and CA3 there are no regional differences (Derdikman and Knierim 2014), with the exception that the respective projections target different proximodistal positions on the apical dendrites of the innervated neurons. There are also some morphological and physiological differences between MEC and LEC, although these are mostly seen in LII (Tahvildari and Alonso 2005; Stranahan and Mattson 2010; Brandon, Koenig et al. 2014). The differences between LEC and MEC have been hypothesized to be due to the possibility of distinct origins in the pallium during embryonic development (Abellan, Desfilis et al. 2014).

The functional boundary between MEC and LEC is more like a gradient, likely because the dendrites and axons of LII neurons cross the border between the two regions (Canto and Witter 2012). In line with this, intrinsic long-range connectivity between the two regions has been shown, connecting LEC and MEC along a rostrocaudal axis, although the density of these longrange projections might be less compared to the connectivity between superficial and deep layer neurons within each region (Dolorfo and Amaral 1998).

4.2. Cell types in the entorhinal cortex

The brain contains an incredible morphological, molecular, and functional diversity of neurons (Lodato, Shetty et al. 2015; Molyneaux, Goff et al. 2015). The identity of each neuronal subtype appears to be determined by different combinations of regulatory factors known as selector genes (Arlotta and Hobert 2015), and the neuronal subtypes are generally grouped based on neurotransmitter phenotype, morphology, synaptic partners, and the location and types of specific proteins (e.g. ion channel and cell adhesive proteins) (Rosenberg and Spitzer 2011; Puelles and Ferran 2012).

In the EC, the characteristics of entorhinal cells vary between regions and layers (Figure 4). LI, the molecular layer, is fiber rich and contains some horizontal neurons and calretinin

positive multipolar neurons, both GABAergic (Cappaert, Strien et al. 2015). In LEC, some of the horizontal neurons stain positive for vasoactive intestinal polypeptide (VIP), whereas some are positive for cholecystokinin (CCK) in MEC (Canto, Wouterlood et al. 2008).
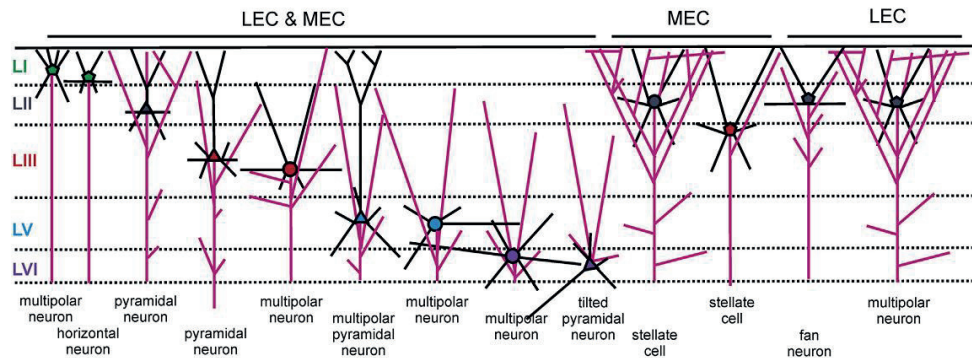
LII is a cell rich layer and displays the most variability in neuron morphology between the lateral and medial parts of the EC and also along the rostral-caudal axis (Canto, Wouterlood et al. 2008). The main principal neuronal cell types in MEC LII are the large star-shaped, reelin positive stellate neuron (67% of cells) and the calbindin and wolfram syndrome 1 positive pyramidal neuron (17% of cells) (Canto, Wouterlood et al. 2008; Gatome, Slomianka et al. 2010). The stellate neurons are the main source of the perforant path projections to the dentate gyrus and CA3, and unlike the pyramidal cells, display subthreshold oscillatory behavior appearing at P22 (Klink and Alonso 1997; Wills, Barry et al. 2012; Cappaert, Strien et al. 2015). Recently, Fuchs et al (2016) also identified intermediate pyramidal and intermediate stellate cells based on morphological and physiological properties (Fuchs, Neitz et al. 2016). While stellate neurons dominate MEC LII, fan cells are in majority in LEC LII (Figure 4 and Figure 5, (Canto, Wouterlood et al. 2008)). Fan cells display different physiology than the stellate cells, and also lack the oscillatory behavior (Tahvildari and Alonso 2005).

A variety of interneurons are found in LII. Based on morphology, EC interneurons have been classified as multipolar neurons, basket, chandelier, and bipolar cells (Canto, Wouterlood et al. 2008). Recently, Ferrante et al. (2017) identified five main classes of interneurons in EC based on molecular markers (parvalbumin, somatostatin, serotonin receptor 3a, regulator of calcineurin 2, neuropeptide Y, VIP, and neurogliaform) and electrophysiology (Ferrante, Tahvildari et al. 2017). While basket and chandelier cells tend to be positive for the same markers in MEC and LEC, multipolar neurons and bipolar cells may stain with additional markers to their correlates in the MEC (neuropeptide Y in LEC multipolar cells, and encephalin, CCK, and neuropeptide Y for LEC bipolar cells) (Canto, Wouterlood et al. 2008). The interneurons are also differentially distributed between the two regions in LII, something which is also seen in LI. LEC has fewer parvalbumin positive interneurons, and weaker staining for this interneurons marker in general (Miettinen, Koivisto et al. 1996). MEC fast-spiking parvalbumin positive basket cells tend to connect with stellate neurons, while parvalbumin-CCK positive interneurons tend to connect with pyramidal cells (Varga, Lee et

al. 2010). Indeed, MEC stellate cells have been found to interact through interneurons (Couey, Witoelar et al. 2013).
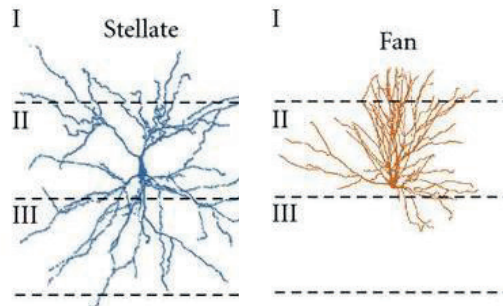
In the deeper layers there are fewer differences in morphology between MEC and LEC. Large-to-medium sized pyramidal cells dominate LIII and the superficial part of LV, while a smaller type is found in the deep part of LV (Canto, Wouterlood et al. 2008; Cappaert, Strien et al. 2015). LVI contains multipolar neurons and pyramidal cells, and varies in appearance along the lateromedial and rostrocaudal axes (Canto, Wouterlood et al. 2008). LIV, known as the lamina dissecans, is cell-sparse (although pyramidal-like neurons and bipolar cells have been observed) and more poorly defined in LEC than in MEC (Tahvildari and Alonso 2005; Canto, Wouterlood et al. 2008). With respect to interneurons, LIII and LV both contain multipolar neurons and bipolar cells. In addition, LIII contains pyramidal looking interneurons, and LV fusiform cells. LVI also contains multipolar neurons (Canto, Wouterlood et al. 2008). In general, the number of interneurons increases from LV to LII, as do their diversity and level of connectivity (Greenhill, Chamberlain et al. 2014).

4.3. The medial entorhinal cortex and spatial memory

A number of neurons tuned to navigational properties have been discovered in the medial part of the EC, including grid, border, head direction, and speed cells (Figure 6). These cells are unevenly dispersed over the MEC layers, with grid cells dominating LII, head-direction cells dominating LIII, and conjunctive cells dominating LV (Greenhill, Chamberlain et al. 2014).

The grid cells, the most abundant navigational neurons in the MEC, fire when an animal is at certain locations in an environment (Hafting, Fyhn et al. 2005; Zhang, Ye et al. 2013). The locations are regularly spaced, forming a hexagonal grid across the space available to the animal (Hafting, Fyhn et al. 2005). It is believed that this is a special metric to estimate distance when an animal is moving. The grid properties persist with the removal of olfactory and visual landmarks, and seem to arise from the animal's movement (Moser, Moser et al. 2014). The distance between the grid firing fields increases in a discrete fashion along the dorsoventral axis of the MEC, with a scaling factor of 1.42 between each module (Stensola, Stensola et al. 2012). The highest density of pure grid cells is found in LII of the MEC. Cells with grid firing properties are also found in the deeper layers, but many of these are also tuned to head direction (Sargolini, Fyhn et al. 2006). The grid cells are dependent on input

from place cells, with near elimination of the grid structure after place cell inactivation (Bonnevie, Dunn et al. 2013). Although they were discovered in the rat, grid cells have also been reported in mice, bats, and monkeys, and evidence also exists for their presence in humans (Moser and Moser 2013). Rough grid fields begin to appear around P16, but they are not stable until P20-P22, and continue to develop until at least P34 (Langston, Ainge et al. 2010; Wills, Cacucci et al. 2010; Witter, Canto et al. 2014). The number of grid cells also increase during this time span (Langston, Ainge et al. 2010).
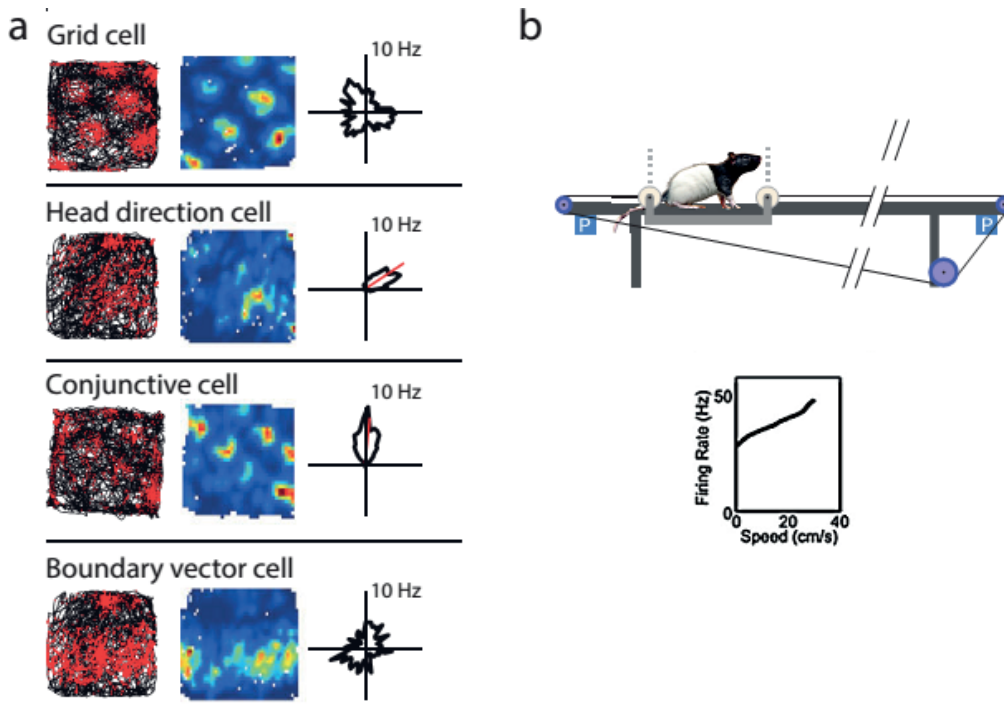
Figure 6 Specialized neurons in the MEC. a) The left column shows the path of a rat in an open field (black line), and the position of the rat during firing of action potentials (red dots) for a representative grid cell, head direction cell, conjunctive cell, and boundary vector cell. The central column shows a color-coded firing rate map for the same area as shown in the left column (blue = low firing rate, red = high firing rate). The right column show polar plots with the firing rate as a function of the animal's head direction. Reprinted from (Brandon, Koenig et al. 2014) with permission under the Creative Commons License. b) Car used in the discovery of speed-responsive cells. The firing rate of these cells corresponds with the speed of the animal as it moves along a linear track. Adapted from (Kropff, Carmichael et al. 2015), with permission from Macmillan Publishers Ltd. Nature.

Border cells are neurons which fire when an animal approaches a border or a drop off in an environment (Savelli, Yoganarasimha et al. 2008; Solstad, Boccara et al. 2008). These cells are present in lower numbers (~10%) in the MEC, and are found in both superficial and deep layers (Solstad, Boccara et al. 2008). Border cells appear adult-like when rat pups begin to explore their environment at P16-18 (Bjerknes, Moser et al. 2014). It is thought that border cells provide very important input for place cells and grid cells, providing boundary information which potentially could contribute to the formation of grid and place fields (Buzsaki and Moser 2013; Wills, Muessig et al. 2014).

The head direction cells function somewhat akin to a compass, firing whenever an animal's head is turned in a certain direction (Taube 2007). These cells are found in several interconnected brain regions, including the entorhinal cortex, where they may be imperative for the generation of grid fields (Winter and Taube 2014). Self-motion and visual information can modulate these cells. Together, the head direction cells cover all possible directions (Taube, Muller et al. 1990). Head direction cells are abundant in MEC LIII and LV, but scarce in LII (Sargolini, Fyhn et al. 2006). In the deeper layers of the MEC, particularly in LV, cells with simultaneous grid and head direction properties (so-called conjunctive cells) can be found (Greenhill, Chamberlain et al. 2014). The head-direction cells are adult-like already when the rats open their eyes around P15, and have been measured as early as P11 (Langston, Ainge et al. 2010; Bjerknes, Moser et al. 2014).

The most recent cell type to be discovered is the speed cell, which fires more rapidly as the animal's speed increases (Kropff, Carmichael et al. 2015). The speed cells are quite numerous, making up about 15% of all MEC neurons, and seem evenly distributed across all MEC layers.

When the grid cells were discovered, it was believed that the place cells depended solely on their input (Solstad, Moser et al. 2006). However, subsequent work revealed that place cells display stable firing at P16, whereas grid cells are not adult-like until P21 (Langston, Ainge et al. 2010; Wills, Cacucci et al. 2010). Now it is believed that the place cells integrate the input from all the navigational cells of the MEC, and that the signals from border and head-direction cells are sufficient for place cell function before the maturation of grid cells (Derdikman and Moser 2014).

It has been widely debated whether these navigational neurons correlate with certain neuronal morphologies. As the stellate neuron dominates LII, where grid cells also are numerous, it has been hypothesized that grid cells are stellate neurons. There was evidence for this hypothesis (Domnisoru, Kinkhabwala et al. 2013; Schmidt-Hieber and Hausser 2013), but others reported that grid cells mostly correspond to pyramidal cells, and that border cells are mostly stellate cells (Tang, Burgalossi et al. 2014). Another possibility is that the spatial cells do not correspond to a particular morphology, but that the identity of the surrounding interneurons determines the properties of the principal neuron (Couey, Witoelar et al. 2013; Craig and McBain 2015; Eichenbaum, Amaral et al. 2016). According to the latest evidence, neurons with grid properties can be found both amongst cells with stellate as well as pyramidal morphologies (Sun, Kitamura et al. 2015).

4.4. The lateral entorhinal cortex and object recognition memory

The lateral part of the entorhinal cortex is not as well studied as the medial part. For a long time the consensus was that the medial entorhinal cortex channeled the "where" part of episodic memory to the hippocampus, while the lateral entorhinal cortex channeled the "what" part, or the content of the memory (van Strien, Cappaert et al. 2009). This was based on the absence of spatially tuned neurons (Hargreaves, Rao et al. 2005; Yoganarasimha, Rao et al. 2011) and the discovery of neurons responding to odors (Young, Otto et al. 1997) and objects in the LEC (Zhu, Brown et al. 1995; Wan, Aggleton et al. 1999; Deshmukh 2014).

Later evidence has shown that the LEC also has a spatial aspect, although this is related to the presence of objects (Deshmukh 2014). Neurons in the LEC fire at or near objects, or

where the object used to be after object removal (Figure 7; (Tsao, Moser et al. 2013)). It seems that for some neurons, the "what" and "where" of the memory converges in the LEC in the form of conjunctive place + object cells (Deshmukh 2014). Because of the reciprocal connections between MEC and LEC, it is possible that the non-spatial and spatial information (to a certain degree) already converges in the EC (van Strien, Cappaert et al. 2009).
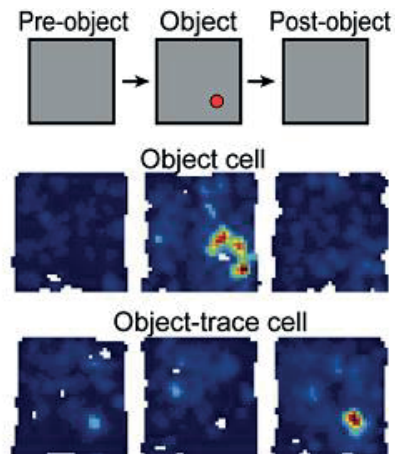
Figure 7 Firing properties of object and object-trace cells. The top panel shows before, during and after the placement of an object in a square space. The bottom two panels show firing rate maps of an LEC object cell (middle panel) and an LEC object-trace cell (bottom panel) for that object. Reprinted from (Igarashi 2016) with permission from Elsevier.

4.5. Disease susceptibility in the entorhinal cortex

Several debilitating diseases affect the entorhinal cortex, including Alzheimer's disease, schizophrenia, Parkinsons' disease, and epilepsy (Braak and Braak 1985; Du, Whetsell et al. 1993; Braak, Rub et al. 2006; Baiano, Perlini et al. 2008). The effect of most of these diseases is unevenly distributed across the EC layers. The neurons in LIII display vulnerability to death after epileptic seizures (Schwarcz, Eid et al. 2000). For Alzheimer's disease, there is more neuronal loss in LII when compared to the other layers. It is hypothesized that the vulnerability of LII cells could be due to more complex morphology and higher energy requirements (Stranahan and Mattson 2010). Interestingly, an early symptom of Alzheimer's disease is spatial navigation deficits (Allison, Fagan et al. 2016), which further supports the importance of the EC, LII in particular, in navigation. Evidence suggests that MEC excitatory neurons and grid cell function are vulnerable to tau pathology (Fu, Rodriguez et al. 2017), and that MEC stellate neurons express increased amounts of amyloid β in early stages of Alzheimer's disease (Kobro-Flatmoen, Nagelhus et al. 2016).

In schizophrenic individuals, altered cytoarchitecture and smaller neuron size is common in EC LII and LIII (Arnold 2000). Gene expression analysis of EC stellate neurons in schizophrenic patients showed altered expression of certain transcription factors, ion channels, and proteins involved in synaptic function (Hemby, Ginsberg et al. 2002).

5. Postnatal development of the rodent brain

The general architecture of the brain, with area patterning and lamination of the cortex, is largely complete at birth (Rice and Barone 2000; Jiang and Nardelli 2016). This is mainly because the vast majority of neurogenesis and neuronal migration take place during

embryonic development, with the notable exceptions of the dentate gyrus and the subventricular zone, which reach peak neurogenesis rates after birth (Cayre, Canoll et al. 2009; Semple, Blomgren et al. 2013). The differentiation of neurons begins after neurogenesis, but specialization and subtype specification continues into the postnatal stages (Figure 8; (Southwell, Nicholas et al. 2014; Harb, Magrinelli et al. 2016)).

The same progenitor cells that give rise to neurons during the embryonic stage switch their developmental program and begin to give rise to glial cells (Jiang and Nardelli 2016). There are three waves of gliogenesis, of which the third begins after birth (Rowitch and Kriegstein 2010). The formation of both oligodendrocytes and astrocytes peaks during the first postnatal month in rodents (Jiang and Nardelli 2016). After maturation and association with neuronal axons, the oligodendrocytes begin forming the myelin sheaths, a process that begins around P10, peaks around P20, and reaches adult-like distribution around P25 (Meier, Brauer et al. 2004; Semple, Blomgren et al. 2013). New astrocytes originate from differentiated, local astrocytes that migrated from the subventricular zone during embryonic development. After cell division, the new astrocytes integrate into the existing network, where they regulate the neuronal environment and synaptic transmission, and form part of the blood brain barrier (Clarke and Barres 2013; Jiang and Nardelli 2016). The blood-brain barrier is present, but immature, at birth. The capillaries become adult-like from P14-21 in the rat, and are increasingly covered by pericytes and astrocytic endfeet during the first three weeks (Semple, Blomgren et al. 2013; Zhao, Nelson et al. 2015).
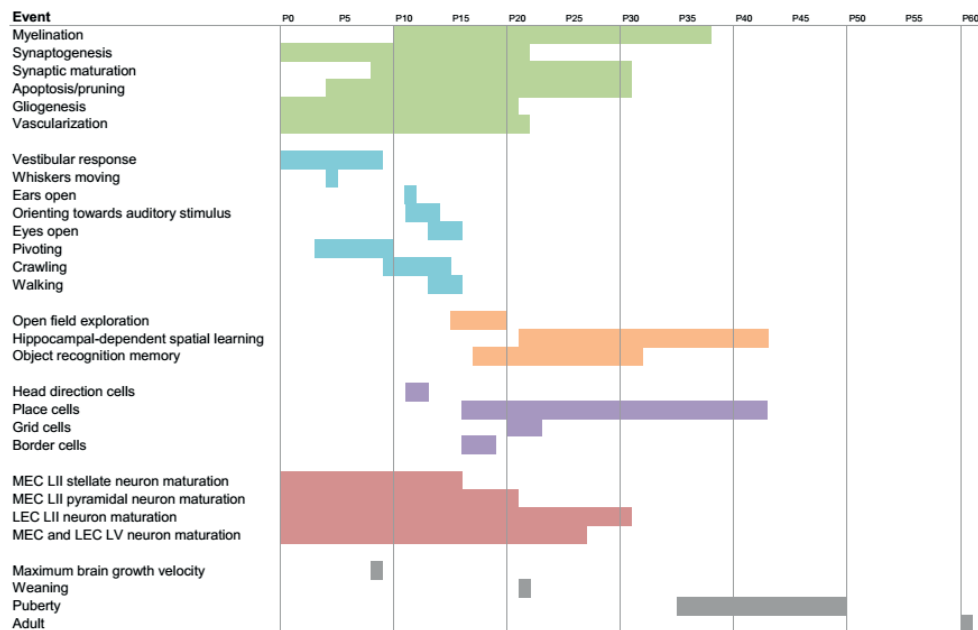
Figure 8: Time line of developmental events in rat brain from birth (P0) to adulthood. Based on (Howdeshell 2002; Watson, Desesso et al. 2006; Le Magueresse and Monyer 2013; Pressler and Auvin 2013; Semple, Blomgren et al. 2013; Sengupta 2013; Bjerknes, Moser et al. 2014; Downes and Mullins 2014; Engelhardt and Liebner 2014; Wills and Cacucci 2014; Bjerknes, Langston et al. 2015; Ramsaran, Sanders et al. 2016; Ramsaran, Westbrook et al. 2016; Donato, Jacobsen et al. 2017).

Unlike the other glial cells, microglia have mesodermal origins, and begin to colonize the CNS during embryonic development (Chan, Kohsaka et al. 2007; Prinz and Priller 2014). Postnatally, these resident microglia undergo substantial cell division, with their numbers increasing around 20-fold from P0 to adulthood (Alliot, Godin et al. 1999). As a consequence of the increase in the number of macro- and microglial cells together with myelination, there is large increase in brain volume during the first postnatal weeks (Figure 9ab). In the rat MEC, the thickness of both superficial and deep layers increases around 2-fold from P0 to P12 (Figure 9c; (Ray and Brecht 2016)).
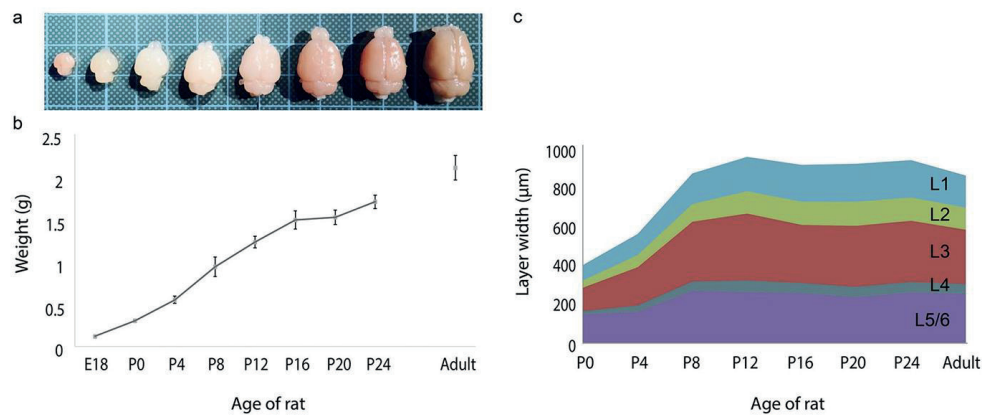
Figure 9 Volumetric development of rat brain in general and the MEC in particular. a) Rat brain size from E18, P0, P4, P8, P12, P16, P20 to adult. b) Mean weight (g) of E18, P0, P4, P8, P12, P16, P20, P24 and adult brains. c) MEC layer width (μm) for P0, P4, P8, P12, P16, P20, P24 and adult rats. Layer 1 (light-blue), layer 2 (green), layer 3 (red), layer 4 (gray-blue) and layer 5/6 (purple). Reprinted from (Ray and Brecht 2016), with permission under the Creative Commons License.

Along with the increase in cell numbers, there is also maturation of the different cell types alongside ramification. The latter includes axonogenesis and dendritogenesis on neurons and the subsequent formation of synapses, a process which underlies the establishment of functional neuronal circuitry (Figure 10). For instance, the projections from the pre- and parasubiculum to the MEC become functional around P9/10, and continue developing until P30 (Witter, Canto et al. 2014). Also, the stellate neurons increase their dendritic spine density almost 3-fold between the second and fourth postnatal weeks (Boehlen, Heinemann et al. 2010). Synaptogenesis begins at the embryonic stage, but the synapses are rudimentary, few, and localized to dendritic shafts or filopodia (Lohmann and Kessels 2014). The process continues after birth, with extensive synapse formation during the first three weeks after birth, most on dendritic spines. (Semple, Blomgren et al. 2013; Lohmann and Kessels 2014; Jiang and Nardelli 2016). The rate of synapse formation slows down during the fourth postnatal week. Alongside synaptogenesis there is also development of molecular synaptic diversity, with corresponding differences in types and expression levels of proteins (O'Rourke, Weiler et al. 2012). It also seems that the subcellular localization of the synapse on the postsynaptic partner is of importance for the properties of the neural circuit, and this must also be guided (Maeder and Shen 2011).
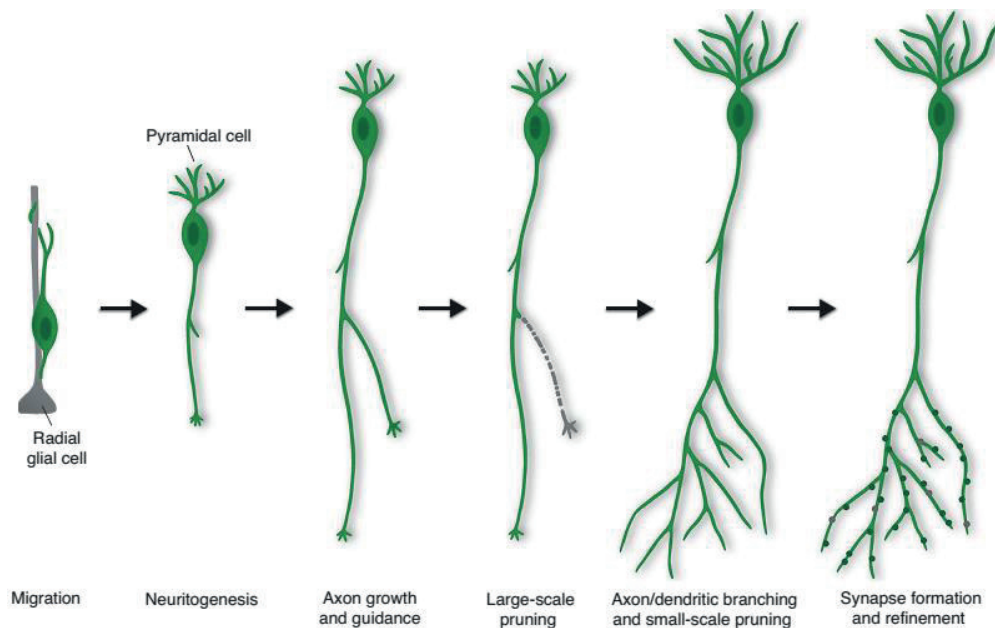
Figure 10 Maturation of neurons, from migration through neuron projection and pruning to synapse formation and refinement. Reprinted from (Navarro and Rico 2014), with permission from Elsevier.

Neuronal activity is dominated by electrical transmission over gap junctions at birth, and gradually transitions to chemical transmission during the next weeks, especially after P16 (Pereda 2014; Luhmann, Sinning et al. 2016). This early spontaneous network activity regulates the development and connectivity of neurons (Blankenship and Feller 2010). The hippocampal CA1 pyramidal neurons are mostly silent at birth, whereas a majority of interneurons in the same location display immature forms of activity. Their GABAergic synapses develop before the glutamatergic synapses, and aid in the maturation of hippocampal synapses (Khalaf-Nazzal and Francis 2013). GABA starts out having a depolarizing function during the first postnatal week, and becomes inhibitory during the second week (Lohmann and Kessels 2014). The maturation of GABAergic interneuron firing properties is protracted and not even complete at P30, at least in the mouse (Le Magueresse and Monyer 2013). On the other hand, cortical pyramidal neurons display mature firing properties around P20-22 in the rat. As the physiology of the individual neurons develops, the currents of neurons in the developing circuits begin to synchronize to generate brain rhythms (Colgin 2016). For instance, theta oscillations that occur during locomotion and exploration of animals appear at P8 and increase gradually during postnatal development (Wills and Cacucci 2014). Gamma oscillations appear already at P2, and sharp wave ripples at P7. Synaptic plasticity mechanisms, such as LTP, gradually mature until reaching adult-like function within the sixth postnatal week (Lohmann and Kessels 2014).

Following the overproduction of synapses during early postnatal development, comes a period of apoptosis and synapse pruning and stabilization (Nikolic, Gardner et al. 2013; Jiang and Nardelli 2016). This is thought to be a method of refinement of the cortical circuitry to remove wrong or superfluous connections (Low and Cheng 2006). Astrocytes signal the elimination of synapses, triggering the phagocytosis of synaptic materials by microglia (Clarke and Barres 2013). Microglia also engulf the remains after apoptosis (Bilbo and

14

Schwarz 2012). Recent findings indicate that pruning of the dentate granule cells, where perforant path projections terminate, is of a subtle and more homeostatic nature to prevent excessive branching (Goncalves, Bloyd et al. 2016; Radic, Jungenitz et al. 2017).

The brain's state of immaturity at birth is also seen in the behavioral and cognitive skills of the animal (Egorov and Draguhn 2013). Most of the behavior at birth is based on reflexes, and the vestibular and olfactory systems develop around this time (Lohmann and Kessels 2014; Wills and Cacucci 2014). Evidence of tactile exploration starts at P4, and the emergence of auditory system function occurs around P8-9 (Wills and Cacucci 2014). Rats are born with their eyes closed, and the eyes stay closed until around P14-15 (Langston, Ainge et al. 2010). The first two weeks are spent in the nest with very simple motor behavior. The pups begin moving independently at P13, and shortly afterwards (between P15 and P20), they begin to explore their environment (Langston, Ainge et al. 2010; Wills and Cacucci 2014). From P21 and on, the ability to perform spatial learning tasks that depend on the hippocampus emerges (Wills, Muessig et al. 2014). Spatial learning is accompanied by the restructuring of the hippocampal circuitry (Tronel, Fabre et al. 2010).

6. Gene expression and regulation in the brain

The complexity and adaptability of mammalian brains depend on a well-conserved array of molecular mechanisms. These mechanisms are spatially and temporally controlled by programs of gene expression together with environmental input to drive the development of the different cell types and the formation of brain connections. A gene can be defined as a stretch of DNA encoding an RNA molecule which is protein-coding (a messenger RNA or mRNA) or which has some other cellular function (non-coding RNA or ncRNA). Gene expression is subjected to regulation at many levels, including transcriptional, post-transcriptional, translational, and post-translational regulatory mechanisms. This introduction will focus on regulatory aspects affecting RNA levels.

DNA accessibility is regulated through DNA methylation and histone modifications and controls binding of transcription factors, which promote or repress transcription (Lelli, Slattery et al. 2012). Long ncRNAs (lncRNAs) can influence transcription through a variety of mechanisms, including competitively binding to the transcription machinery or transcription regulatory factors, forming scaffolds for protein complexes necessary for transcription or chromatin modification, and acting as decoys by sequestering proteins or small RNAs (Geisler and Coller 2013; Quinn and Chang 2016). Elongation and transcript processing rates are other aspects of transcriptional regulation, but alternative splicing and imprinting of mRNA binding partners, which occur during transcription, can also affect mRNA export and decay (Hocine, Singer et al. 2010). Other post-transcriptional mechanisms include mRNA transportation, microRNA (miRNA) regulation and mRNA degradation (McKee and Silver 2007).

The brain has the highest number of organ-specific genes, and exhibits the highest level of alternative splicing of all tissues (Yu, Fuscoe et al. 2014). Gene expression differs between brain structures, cortical layers, and also between cell types in the brain (Stansberg, Ersland et al. 2011; Fertuzinhos, Li et al. 2014; Zeisel, Munoz-Manchado et al. 2015). Cell type specific studies have shown robust transcriptional differences between the main cell types in the brain, and have indicated the existence of subtypes for each cell type (Zeisel, Munoz-Manchado et al. 2015; Bakken, Miller et al. 2016). Of the cell types present in the brain, neurons have the highest number of genes expressed (Harbom, Chronister et al. 2016). The

structure of neuronal cells also has special requirements for long-distance transport of transcripts and localized translation of proteins (Di Liegro, Schiera et al. 2014). In addition, post-transcriptional regulatory mechanisms allow for temporal control of translation in response to environmental input (Rosenberg, Gal-Ben-Ari et al. 2014). The following sections review aspects of brain transcriptome dynamics during postnatal brain development, first focusing on protein coding mRNAs before turning to the roles of lncRNAs and miRNAs in the brain.

6.1. Gene expression dynamics during postnatal brain development

The formation of the different cell types in the brain and the connections between them are accompanied by variation in gene expression between developmental stages and between cells. The advent of microarrays and deep sequencing technologies has allowed analysis of the global transcriptome of the brain during development. Different areas and cell types in the brains of several species, including the rat, have been analyzed in this way, and the data is complemented by findings from *in situ* hybridization (ISH) studies, such as those of the Allen Brain Atlas (Lein, Hawrylycz et al. 2007; Dillman and Cookson 2014). Gene expression analyses of the hippocampus has been conducted in humans, monkeys and mice (Leonardo, Richardson-Jones et al. 2006; Thompson, Pathak et al. 2008; Dong, Swanson et al. 2009; Christensen, Bisgaard et al. 2010; Bakken, Miller et al. 2016; Cembrowski, Bachman et al. 2016; Cembrowski, Wang et al. 2016), even at a single cell level (Zeisel, Munoz-Manchado et al. 2015; Shah, Lubeck et al. 2016).

Transcriptomic analyses have shown that the rodent brain transcriptome changes greatly during postnatal development, with the onset of adolescence and adulthood seeing large increases or decreases in the expression of many genes (Yu, Fuscoe et al. 2014). Several studies have found that the genes decreasing in expression from embryonic to postnatal stages are involved in neuronal proliferation, which is thought to reflect the transition from neuronal precursor cells to post-mitotic, mature neurons (Dillman and Cookson 2014). Genes increasing from embryonic to postnatal stages appear to be involved in glycolysis and synaptic maturation. Many of the same pathways that are involved in embryonic development have different functions in postnatal development and plasticity (Guillemot and Zimmer 2011; Mulligan and Cheyette 2012). The expression trajectories of a large portion (~70%) of these developmental genes are conserved in species from rodent to human (Bakken, Miller et al. 2016). Much of these expression trajectory dynamics are due to epigenetic modifications, which have been shown to be prevalent during the development of the human and mouse brain, although the rate of DNA methylation changes displays a gradual decrease after birth (Dillman and Cookson 2014).

In addition to the differences in expression levels of genes during development, the presence and levels of some isoforms also vary with age. In fact it seems alternative splicing is necessary for normal brain development and function both at the embryonic and postnatal stages (Dillman and Cookson 2014; Vuong, Black et al. 2016), and it is likely involved in most aspects of neuronal cell development, including subtype specificity (Iijima, Hidaka et al. 2016). Neuronal activity can alter splicing patterns through Ca^{2+}-mediated signaling (Razanau and Xie 2013). Another aspect of RNA mediated developmental mechanisms is RNA editing, with the proportion of transcripts subjected to RNA editing varying across brain development and increasing with age (Dillman and Cookson 2014).

6.2. Key genes and pathways guiding main aspects of postnatal brain development

The research findings on single genes and pathways that have been found to be involved in the different aspects of brain development are vast, and a thorough coverage is outside the scope of this work. I will however describe certain key genes and pathways known to be involved in the most important postnatal developmental processes. Different classes of protein-coding genes are involved in development, including transcription factors, signaling molecules, signal receptors, elements in signal transducing pathways, and extracellular enzymes. The sequence of events is guided by cascades of transcription factors (Ben-Ari and Spitzer 2010). Transcription factors are also important for neuronal subtype specification and maintenance (Dillman and Cookson 2014; Ohtaka-Maruyama and Okado 2015). The following paragraphs will review some of the protein-coding genes and pathways involved in important aspects of postnatal brain development, including neuron migration, neuron projection formation, synaptogenesis, gliogenesis and glial differentiation, and vascular formation.

Although neuronal migration mostly takes place during embryonic development, there is also limited migration at the postnatal stage. The migration itself, as well as changes in neuronal shape and morphology during migration, is caused by changes to the cytoskeleton, and the migration process requires the activity of motor proteins (Jiang and Nardelli 2016). The migration is guided by integration of attractive and repellant signals, which are thought to be integrated by the Rho-GTPases (Lambert de Rouvroit and Goffinet 2001). Cell adhesion molecules mediate the interaction between the migrating neuron and the radial glial fibers they migrate along (Marin, Valiente et al. 2010). Molecules such as Reelin, ephrins, Wnts, and retinoic acid function as extracellular cues for guidance (Marin, Valiente et al. 2010; Jiang and Nardelli 2016).

Once the neurons are in place, axons are carefully guided to their targets by the presence of attracting and repellant molecules, both secreted and membrane proteins. The process is controlled in a spatiotemporally dynamic manner to ensure correct targeting of the axon to the appropriate subcellular localization on the appropriate neuron (Maeder and Shen 2011; Hassan and Hiesinger 2015). Important molecules include cell-surface adhesion molecules (e.g. the neuronal cell adhesion molecule NCAM, N-cadherin, and integrins) and guidance proteins, including some of the classical morphogens (Stranahan, Erion et al. 2013; Jiang and Nardelli 2016). The four main families of guidance cues are the Semaphorins, Netrins, the Slit–Robo system, and ephrins (Kolodkin and Tessier-Lavigne 2011). These are also known to be involved in the formation of the hippocampal projections (Forster, Zhao et al. 2006). Some of the other proteins involved are also involved in neuronal migration and embryonic patterning, such as Wnt, Shh and BMP (Borodinsky, Belgacem et al. 2015; Hassan and Hiesinger 2015). These substances will subsequently exert their effect on cytoskeletal components, such as actin and microtubules, to further extend the axon (Dent, Gupton et al. 2011).

Dendrite formation involves changes in cytoskeletal protein levels and polymerization structures guided by many of the same pathways as used in axon guidance (Dent, Gupton et al. 2011; Kolodkin and Tessier-Lavigne 2011). Some axon guidance molecules, such as the semaphorins and the ephrins, are also involved in synaptic pruning together with the transforming growth factor β and death receptors (Schuldiner and Yaron 2015). There is

increasing evidence that pruning is controlled by a transcriptional program, although it is not clear whether this is instructive or merely permissive.

Following arrival of the growth cone at its target, there is coordinated structural and functional maturation of the synapse, including the accumulation of synaptic vesicles, changes in types and subunit composition of channel proteins and neurotransmitter receptors, and bridging of the transynaptic space with cell adhesion molecules (Jiang and Nardelli 2016). Wnts, bone morphogenic protein (BMP), and sonic hedgehog are also involved in synaptogenesis and synapse maturation (Borodinsky, Belgacem et al. 2015). Neuronal synaptic activity causes influx of Ca^{2+}, which again leads to a cascade of signaling events ultimately activating gene expression programs (Greer and Greenberg 2008). Such gene products include neurotransmitter receptors and kinases modulating synaptic plasticity (Lohmann and Kessels 2014). In addition to alterations in neurotransmitter receptor compositions, changes in the ion channel types and levels leads to maturation in firing properties (Kaila, Price et al. 2014; Lohmann and Kessels 2014). The cell and stage-specific expression of these proteins determines the state of differentiation and subtype identity development of neurons (Ben-Ari and Spitzer 2010; Semple, Blomgren et al. 2013). For instance, the expression of glutamate receptor subunits is known to increase substantially postnatally (Semple, Blomgren et al. 2013). Another example includes the hyperpolarization-activated cyclic nucleotide-gated (Hcn) channels important for the physiological properties of stellate neurons, which increase in density with age, reaching a peak around 3 weeks after birth (Pastoll, Ramsden et al. 2012). Other molecules that participate in synaptic function and plasticity, such as kinases and phosphatases like Ca^{2+}/calmodulin-dependent protein kinase-II and protein kinase A, increase in expression until the end of the fourth postnatal week (Lohmann and Kessels 2014).

Alongside neuronal maturation there is extensive formation and maturation of glial cells. The proliferation and migration of oligodendrocyte precursor cells is stimulated by platelet-derived growth factor A (Cayre, Canoll et al. 2009), while transcription factors (e.g. oligodendrocyte transcription factor 1/2, SRY-box 10, and NK 2 Homeobox 2) and certain miRNAs, lncRNAs, and chromatin remodeling enzymes promote their differentiation into mature oligodendrocytes (Jiang and Nardelli 2016). The Src kinase Fyn is also involved in oligodendrocyte differentiation, in addition to serving as an intrinsic stimulant of myelination. In addition, axonal molecules like cell adhesion molecules and neurotrophins, and glutamate or ATP released as a consequence of neuronal activity also influence oligodendrocyte migration, differentiation and myelination.

Differentiation of precursor cells to astrocytes begins with Notch signaling, which inhibits differentiation into neuronal and oligodendrocyte lineages (Jiang and Nardelli 2016). BMP and the interleukin-6 family of cytokines also promote astrogenesis. These pathways exert their effects separately or by activating the JAK-STAT pathway. Astrocytes also make up an important part of the blood brain barrier. Other pathways involved in angiogenesis, neurovascular patterning, and blood brain barrier formation include Wnt/β-catenin, platelet-derived growth factor β, sonic hedgehog, vascular endothelial growth factor, and insulin growth factor signaling (Zhao, Nelson et al. 2015).

When reaching adulthood, the rats will have developed neuronal networks based on a combination of genetic programming and environmental factors, and will have specialized cells with distinct biochemistries. Although much is known, the details of the molecular mechanisms behind the postnatal maturation events in the brain are still being elucidated (Cayre, Canoll et al. 2009; Bae, Jayaraman et al. 2015). The complexity of the molecular processes important for brain development and the resources required to probe these processes are still limiting factors in this research field (Bakken, Miller et al. 2016).

6.3. Noncoding RNAs in the brain

It was long believed that the genome's function was exerted exclusively through classical protein-coding genes, even though these genes make up only 2-3% of the genome (Harrow, Frankish et al. 2012; Mudge and Harrow 2015). Apart from the sections of DNA encoding transfer RNAs (tRNAs) and ribosomal RNAs (rRNAs), the rest was long thought of as "junk DNA". It is now known that much of the genome is transcribed at one time or another, and that many of these non-coding transcripts have functions (ENCODE, (2012)). Due to historical reasons, non-coding transcripts are mainly divided into two main classes– lncRNAs (≥200 nucleotides) and small ncRNAs (<200 nucleotides) (Mercer, Dinger et al. 2009).

Small ncRNAs were long overlooked due to limitations in the laboratory methods used to purify RNAs. Intensive efforts have gone into discovering types and functions of small RNAs, greatly aided by the invention of high throughput sequencing technology. The most notable types of small RNAs are miRNAs (see Section 6.4), small interfering RNAs (siRNAs), small nuclear RNAs (snRNAs), small nucleolar RNAs (snoRNAs), and piwi-interacting RNAs (piRNAs), and their functions span from post-transcriptional regulation of gene expression, to involvement in splicing and chromatin modifications (Cech and Steitz 2014).

The different types of lncRNAs are distinguished by the location of their transcriptional start site and the direction of transcription in relation to protein-coding genes, namely antisense, sense intronic, sense overlapping, large intergenic, and processed transcripts (Derrien, Johnson et al. 2012). Some lncRNAs are polyadenylated, while others are not (Cech and Steitz 2014). Their expression is regulated similarly to that of protein-coding genes (Wu, Liu et al. 2014). LncRNAs tend to contain fewer exons than protein-coding genes, and are generally expressed at lower levels (Quinn and Chang 2016).

Although lncRNAs by definition do not encode any proteins, some have been found to encode small peptides (de Andres-Pablo, Morillon et al. 2017). The functions of lncRNAs are still being elucidated, but they have been found to be important for processes such as imprinting, regulation of gene expression, and modulation of splicing (Quinn and Chang 2016).

Many lncRNAs have tissue-specific expression, with an estimated 40% of the known lncRNAs being specific to the brain (Derrien, Johnson et al. 2012). This expression seems developmentally regulated (Briggs, Wolvetang et al. 2015) and cell-type specific (Molyneaux, Goff et al. 2015). In fact, lncRNAs seem to be more cell-type specific than protein-coding genes. LncRNAs have been implicated in neurogenesis and neural lineage differentiation, and the knockout of certain lncRNAs has led to neonatal or perinatal lethality (Ramos, Attenello et al. 2016). Neuronal activity has been shown to alter their expression (Briggs, Wolvetang et al. 2015). The importance for lncRNAs in the brain is further supported by perturbations

in certain neurological disorders, such as Alzheimer's disease, schizophrenia, and autism (Luo and Chen 2016; Ramos, Attenello et al. 2016).

6.4. miRNAs and their importance for the brain

MiRNAs are short, non-coding RNAs of 21-24 nucleotides that are important regulators of gene expression (Pasquinelli 2012). Genes encoding miRNAs are transcribed by RNA polymerase II into long primary transcripts (pri-miRNA), each with one or more local hairpin structures (Figure 11; (Ha and Kim 2014)). Some miRNAs are encoded close together in the genome, and are then usually co-transcribed. The hairpins within the primary transcripts are processed into precursor miRNAs (pre-miRNAs) by the Microprocessor complex containing RNase III enzyme Drosha and its binding partner DGCR8, except for a minority of pri-miRNAs (mirtrons) which are processed by the splicing machinery. The pre-miRNA forms a complex with the proteins exportin-5 and Ran-GTP for export into the cytoplasm. The cytoplasmic RNase III enzyme Dicer then cleaves the terminal loop of the pre-miRNA, producing a double-stranded duplex, which in turn may yield two mature miRNAs, one from the 5' end and the other from the 3' end of the hairpin structure. The mature miRNA associates with an Argonaute protein, and together they constitute the main components of the miRNA-induced silencing complex (miRISC, (Krol, Loedige et al. 2010)).

Usually one of the two mature miRNAs is more commonly incorporated into the miRISC, and is then called the "guide" strand, while the other strand is called the "passenger" strand, and has been historically denoted miRNA* (Ha and Kim 2014; Kozomara, Hunt et al. 2014). In the latest miRNA nomenclature, miRNAs are instead denoted with the suffix -5p or -3p, depending on the hairpin end they from which they are derived (Kozomara, Hunt et al. 2014). The miRNA repository miRBase has designated miRNAs with a three-letter prefix followed by a numerical suffix (i.e. "miR-1"; (Griffiths-Jones, Grocock et al. 2006)). Mature sequences are identified with the prefix "miR", and precursor hairpins "mir". To identify the organism, a three or four letter code is used in front of the miRNA name (e.g. "rno-miR-1" for Rattus Norvegicus). Several miRNAs are encoded at multiple loci, and the precursor hairpins for these are identified with an additional numeric suffix (e.g. mir-124-1 and mir-124-2). For orthologous miRNAs an additional letter is added to the core nomenclature (e.g. "miR-10a and miR-10b").

The mature miRNA in the miRISC complex will bind to its target mRNA through a sequence with high complementarity. It is typically the nucleotides in positions 2-7 from the 5' end of the miRNA, known as the seed sequence, which binds the target site in the mRNA, most often in the 3'UTR (Yates, Norbury et al. 2013). This will most often lead to either degradation of the target mRNA, or repression of its translation, depending on the level of complementarity and the target site context (Pasquinelli 2012). However, instances where miRNAs bind to instability elements in the 3'UTR of the target mRNA, subsequently increasing its stability, have been reported (Fabian, Sonenberg et al. 2010). One miRNA can target hundreds of mRNAs, and one mRNA can be targeted by several different miRNAs (Pritchard, Cheng et al. 2012). Their function can vary between cell types and with different conditions (Erhard, Haas et al. 2014). MiRNAs thereby represent an important mechanism for post-transcriptional regulation of gene expression, and have been shown to play a role in development, homeostasis, and pathology (Ambros 2011; Sayed and Abdellatif 2011). However, the roles of each miRNA can change depending on the developmental and cellular context (Gao 2010).
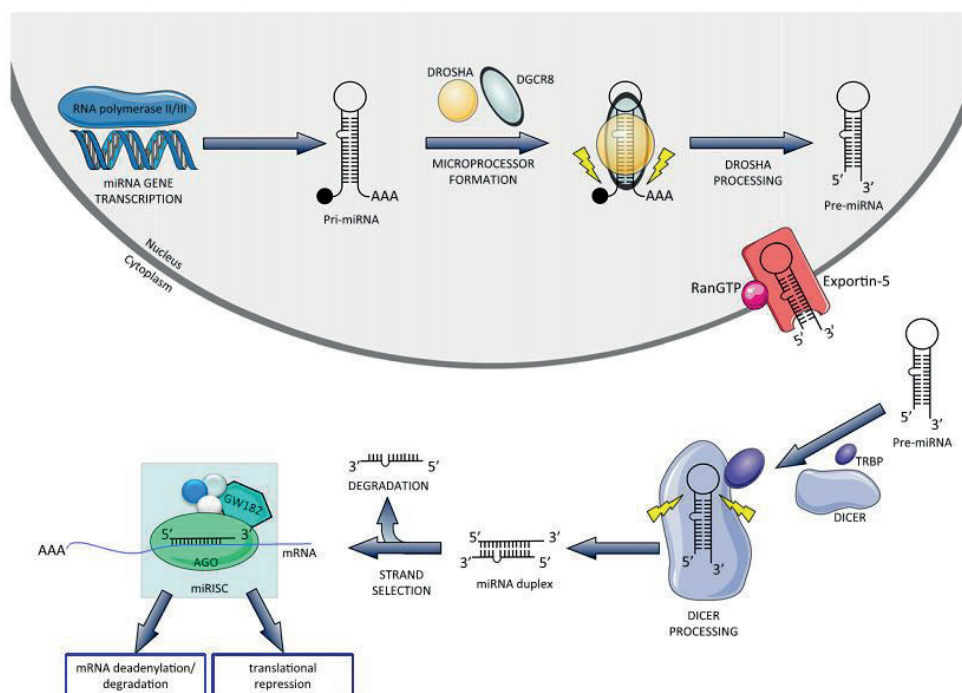
Figure 11 miRNA biogenesis and function. Pri-miRNAs are transcribed by RNA polymerase II or III, and processed into pre-miRNAs by the Microprocessor complex consisting of Drosha and DGCR8. The pre-miRNA is transported into the cytoplasm mediated by Exportin-5, and further processed into the miRNA duplex by Dicer. One of the strands is usually selected for loading into the miRISC complex, which is capable of post-transcriptional regulation of gene expression. Reprinted from (Luoni and Riva 2016), with permission from Elsevier.

About 70% of all known miRNAs can be detected in the brain, and some of these are expressed at a higher level in the brain compared to other organs (Nowak and Michlewski 2013). Protein coding genes expressed in the brain tend to have longer 3' untranslated regions (UTRs) than in other tissues, which increases the potential for miRNA regulation of these genes (Miura, Shenker et al. 2013). Indeed, these brain-specific 3'UTR isoforms are enriched for target sites of miRNAs with known neuronal functions. MiRNAs also display cell-type specific expression, and a large proportion of miRNAs have great fluctuations in expression levels during brain development (Fiore, Siegel et al. 2008; He, Liu et al. 2012).

The importance of miRNAs for brain development first became clear from global and targeted knockout studies of the components of miRNA biogenesis. Global knockout of Argonaute 2 led to failure of neural tube closure, and various types of Dicer knockouts led to defects in neuronal cell differentiation and brain morphogenesis, or even death of the organism (Figure 12; (Saba and Schratt 2010; Sayed and Abdellatif 2011)). It is thought that the role of miRNAs in brain development is to maintain and fine-tune gene expression levels in the presence of developmental stimuli (Dillman and Cookson 2014; Follert, Cremer et al. 2014). Evidence shows the importance of miRNAs throughout brain development and in normal brain function, with roles in neuronal and glial differentiation, neuron migration, neuronal subtype specification, synaptogenesis, and synaptic plasticity (Figure 13; (Saba and Schratt 2010; Bian and Sun 2011; McNeill and Van Vactor 2012; Aksoy-Aksel, Zampa et al. 2014; Dillman and Cookson 2014; Stappert, Roese-Koerner et al. 2015). In fact, miRNAs are

emerging as a powerful cellular mechanism for localized regulation of the protein synthesis required for dendritic spine growth and synaptic plasticity in the dendrites, which in turn forms the basis for the formation and refinement of neuronal circuits (Saba and Schratt 2010; McNeill and Van Vactor 2012). Evolutionary studies of miRNAs in primate brains have also indicated that miRNAs may be responsible for species-specific traits (Chen and Qin 2015).
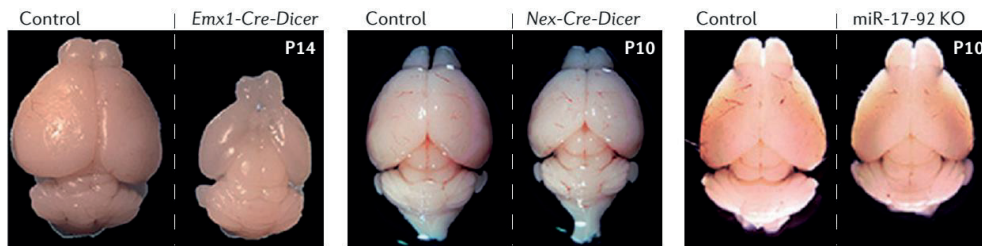
Figure 12 MiRNAs are important for brain development. Knocking out the miRNA processing enzyme Dicer (left and center panels) and miR-17/92 (right) reduces brain volume. Reprinted from (Sun and Hevner 2014), with permission from Macmillan Publishers Ltd: Nature Reviews Neuroscience.
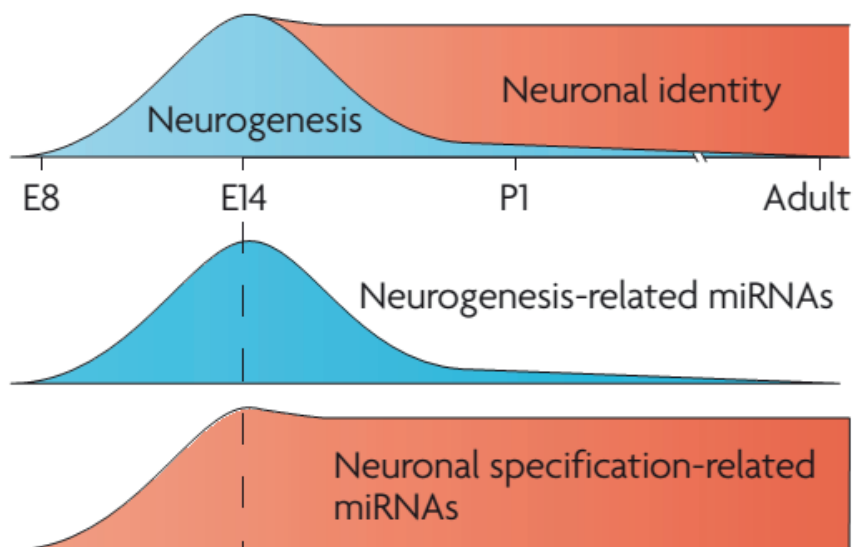
Figure 13 Expression of miRNAs in neuronal development. The top panel shows relative levels of neurogenesis during embryonic and postnatal development. The expression of some miRNAs mirror levels of neurogenesis (center panel), while other miRNAs are induced during neurogenesis, and maintain high expression levels (bottom panel). Reprinted from (Li and Jin 2010), with permission from Macmillan Publishers Ltd: Nature Reviews Neuroscience.

Underscoring the importance of miRNAs for brain development and function, altered miRNA levels are seen in several psychiatric disorders as well as neurodevelopmental and neurodegenerative diseases. Altered miRNA levels are also seen for the diseases known to affect the EC, including Alzheimer's disease, epilepsy, Parkinson's disease, and schizophrenia (Fiorenza and Barco 2016). Several of the protein-coding genes known to be involved in these diseases have target sites for the miRNAs displaying altered levels, and have anti-correlated expression patterns with the miRNAs targeting them (Wang, Rajeev et al. 2008; Beveridge and Cairns 2012). There are also examples of SNPs in miRNA recognition elements in the 3'UTRs of target genes which may be involved in human neurological disease (Nowak and

22

Michlewski 2013) in addition to genome wide associations to the miRNAs themselves (Ripke, O'Dushlaine et al. 2013; Forstner, Hofmann et al. 2015; Ghanbari, Ikram et al. 2016). Further, conditional Dicer knock out causes neurodegenerative features (Davis, Cuellar et al. 2008; Tao, Wu et al. 2011). However, much is still unknown about the exact role of miRNAs in these diseases, and also with respect to their role in general brain functions of neuronal excitability, synaptic plasticity and memory (Fiorenza and Barco 2016).

7. Measuring the brain transcriptome

Analysis of the transcriptome is essential in the quest to understand the role of RNAs in guiding and controlling development, homeostasis, and cellular response to environmental factors. The transcriptome consists of all coding and non-coding RNA molecules in a cell, and the study of the expression of these molecules is known as transcriptomics (Roy, Altermann et al. 2011). There are several methods available for analysis of the transcriptome, some measuring the expression of one type of RNA transcript at a time (i.e. one gene), and others measuring the expression levels of thousands of different RNA transcripts simultaneously.

It is common to compare the transcriptomes of different brain parts, cell types, developmental time points, and the brains of diseased individuals with those of healthy individuals to answer biologically relevant questions (Hemby, Ginsberg et al. 2002; Dillman and Cookson 2014; Zeisel, Munoz-Manchado et al. 2015; Bakken, Miller et al. 2016). RNA from tissue samples gives an average measure of gene expression across the cell types present in the sample. To obtain one or more cells from a single cell type, it is possible to label the cells of interest with transgenic or retrograde labeling methods, and to then select the cells using laser microdissection, fluorescence activated cell sorting, or manual sorting under a microscope (Okaty, Sugino et al. 2011). Alternatively, the content of a single cell can be aspirated following patch-clamp recordings. Through new advances in microfluidics, coupled with single cell sequencing, it is also possible to analyze single cells in cell populations in a data driven way (Grun and van Oudenaarden 2015). The following sections will touch upon the methods in transcriptomics relevant for this work, including microarrays, TaqMan arrays, deep sequencing of large and small RNAs, as well as ISH.

7.1. Microarray analysis

Microarrays represent a well-established, probe-based method to study the expression of thousands of RNA transcripts simultaneously, including protein-coding genes and miRNAs (Bassani, Ambrogi et al. 2014; Jaksik, Iwanaszko et al. 2015). The RNA sample is reverse transcribed and fluorescently labeled, and is subsequently hybridized to a chip containing DNA probes which are reverse complimentary to the nucleotide sequences of interest. The fluorescent signal for each probe is a measure of how highly the RNA molecule is expressed, and can be compared between samples after adjusting for technical sources of variation (normalization).

The drawbacks of microarrays are that they can only measure known genes, the dynamic range is limited, and the accuracy is lower than, for example, RNA sequencing (Pritchard, Cheng et al. 2012; Zhao, Fung-Leung et al. 2014). There is also a considerable batch effect (Jaksik, Iwanaszko et al. 2015). In the case of miRNAs, the high sequence homology between members of miRNA families can make it difficult to distinguish between the different members, as they may cross-hybridize (Sato, Tsuchiya et al. 2009). Cross-hybridization may also be a problem for other types of transcripts (Koltai and Weingarten-Baror 2008).

7.2. TaqMan array analysis

The TaqMan Low Density Array is a quantitative reverse transcription polymerase chain reaction (qRT-PCR) based microfluidic array that can be used to measure the expression of hundreds of genes or miRNAs simultaneously. The method has been shown to have high specificity and sensitivity, and has a broad dynamic range (Chen, Gelfond et al. 2009; Wang, Howel et al. 2011; Mestdagh, Hartmann et al. 2014). The sensitivity can be further increased with the use of pre-amplification, although this can increase variability (Chen, Gelfond et al. 2009).

In the case of miRNAs, stem-loop primers are used to detect mature miRNAs, since their small size is not suitable for normal primers (Pritchard, Cheng et al. 2012). It is common to normalize against other short RNA species, such as snRNAs, and to use the ddCt method to calculate differential expression (Chugh and Dittmer 2012; Pritchard, Cheng et al. 2012). The use of such endogenous controls is based on the assumption that they are independent of the biological process of study, which may not always be the case (Vandesompele, De Preter et al. 2002). Another source of bias for this technology is that PCR methods in general are affected by the GC content in the nucleic acid being amplified (Aird, Ross et al. 2011), and this can cause the optimal reaction conditions for each qPCR assay to vary substantially (Pritchard, Cheng et al. 2012). Like microarrays, the TaqMan arrays are limited to known miRNAs.

7.3. RNA sequencing

With next generation sequencing technology, cDNAs generated from RNA samples can be sequenced through the generation of millions of short reads. The most commonly used RNA sequencing platform is that of Illumina with their sequencing by synthesis technology (Reuter, Spacek et al. 2015), providing reads from one or both ends of an RNA molecule at lengths up to 2x300 base pairs (Illumina). Sample barcoding allows many samples to be run on one sequencing lane, although with a reduction in sequencing depth for each sample (Campbell, Liu et al. 2015). It is also possible to get strand information, which is crucial for the identification of antisense lncRNAs (Head, Komori et al. 2014). Strand information can be obtained by incorporating uracil during second strand cDNA synthesis, followed by the use of a PCR polymerase which cannot recognize this nucleotide. Other methods include the use of end-specific adapters added sequentially to the mRNA before reverse transcription, or the use of Moloney murine leukemia virus reverse transcriptase, which adds multiple cytosines to the end of the cDNA (Levin, Yassour et al. 2010).

In most library preparation protocols, purified RNA is fragmented and reverse transcribed to cDNA with the addition of oligonucleotide adapters to the ends (Head, Komori et al. 2014). There is also typically a selection step for the RNA transcripts of interest, with the most common selection method being the use of polyT beads to capture polyadenylated RNA transcripts (Zhao, He et al. 2014). Alternatively, highly abundant transcripts, such as rRNA or beta-globin mRNA (highly expressed in blood), can be diminished from the sample, as such transcripts can mask the presence of the RNA transcripts of interest. Depletion of rRNAs enables inclusion of non-polyadenylated RNA transcripts in the sample, reduces the 3' bias of the polyA capture method, and is suitable for RNA of poorer quality. However, the sequencing output from ribosomal depletion also results in more reads mapping to intronic or intergenic regions, which in addition to lncRNAs could represent pre-mRNAs, products of transcriptional noise, or DNA contamination (Cui, Lin et al. 2010; Capobianco 2014; Zhao, He

24

et al. 2014). Several groups have reported some variations in results depending on the selection method (Cui, Lin et al. 2010; Lahens, Kavakli et al. 2014; Zhao, He et al. 2014; Weedall, Irving et al. 2015).

Unlike microarrays, RNA sequencing allows analysis of expression levels and sequence features like splicing patterns and sequence variants in the same run, although to a limited extent this can also be achieved with tiling arrays (Malone and Oliver 2011). RNA sequencing has a broader dynamic range, and can detect transcripts expressed at lower levels, although this depends on the sequencing depth. Also, the method represents a more unbiased analysis of the RNAs present in the sample, as it is not probe-dependent. The sequencing depth influences identification and quantification of transcripts. With relevance for the brain, where isoforms are known to be of particular importance (Bae, Jayaraman et al. 2015; Vuong, Black et al. 2016), alternative splicing can be determined by analysis of RNA sequencing data (Garber, Grabherr et al. 2011). The limitations to the RNA sequencing technology include PCR and ligation related biases, failure to detect lowly expressed transcripts, and difficulty in comparing runs if different library preparation methods have been used (Oshlack, Robinson et al. 2010; Aird, Ross et al. 2011; Chugh and Dittmer 2012; Head, Komori et al. 2014).

7.4. miRNA sequencing

MiRNA sequencing uses similar methodology as RNA sequencing, except for the adaptor ligation and RNA size selection steps. After purification of total RNA with an isolation method that includes small RNAs, rRNAs and mRNAs will dominate the samples, and impede the subsequent detection of miRNAs by sequencing (Motameny, Wolters et al. 2010). To circumvent this problem, the adapter ligation or enzymatic steps may target miRNA species by only ligating transcripts with a 5' phosphate and 3' OH, although such transcripts also include tRNAs and snoRNAs (Zhuang, Fuchs et al. 2012; Head, Komori et al. 2014). In addition, the library undergoes size selection using gel or bead based methods either before or after adapter ligation and PCR amplification to enrich for RNAs of an appropriate size. Similar to regular RNA sequencing, miRNA sequencing allows for analysis of sequence variation, for instance the detection of isomirs or disease-associated variants (Chugh and Dittmer 2012).

7.5. In situ hybridization

With ISH it is possible to get information about where in the tissue a certain gene is expressed; whether it can be found in a certain region or cell type (Nuovo 2008; Cassidy and Jones 2014; Zhang, Xie et al. 2015). The tissue can be used whole, or sectioned if too large. The method entails the use of an antisense DNA or RNA probe to bind to the nucleic acid of interest (Warford 2016). The probe is labeled to allow subsequent detection, and is added to the tissue of interest at a temperature optimal for hybridization with the target molecule. Detection may be by fluorescence, radioactivity or chromophore (Cassidy and Jones 2014). The signal from the bound probe can be seen under a microscope, where its intensity provides a semi-quantitative measurement of the nucleic acid of interest. It is possible to increase the throughput by automation or by tissue microarray. The quality of the result depends on the specificity and sensitivity of the probe used, and optimization to maximize probe access to the target molecule and minimize background signal (Cassidy and Jones 2014; Zhang, Xie et al. 2015).

Due to the small size of miRNAs, the conventional probes are not suitable for their detection, as the resulting complex is unstable (Nuovo 2008). In addition, such analyses are further

complicated by a high degree of sequence similarity between certain miRNA family members (Urbanek, Nawrocka et al. 2015). The problem of specificity is most commonly solved by the use of probes containing modified nucleotides, locked nucleic acids (LNA) (Urbanek, Nawrocka et al. 2015; Zhang, Xie et al. 2015). The nucleotides contain an extra methylene bridge between the 2'-O and the 4'-C in the sugar moiety of the ribonucleotide (Petersen, Nielsen et al. 2000). This locks the molecule conformation in a way that creates more efficient nucleobase stacking, thereby increasing the melting temperature of the probe-nucleic acid duplex and increasing its specificity and affinity (Petersen, Nielsen et al. 2000; Thomsen, Nielsen et al. 2005; Cassidy and Jones 2014).

8. Analysis of the brain transcriptome

There are a variety of methods available for the analysis of transcriptomic data, and there is therefore still a great need for standardization of the research field, as the choice of analysis pipeline can influence the results (Garber, Grabherr et al. 2011). It is imperative to choose analysis methods suited to deal with the biases present in the technology used. The following sections describe common processing steps for microarray and RNA sequencing data, as well as both supervised and unsupervised methods to analyze the data. Finally, tools for *in silico* functional analyses are reviewed.

8.1. Data processing

Particularly for the transcriptomic methods involving the testing of multiple RNA transcripts simultaneously, the resulting data needs preprocessing to minimize errors and to alter the distribution of the data to be suitable for the chosen statistical methods. The first step is quality control (Figure 14). In the case of microarrays, this includes background correction and removal of low quality spots as determined by the image processing.

RNA sequencing data is computationally more challenging than microarray data, and requires more preprocessing (Garber, Grabherr et al. 2011). The quality of the raw data must be assessed by quality control software, and based on the outcome; the need for preliminary pre-processing is assessed. Pre-processing steps could include adapter trimming and the removal of low quality reads and bases, short reads, and PCR artifacts (Conesa, Madrigal et al. 2016). Subsequently, the reads need to be mapped to the relevant genome, or assembled *de novo*. Genome alignment can be complicated by reads aligning several places in the genome, as well as biological variations with respect to the reference genome and reads spanning exon-exon junctions. The use of paired-end sequencing or the preliminary alignment against a known transcriptome can alleviate multi-mapping and aid in the identification of exon junctions (Oshlack, Robinson et al. 2010; Zhao 2014).

Next, using the annotation information, the reads must be summarized across the RNA type of interest, e.g. transcript isoforms, exons, genes, lncRNAs, or miRNAs. The choice of reference annotation can impact the results (SeqQC Consortium, (2014)). Unannotated reads can be analyzed for novel transcripts (Conesa, Madrigal et al. 2016).
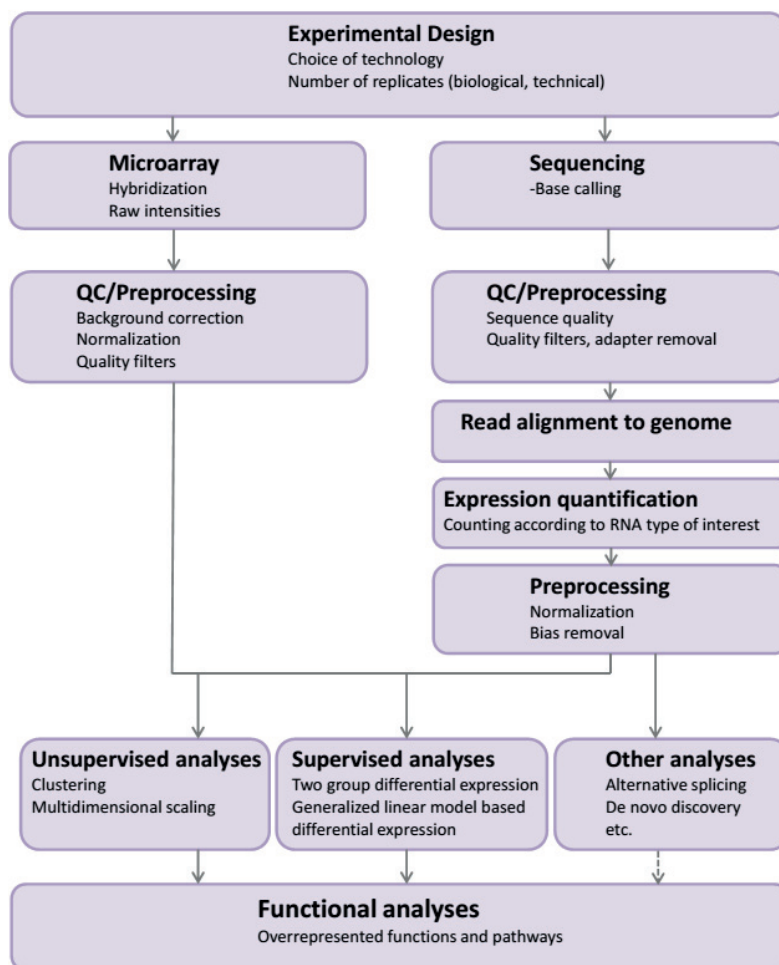
Figure 14 Microarray and RNAseq data analysis workflow. Adapted from (Fang, Martin et al. 2012) with input from (Conesa, Madrigal et al. 2016), with permission under the Creative Commons license.

Once there is a signal for each annotated transcript, the data should be normalized to reduce the effect of technical variability (Pritchard, Cheng et al. 2012). For TaqMan arrays, it is common to normalize against housekeeping genes or other transcripts with stable expression profiles. There are several normalization methods available for microarray and RNA sequencing data, and the suitability of the method chosen should be evaluated by visualization of the data before and after normalization (Quackenbush 2002; Slonim and Yanai 2009; Li, Piao et al. 2015). One generally well-performing method that can be used for both is quantile normalization, which matches the signal distributions across the samples in an experiment (Bolstad, Irizarry et al. 2003; Dillies, Rau et al. 2013). There is still some debate about the most suitable normalization method for RNA sequencing data, due to the complexity in the data (Hansen, Irizarry et al. 2012; Dillies, Rau et al. 2013; Law, Chen et al. 2014; Risso, Ngai et al. 2014). As a minimum, reads from RNA sequencing should be normalized according to library size. It is also beneficial to normalize according to gene length, as longer genes will have more reads than shorter genes at the same expression level and thereby provide greater statistical power for detection of differentially expressed genes

(Oshlack, Robinson et al. 2010). A common method for gene length normalization is to calculate reads per kilobase of exon model per million mapped reads (RPKM).

Another issue with RNA sequencing data is that the count distributions can be skewed by highly variable features or features expressed at high levels. Dillies and coworkers (2013) compared different normalization methods and recommended the use of Trimmed mean of M-values or DEseq normalization methods, which both solve the skewed distribution problem (Dillies, Rau et al. 2013; Conesa, Madrigal et al. 2016). These methods entail calculating a scaling factor based on the assumption that most genes are not differentially expressed (Dillies, Rau et al. 2013). There are also normalization methods controlling for the GC-content in the reads (Hansen, Irizarry et al. 2012).

To allow the use of statistical tests suitable for microarray data on RNA sequencing data, Law et al (2014) introduced the voom function in the limma package (Law, Chen et al. 2014). This function normalizes and log-transforms the raw read counts, and adds precision weights to adjust for the lack of independence between the variance and the mean for RNA sequencing data.

Once the preprocessing is complete, the next step is to look for transcripts that are differentially expressed between conditions, follow some expression pattern depending on the biological question of interest, or that display sequence variants. For analysis of splice variants, a commonly used approach is to look for differentially expressed exons. However, the detection of unknown splice junctions remains a challenge with today's analysis methods (SeqQC Consortium, (2014)).

8.2. Supervised analyses

A common purpose when using transcriptomic technologies is to determine whether one or more transcripts differ in expression level between known conditions (Scholtens and von Heydebreck 2005). This requires the use of supervised statistical methods to assess the significance of such differences when experimental and biological variation is present. The methods assume a null hypothesis of no differential expression of a gene between the conditions.

When testing the differential expression of one single gene, such as in singleplex quantitative PCR, a simple parametric t-test or a non-parametric Wilcoxon test can be applied after normalization to test whether the mean expressions of the two conditions are equal and determine the statistical significance of the result (Yuan, Reed et al. 2006). For the multivariate scenarios, such as microarrays and RNA sequencing, traditional statistical methods often fail due to the dimensionality and noise levels (Clarke, Ressom et al. 2008). This is further complicated by the use of a limited number of replicates due to the high cost of microarray and RNA sequencing experiments, which makes it challenging to estimate variation (Nadon and Shoemaker 2002; Jeffery, Higgins et al. 2006). To allow the use of parametric tests, data can be transformed to the log scale, often providing a more symmetrical, approximately normal data distribution (Scholtens and von Heydebreck 2005). No statistical model has been shown to fit with all types of data, and the choice of method can influence the results (Conesa, Madrigal et al. 2016).

Most analysis methods used for microarray data depend on an approximately normal distribution of the data, whereas the count-based nature of RNA sequencing data fits well with discrete probability distributions. However, data transformation methods (e.g. the mean-variance adjustment in the limma-voom method) combined with borrowing information (e.g. variance) across all genes tested also allows for the use of statistical methods based on normal distribution also for RNA sequencing data (e.g. linear models, (Law, Chen et al. 2014; Conesa, Madrigal et al. 2016)).

Linear modeling, as implemented in the limma package, have been shown to perform well for both microarray and RNA sequencing data (Smyth 2004; Jeanmougin, de Reynies et al. 2010; Soneson and Delorenzi 2013; Law, Chen et al. 2014). The linear model is fitted to the expression data for each gene. The limma method solves the variance problem caused by a limited number of replicates by calculating an estimate based on the variance of all genes, and using it to obtain a moderated t-statistic with increased degrees of freedom (empirical Bayes method, (Smyth 2004)).

In addition to pairwise analyses, limma can also be used for multiple comparisons through the use of an F-statistic (Smyth 2004; Law, Chen et al. 2014). This is an empirical Bayes extension of the analysis of variance test (ANOVA), where the residual mean squares between genes have been moderated (Smyth 2005). A regular ANOVA can also be used when comparing more than two groups outside of limma, most commonly after fitting the data to a linear model (Cui and Churchill 2003).

When analyzing the expression of many genes simultaneously, it is important to reduce the probability of false positives (type I statistical errors). The simplest way to correct for multiple testing is the Bonferroni method, where the p-value is adjusted by the number of tests (Hastie, Tibshirani et al. 2009). This works well with fewer tests, but becomes too conservative with many tests, increasing the risk of false negative findings (type II statistical errors). The Benjamini-Hochberg method is more suitable for high numbers of tests. This approach adjusts the p-value according to the proportion of false negatives expected, assuming a uniform distribution of p-values under the null hypothesis (Noble 2009). In addition to adjustment of p-values, it is advised to apply a threshold of $|\log_2 \text{fold-change}|>1$ and a threshold for the adjusted p-value to obtain a list of reliably differentially expressed genes (SeqQC Consortium, (2014)).

8.3. Unsupervised analyses

Unsupervised methods are hypothesis-free methods which can be useful in exploration and organization of transcriptome data (Greene, Tan et al. 2014). The complexity of the high-dimensional data generated can be simplified by dimension reduction methods, where some measure of similarity between samples or transcripts is used to display relatedness. Two commonly used similarity measures for transcriptome data include leading log2 fold change (MDS plotting in the limma package, (Ritchie, Phipson et al. 2015)) and covariance (principal components analysis, (Ringner 2008)).

Clustering methods group the data into categories based on similarities, such as Euclidean distance or correlation, without prior assumptions (Kerr, Ruskin et al. 2008). This can be used to find new classes in the samples, or to identify co-expressed genes. In the widely used hierarchical clustering method, the results are presented as a dendrogram with hierarchy,

which can be partitioned to arrive at potentially meaningful groups for further exploration. For instance, genes with correlating expression patterns may be co-regulated by the same transcription factor, or be part of a particular pathway (Allocco, Kohane et al. 2004; Huang, Wallqvist et al. 2006).

8.4. Functional analyses

The final step is to infer some biological sense of the resulting list(s) of significant genes, either by using existing knowledge databases, looking for enriched or overrepresented gene sets, or performing network analyses (Oshlack, Robinson et al. 2010; Conesa, Madrigal et al. 2016). The Gene Ontology initiative was introduced to classify gene function, and links genes to molecular function, cellular components, and biological processes (Ashburner, Ball et al. 2000). The annotations are based on mainly experimental or computational sources, which are shown in the evidence code (du Plessis, Skunca et al. 2011).

An array of bioinformatics tools exist to look for significant overrepresentation of the genes in the result list in ontological terms, using methods like the Fisher's exact test, Chi-squared, or hypergeometric test to ascertain statistical significance (Huang da, Sherman et al. 2009). It is also common to test for overrepresentation in known pathways, using data from e.g. the Kyoto Encyclopedia of Genes and Genomes (KEGG) or the Reactome databases (Ogata, Goto et al. 1999; Joshi-Tope, Gillespie et al. 2005). The results can indicate functional differences between the conditions tested. Other methods include more of the richness in the expression data in that they can identify small changes that are coordinated in the same pathways, or use biological information about the position and role of a gene in a network through topology-based approaches (Khatri, Sirota et al. 2012; Garcia-Campos, Espinal-Enriquez et al. 2015). Regardless of the method, there are still limitations due to incomplete or inaccurate annotations and ontologies, and because most of the existing knowledge may be condition or cell-type specific (Khatri, Sirota et al. 2012).

To get a better understanding of the molecular processes in biological entities at a systems level, it is possible to analyze different data sets in conjunction, for instance to gain insight on regulatory mechanisms (Pritchard, Cheng et al. 2012). One such example includes the combination of miRNA and mRNA expression data in probing potential functions of miRNAs. The combination of such data can indicate the effect of miRNA regulation of the steady state mRNA expression levels (Conesa, Madrigal et al. 2016). Due to the nature of miRNA regulation of transcripts, most miRNA-mRNA expression patterns are expected to be anti-correlated. This type of analysis can help increase or decrease the confidence of the predicted targets (Steinkraus, Toegel et al. 2016).

There are several tools available to predict potential miRNA targets, such as TargetScan, PicTar, miRanda, and PITA (Saito and Saetrom 2010). Most of the methods look for complementarity between the seed and target gene sequences, thermodynamic properties (e.g. accessibility of the target sequence based on predicted 3-dimensional structure), and evolutionary conservation (Pasquinelli 2012; Steinkraus, Toegel et al. 2016). Others also make use of machine learning approaches on training sets (Steinkraus, Toegel et al. 2016). Of the target prediction tools, TargetScan has been found to perform well when compared to in vivo findings (Witkos, Koscianska et al. 2011). The TargetScan algorithm uses several different sequence features in both the miRNA and the mRNA to arrive at a context score, a qualitative measure of the predicted efficacy of the target site and target site abundance

(Grimson, Farh et al. 2007; Garcia, Baek et al. 2011). The latest version of TargetScan gives a context++ score, which also takes into account evolutionary conservation information and available 3'UTR isoform information (Agarwal, Bell et al. 2015). The context score seems to correlate well with protein downregulation (Witkos, Koscianska et al. 2011). However, CLIP-seq data (sequencing of RNAs bound to the Argonaute protein) shows low sensitivity for TargetScan (Reyes-Herrera and Ficarra 2012). There are also databases for validated miRNA targets, with increasing number of interactions (miRTarBase, TarBase, miRWalk and miRecords, (Xiao, Zuo et al. 2009; Chou, Chang et al. 2016)).
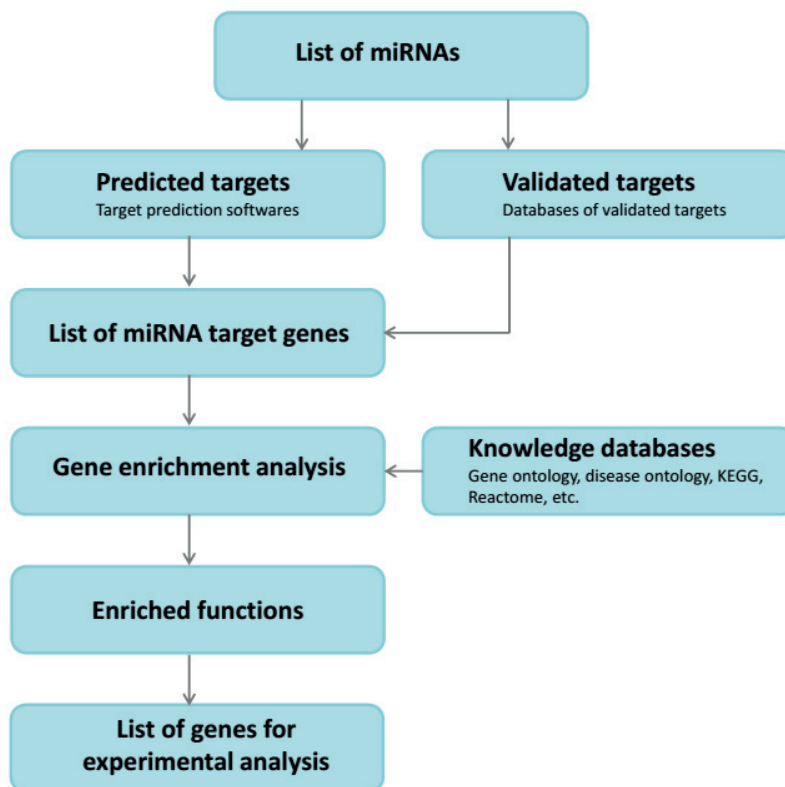
Figure 15 *In silico* **methods in miRNA functional analyses. Adapted from (Liu, Li et al. 2014) with permission under the Creative Commons license.**

Once the analysis provides a list of interesting target genes, this can be further analyzed for potential functions in the same way as any gene list (Figure 15). However, much of the information in the validated target databases was incomplete or inaccurate as of 2015 (Lee, Kim et al. 2015). This, combined with weaknesses in the target prediction algorithms, has made miRNA/mRNA conjunctive analyses messy (Steinkraus, Toegel et al. 2016). The situation is further complicated by differences in bona fide target genes in different tissues for the same miRNA (Clark, Loher et al. 2014). On top of this, the miRNA database miRBase most likely contains many false annotations because they are only based on high-throughput sequencing data without functional validation, and could thereby be intermediate molecules from other RNA species (Kozomara and Griffiths-Jones 2014).

All of these *in silico* functional analyses are limited to the current biological content of the databases used, and should be accompanied by verification in the lab for further support.

AIMS OF THE STUDY

The main objective of the study was to find genes and miRNAs that could shed light on the development of functional differences between different regions within the entorhinal cortex and the hippocampus.

Subgoals

Paper I
To investigate at what time point during postnatal development the dorsal and ventral parts of the hippocampus were comparable to that of the adult rat, displaying topographical connections and differential gene expression.

Paper II
To elucidate spatiotemporal expression of miRNAs and their predicted mRNA target genes in the medial entorhinal cortex during postnatal development, and to identify miRNAs of potential importance for stellate cell function.

Paper III
To characterize transcriptional differences between the medial and lateral entorhinal cortices and their layers during postnatal development to identify potential molecular substrates that may explain functional differences in these areas.

SUMMARY OF PAPERS

Paper I

The HF appears functionally differentiated along its dorsal-ventral axis. In paper I we investigated at what age this differentiation is adult-like with respect to general morphology, projection topography, and gene expression.

Examination of coronal sections revealed that the dorsal part of the hippocampus appeared at approximately the same anterior-posterior position of the cortex at all postnatal ages examined. However, the ventral part was found in a more posterior position in neonates compared to older animals. To examine this apparent change in positioning more closely, we injected a fluorescent dye into the ventral hippocampus at P7. The labeled sites were still found to be in the ventral hippocampus when reexamined at P15. Next, we used anterograde and retrograde tracers to examine if the projections from the EC to the hippocampus were organized along the dorso-ventral axis, as they are in the adult rat. We found adult-like topographical organization as early as P2-4.

Finally, we examined the gene expression of dorsal, intermediate, and ventral hippocampus at four postnatal ages (P0, P9, P18 and P60) by microarray analysis. We found 27 genes to be consistently differentially expressed more than two-fold between dorsal and ventral hippocampus at all time points, several of which were known from previous gene expression studies in adults. The differential expression of six genes was verified with qPCR.

These findings show that the differences along the dorsal-ventral axis of the hippocampus are present within the first postnatal week. Hippocampal projections from the entorhinal cortex display adult-like topography, and there is differential gene expression between the dorsal and ventral hippocampus as early as P0.

Paper II

The MEC has a laminar topography, and it is known that cell morphology, physiology, disease susceptibility and gene expression vary across MEC layers. There are also differences in the function and morphology of the cell types within single layers. MiRNAs have been shown to be important for brain development in general and neuronal subtype specification in particular by regulating the expression of their target mRNAs. We investigated how miRNA and mRNA expression differs between MEC layers (LII vs. LIII-LVI (LDeep)) at the postnatal time points P2, P9, P23, and P45. We also compared the miRNA expression in stellate neurons with the rest of the MEC at P4/5. The tissue expression analysis revealed laminar differences in miRNA expression at all time points examined, although the differences between ages were greater, in particular between P9 and P23. Enrichment analyses of validated and predicted, conserved target mRNAs of these laminar miRNAs that were expressed in the MEC revealed terms important for neuronal differentiation and function. Several of the miRNAs with laminar and temporal expression profiles have previously been implicated in Alzheimer's disease and schizophrenia.

We looked closer at the potential functions of miRNAs with similar expression patterns by clustering of miRNAs with correlated expression into modules, and performing enrichment analyses of the validated and predicted, conserved target mRNAs displaying negatively correlated expression patterns to the miRNAs in each module. The main trends were that miRNAs that increased in expression from young to older animals targeted mRNAs involved in cell cycle, neuron differentiation, and axon guidance, while miRNA that decreased across development targeted mRNAs involved in myelination, synapse organization and function, ion channel activity, and locomotory behavior.

MiR-143 was upregulated both in stellate cells and in LII, where stellate neurons dominate, at all time points examined. ISH showed that miR-143 expression was high in stellate neurons, but far from exclusive to this cell type. Bioinformatics analysis of conserved, predicted targets of miR-143 with negatively correlated expression patterns revealed that the most likely targets of this miRNA in the MEC are the genes Lmo4, Tpm2, and Cachd1. We also looked closer at the miRNA that displayed the most significant upregulation in layers III-VI across all time points examined, namely miR-219-5p. Both ISH and bioinformatics analyses suggested involvement in oligodendrocytes and myelination for this miRNA, which is also known from other brain areas.

This work represented the first view of miRNA expression in the MEC, and showed the highly dynamic changes in miRNA expression during postnatal development of this area. Our work indicates that miRNAs do contribute to the laminar functional differences seen in the MEC.

Paper III

The EC has two regions, the MEC and the LEC, which differ with respect to morphology, connectivity, physiology, and memory function. The well-studied MEC is important for spatial memory, whereas the LEC seems to be important for odor and object recognition memory. To elucidate the molecular mechanisms behind these functional differences and their development, we analyzed the expression of coding and non-coding RNAs in rat MEC and LEC layers (LII vs. LDeep) at four different time points during postnatal development (P2, P9, P23, and P45).

We found that the expression of both coding and non-coding RNAs, as well as the level of alternative splicing, differed most between ages, then layers, and least between MEC and LEC. Most of the differences between regions lay in LII at most time points. Gene ontology enrichment analysis of differentially expressed mRNAs between regions yielded potentially important differences in neuromodulation, especially in expression of neuropeptides and their receptors, as well as the dopaminergic system. In addition, terms related to dendritic formation and ion transport were enriched in the regional contrast. Important laminar differences included extracellular matrix proteins, blood vessel formation, synaptic function, and ion transport. When looking at genes belonging to ontological categories relevant for EC function, including ion transport, plasticity, and memory, we found a laminar component for genes involved in long term depression and associative memory.

Using cell type specific gene signatures, we found a general regional upregulation of oligodendrocyte marker genes in MEC LDeep at P23/P45, and that oligodendrocyte marker

genes were generally enriched in LDeep (vs. LII). We also found a weak enrichment of ependymal cells in LEC. The gene signatures for cell types related to vascularization and the blood brain barrier (pericytes, astrocytes, microglia) were generally upregulated in LII (vs. LDeep).

Finally, analysis of genes dysregulated in Alzheimer's disease and schizophrenia revealed that genes upregulated in each of the two disesase tended to be upregulated in LII compared to LDeep. Similarly genes downregulated in Alzheimer's were also downregulated in LII (vs. LDeep), but the same was not the case for genes downregulated in schizophrenia. These findings point to a potential underlying molecular susceptibility for the laminar effect seen in these diseases.

This work represented the first thorough profiling of the LEC, and points to molecular aspects underlying the phenotypical differences seen between MEC and LEC and their layers. The data is available for others as an online resource for further study of the development and molecular properties of MEC and LEC.

DISCUSSION

In the current thesis we have used different transcriptomic methods to elucidate area differences within the hippocampus and the entorhinal cortex at specific time points during postnatal development at an RNA level. In all three papers we have used rats, which have long been the main model organism for the study of hippocampal and entorhinal functions. The presence of differentially expressed transcripts in all the contrasts examined indicates a molecular basis for the functional and morphological differences seen along the dorsal-ventral axis of the hippocampus and between layers and regions of the entorhinal cortex during postnatal development.

Common methodological considerations for papers I-III
The common methods shared between the papers in this dissertation have involved measurements of the transcriptome, with no *in vivo* follow-up studies to determine function of candidate RNA molecules in the hippocampus and the EC. Consequently, the contribution of this work to the research field is largely the generation of hypotheses that our group or others can test in the future. Tables of transcripts of interest for the different contrasts and typical expression profiles have been made available for use by the community.

During the course of this work, there have been great developments in transcriptomic methodologies. For instance, the use of microarrays and TaqMan arrays would now likely have been replaced by deep sequencing. Although the array technologies are sound and well established, we may have missed mRNAs or miRNAs for which there was no assay or probe on the arrays used. Also, the more limited dynamic range may have made it more difficult to detect differential expression among highly expressed transcripts. For miRNAs in particular, the members of certain miRNA families may differ by only one or two nucleotides, leading to potential cross-hybridization issues when using microarrays. The high cost of microarray and sequencing experiments restricts the number of samples possible. As there are great strides in development between P9 and P18/P23, the change in transcription between these two time points was particularly abrupt in our studies, missing much of the dynamics taking place.

The main source of study material in all three papers was tissue samples, which has the benefit of yielding high RNA concentrations when compared to the selection of fewer or single cells. The likelihood of the detection of lowly expressed transcripts is increased, but this approach only measures the average gene expression across all cells in a sample, and does not provide the profiles for the different cell types present, nor does it provide fine locational information. For instance, high expression of certain genes in rare cell populations will be detected as low levels. The localized enrichment of molecules, such as miRNAs, at specific synapses will also be missed. We can only detect large average changes between areas, and we miss any gradual changes across the tissue. Paper I has attempted to address the gradient problem by including the intermediate part of the hippocampal dorsal-ventral axis. In papers II and III, we were mostly interested in the special role of LII cells, and disregarded the known functional and molecular gradient present along the dorsal-ventral axis of the MEC (Giocomo, Hussaini et al. 2011; Giocomo, Moser et al. 2011; Stensola, Stensola et al. 2012; Ramsden, Surmeli et al. 2015). In addition, the boundary between MEC

and LEC has been reported to be gradual (Canto and Witter 2012), with possible implications for our findings in paper III.

For all three papers we used information from the Gene Ontology (GO) Consortium to deduce potential functional implications of our findings. Due to the time consuming nature of manual curation, most annotations in the GO are electronically inferred. Since the curated information is not weighted in our analysis, this creates a bias towards findings of lower quality. We could have limited this problem by only running the analysis against the curated results, but doing so would likely further increase the bias towards what has already been thoroughly studied. The databases are continuously updated, and this dynamic nature can change the results if an enrichment analysis is repeated at a different time point. Despite the extensive information available in the GO, not all genes have annotations. This is largely due to a bias in the research being conducted on genes and gene functions, where extensive work has been done on a small number of genes, whereas few or no studies have been done on the rest of the genes (Pandey, Lu et al. 2014). We also encountered this problem in our work, as several of the genes with the strongest regional or laminar expression patterns have no known function or no known brain function (Paper III). In summary, the findings from gene enrichment analysis point to possible functions for the gene list of interest, and may be a good tool to determine further hypotheses to test, but should not be considered proof.

Paper I
In paper I, we reported that the main features of the differentiation between the dorsal and ventral parts of the hippocampus were in place within the first postnatal week in the rat, including gross-anatomical, circuit, and transcriptional properties.

We first studied the anatomical development of the hippocampus, noting that the curvature changed at the ventral pole from P0 to P15. The length of the hippocampus also increased in this time window, likely due to neurogenesis in the dentate gyrus as well as the genesis of glia, axons, and dendrites (Bayer 1980; Encinas, Sierra et al. 2013; Semple, Blomgren et al. 2013). Myelination begins around P15 in the hippocampus (Meier, Brauer et al. 2004), and would thereby unlikely contribute to this volumetric change.

The entorhinal-hippocampal projections vary along the dorsal-ventral axis of the hippocampus, with the dorsal hippocampus receiving input from the dorsolateral part of the EC, and the ventral hippocampus from the ventromedial part of the EC (Witter, Wouterlood et al. 2000). Using retrograde and anterograde tracers, we confirmed that this connectivity pattern was present as early as P2/P3. The organization of the entorhinal-hippocampal projections is organized as a smooth gradient in adult animals (Strange, Witter et al. 2014), but our discretized injections at different locations did not allow for detection of a gradient in the younger animals.

While adult physiological and anatomical properties along the dorsal-ventral axis of the hippocampus are organized as a gradient, gene expression data indicate the presence of multiple subdomains with more definitive borders (Thompson, Pathak et al. 2008; Dong, Swanson et al. 2009; Strange, Witter et al. 2014). The latter is based on data from multiple ISH, which provide the possibility of more localized information than our dissections. The existence of multiple hippocampal subdomains along the dorsal-ventral axis is also largely

supported by recent *in situ* sequencing findings, although the subdomains appear not to be classified by single cell types, but rather distinct combinations of cell types (Shah, Lubeck et al. 2016). We generated expression data for the three main gene expression domains along the dorsal-ventral axis that have been found with ISH, although multiple subdomains within each domain exist. Due to our sampling method, the contribution from each subdomain would be evened out. Our unsupervised analysis of the data corroborated the three main domains, and showed that the distinction was present already at P0.

The enrichment analysis revealed an enrichment of Notch signaling at the dorsal end and nicotinic signaling at the ventral end of the hippocampus. Both of these play a role in LTP and in spatial learning and memory (Costa, Drew et al. 2005; Kutlu and Gould 2016), properties that vary along the dorsal-ventral axis (Strange, Witter et al. 2014). Genes involved in schizophrenia were enriched at the ventral end of the hippocampus. Interestingly, lesioning the ventral hippocampus at neonatal stages has been a widely used model of abnormal development in rodents relevant for schizophrenia-related studies (Brady 2016). Although volumetric differences have been reported in human posterior hippocampus (Strange, Witter et al. 2014), the greatest differences in anatomy and rates of metabolism between individuals with schizophrenia and controls have been reported in the anterior hippocampus (Small, Schobel et al. 2011). Our data show that dorsally, disease markers related to inflammation were enriched. While this could point to underlying susceptibility for diseases where inflammation is a key factor in the pathophysiology, it could also be related to the importance of the immune system in the homeostasis and function of the brain, including learning and memory (Marin and Kipnis 2013).

The focus of this paper was to find the time point during postnatal development at which the dorsal part of the hippocampus differed from the ventral part, as seen in the adult brain. As a consequence, we looked for genes that were consistently differentially expressed between dorsal and ventral hippocampus at all time points. The data analysis therefore differed from that in papers II and III, as we did not analyze the dynamic changes across time points, but rather similarities. This premise excludes any conclusion about developmental changes, unless the data were to be reanalyzed in another manner. However, several gene expression studies of whole hippocampus at postnatal time points have already been conducted, including for rat (Stead, Neal et al. 2006) and mouse (Mody, Cao et al. 2001). From the methods used, we could conclude that gene expression varies mostly according to age (explaining 56% of the variation in the data) and that the number of differentially expressed genes along the dorsal-ventral axis was highest at P18. The latter indicating highly dynamic events at this time point with probable importance for the dorsal-ventral differentiation of the hippocampus, and corresponding with maturation of spatial and emotional properties (Semple, Blomgren et al. 2013).

Paper II

Methodological considerations
Paper II focused on the role of miRNAs in the laminar and cellular differences in the MEC. We also investigated their role in MEC development. Our methods included miRNA and mRNA expression measurements of MEC layers at postnatal ages P2, P9, P23, and P45, as well as miRNA measurements of FACS-sorted retrogradely labeled stellate as well as non-stellate

cells. Having both mRNA and miRNA expression data for the laminar samples allowed bioinformatics analyses to find likely target genes for the laminar miRNAs. We verified the expression of the most significant laminar miRNAs with ISH.

Transcriptomic data can be analyzed with both supervised and unsupervised methods, and to analyze the spatiotemporal miRNA expression data in Paper II we used both. The supervised approach involved grouping the samples according to laminar identity at each time point, and analyzing for miRNAs differing in expression between layers. This was in line with our interest in the contributions of miRNAs to laminar differences in the MEC. Unsupervised approaches allow the data to drive the analysis, and in addition to the miRNAs with laminar expression profiles from the supervised analysis, this method also yielded information about miRNAs with combined developmental and laminar profiles. The miRNAs with developmental profiles were in majority compared to the laminar miRNAs, as has been seen in other parts of the brain (Fertuzinhos, Li et al. 2014).

MiRNA profiling of stellate cells was achieved using FACS to sort cells from dissociated tissue. FACS is a suitable way of sorting fluorescent from non-fluorescent cells, and we used it to sort retrogradely labeled stellate neurons that project to the hippocampus from surrounding MEC cells. While FACS does not notably affect the transcriptome in cells from other tissues, sorting can be stressful to mature neurons (Arlotta, Molyneaux et al. 2005; Richardson, Lannigan et al. 2015). In addition, the procedure requires dissociation of the tissue by enzymatic and physical means, which can be stressful to the cells and thereby induce stress-related transcription (Richardson, Lannigan et al. 2015). However, with optimized dissociation and the use of live/dead stains, successful cell type specific transcript measurements can be obtained (Lobo, Karsten et al. 2006).

Paper II had a special focus on miRNA expression. While miRNA expression levels are easy to detect, it is challenging to ascertain their particular function. The number of validated miRNA targets is still low, and this necessitates the use of prediction tools. While several programs exist for miRNA target prediction, TargetScan was chosen due to its good performance in comparison with *in vivo* data (Witkos, Koscianska et al. 2011). We focused on predicted conserved targets, as evolutionary conservation increases the likelihood of the target site having biological function. The probability of obtaining a list of real target genes for our miRNAs of interest was further increased by the requirement of negative correlation for miRNA-target gene expression patterns, as decreased mRNA levels is a common consequence of miRNA regulation (Pasquinelli 2012).

There are several weaknesses with our approach of only including target mRNAs with negatively correlated expression patterns. First, this approach does not detect the instances where the miRNA-mediated repression is only at the protein level without reduced mRNA levels, although this is a rare occurrence (Guo, Ingolia et al. 2010). Second, our disregard of all potential targets with positively correlated expression levels could have led us to miss some potentially important target mRNAs, although such targets are less common than those with negatively correlated levels (Fabian, Sonenberg et al. 2010). Third, miRNAs could have different roles in different cell types under different conditions, and it is thereby not certain that the few validated targets included in the analyses we conducted for paper II were targets in rat MEC.

In addition, the target predictions from TargetScan only contain predicted targets that follow the miRNA target prediction rules, focusing on the 3'UTR (Agarwal, Bell et al. 2015) and potentially missing target sites in the coding sequence (Xu, San Lucas et al. 2014). HITS-CLIP and CLIP-seq studies, which are used to determine bona fide miRNA targets, have shown that non-conventional target sites and target sites in the coding sequence are more common than previously thought, although most exhibit modest, if any, repression of their targets (Pasquinelli 2012; Seok, Ham et al. 2016). The identification of bona fide mRNA targets for our differentially expressed miRNAs would require HITS-CLIP analyses conducted on MEC tissue extracts, combined with *in vivo* genetic methods to ascertain actual regulation and function (Pasquinelli 2012). It is also possible to use luciferase reporter-3'UTR constructs with original and mutated sites (Thomson, Bracken et al. 2011).

Potential function of miR-143 in the nervous system
Our clearest finding from paper II was the enrichment of miR-143 in stellate and other neurons. We identified enrichment of miR-143 expression in stellate neurons sorted by FACS and by dense staining of stellate and other neurons with ISH when using a probe against miR-143. Our *in silico* functional analyses of the predicted, conserved and negatively correlated target genes of miR-143 indicated its potential role in neurons. MiR-143 has mostly been studied in relation to vascularization and tumor suppression (Almeida and Calin 2016), since the only obvious effects of its knock out were on vascular smooth muscle cell differentiation (Elia, Quintavalle et al. 2009; Xin, Small et al. 2009). The effect of the knockout seems more profound after stress exposure, both in vascular cells (Xin, Small et al. 2009) and the intestine (Chivukula, Shi et al. 2014). The knock out studies do not report examination of the brain, although Elia *et al.* noted that the knock out mice were viable with no obvious disorders (Elia, Quintavalle et al. 2009). The lack of an obvious phenotype is common in miRNA knock out studies (Vidigal and Ventura 2015).

With regards to a potential function for miR-143 in the nervous system, Edbauer *et al.* (2010) found that miR-143 had no effect on dendrite formation or plasticity on cultured hippocampal neurons (Edbauer, Neilson et al. 2010). Jovicic *et al.* reported astrocyte enrichment of miR-143 (Jovicic, Roshan et al. 2013). Other roles for miR-143 include glycolysis (Fang, Xiao et al. 2012; Xu, Liu et al. 2016), AKT/mTOR pathway (Fang, Xiao et al. 2012; Banerjee, Kim et al. 2016), and regulation of extracellular matrix proteins (Li, Li et al. 2014; Li, Zhang et al. 2014), with possible implications for neuronal functions. The extracellular matrix protein Versican is a validated target of miR-143 (Wang, Hu et al. 2010). Versican is localized to large projection neurons, and its isoforms have known roles in neuron differentiation, neurite formation, and synapse regulation (Horii-Hayashi, Okuda et al. 2008). A known target of miR-143 in intestinal mesenchymal cells is IGFBP5 (Chivukula, Shi et al. 2014), which is also known to be upregulated in Alzheimer's disease (Barucker, Sommer et al. 2015) and whose upregulation causes degeneration of axons (Simon, Rauskolb et al. 2015). Curiously, in a study by Barucker et al. (2015), addition of soluble Amyloid β-42 to neuroblastoma cells was shown to induce both the IGFBP5 gene and the Lmo4 gene (Barucker, Sommer et al. 2015), which was our prime candidate as target gene for miR-143 in the MEC.

Sparse reports of more specific findings for miR-143 neuronal functions do exist. A recent study showed regulation of Notch signaling by miR-143 during neuron differentiation in primates, and that miR-143 levels increased during differentiation (Rani, Nowakowski et al. 2016). Rani *et al.* also showed that overexpression of miR-143 in SHSY5Y cells led to the growth of axon- and dendrite-like processes. Further, miR-143 was upregulated in synaptoneurosomes at terminal stages of neurodegenerative prion disease (Boese, Saba et al. 2016). miR-143 was also detected in a subset of dorsal root ganglion neurons in the peripheral nervous system, where its expression was sensitive to the induction of inflammation *in vivo* (Tam Tam, Bastian et al. 2011). Quaranta *et al.* (2016) identified miR-143 as a regulator of β-dystrobrevin (Quaranta, Spinello et al. 2016), a repressor of synapsin I, which is involved in glutamatergic neurotransmission and hippocampal spatial memory (Gomez-Pinilla, So et al. 2001; Bogen, Jensen et al. 2011; Qiao, Peng et al. 2014). Taken together, these findings point to multiple neuronal functions for miR-143, including a role in glutamatergic neurons, of which the stellate neurons are an example.

In addition, miRNAs may have differing functions in different locations and cell types. Our findings point to the Lmo4 gene as a likely target for miR-143 in the MEC, making it possible that the posttranscriptional regulation of this gene is an important function of miR-143 in the MEC. The Lmo4 gene does have a known role in brain development and neuron differentiation, and has been implicated in hippocampal spatial learning (Azim, Shnider et al. 2009; Qin, Zhou et al. 2012; Cederquist, Azim et al. 2013). The ISH results indicated lower expression of miR-143 in LEC, where Lmo4 expression is higher than in MEC LII, making the high miR-143 and low Lmo4 expression in MEC LII potentially more intriguing. Other highly likely target genes of miR-143 in the MEC included Tpm3 and Cachd1. A known function of Tpm3 is in neuronal shaping (Schevzov, Bryce et al. 2005). Cachd1 has not been studied to date, but is a possible calcium channel regulatory protein, and could thereby influence physiology in MEC cells. All the most likely targets of miR-143 in the MEC thereby have known or likely roles in the brain.

Potential functional contributions from other laminar miRNAs
We also studied miR-219-5p more closely, chosen because it was the most significantly upregulated miRNA in LDeep. This miRNA has a known function in oligodendrocyte maturation and myelination (Zhao, He et al. 2010), which according to our results also appears to be its main function in the MEC. The ISH results showed expression in ependymal cells, oligodendrocytes and glia, and the most likely target genes in the MEC were all involved in oligodendrocyte differentiation and myelination. Known target genes of miR-219-5p displayed negative correlated expression patterns with the miRNA in the MEC, which indicated that these indeed are targets of miR-219-5p also in this brain region. Another miRNA upregulated in LDeep, miR-338, is also known to play a role in oligodendrocyte differentiation (Barca-Mayo and Lu 2012). Together with the general upregulation of oligodendrocyte protein-coding genes in LDeep we saw in paper III, these findings indicate an enrichment of oligodendrocytes in MEC LDeep.

The other laminar miRNAs may also contribute to differences in MEC layers. Some are involved in neuronal differentiation and function, like miR-26b (upregulated LII; (Dill, Linder et al. 2012)) and miR-7a/b (upregulated LDeep; (Horsham, Ganda et al. 2015)), and could thereby contribute to laminar neuronal subtype specialization. We also noted that some of

the laminar miRNAs are known to be differentially expressed in Alzheimer's disease and schizophrenia, which opens the possibility that these miRNAs contribute to the laminar susceptibility to these diseases in the MEC. Higher miR-26b expression induces a similar cellular phenotype as seen in Alzheimer's disease, with tau phosphorylation and apoptosis (Absalon, Kochanek et al. 2013), while miR-126 increases susceptibility to amyloid beta (Kim, Noh et al. 2016). In the case of miR-146a, it is known that higher expression causes an inflammatory gene expression profile (Femminella, Ferrara et al. 2015), which contributes to Alzheimer's disease pathogenesis (Heppner, Ransohoff et al. 2015). In the case of susceptibility for schizophrenia, miR-7 was found to regulate Shank3, a postsynaptic density protein which is involved in neuronal spine and synapse development (Zhang, Sun et al. 2015), of relevance due to the morphological abnormalities reported in affected brains (Arnold 1999). The role of miR-219 in schizophrenia may be a little earlier in development, as elevated levels inhibit neuronal stem cell proliferation, which fits with proliferative defects seen in schizophrenic patients (Murai, Sun et al. 2016).

Contributions of miRNAs to MEC development
In addition to our analysis of laminar and stellate enriched miRNAs, the inclusion of the four time points for the tissue profiling allowed identification of miRNAs that increase or decrease in expression from P2 to P45, and that are of potential importance for fine tuning of developmental processes in the MEC. We addressed the potential functions of developmental miRNAs in the unsupervised analysis, where the two main modules had clear developmental profiles with opposite expression patterns.

Our main findings were that the negatively correlated target genes of miRNAs increasing in expression from early (P2/P9) to late (P23/P45) time points were enriched in cell cycle, neuron differentiation and projection, and synapse organization terms. During the first few weeks of postnatal development there is extensive gliogenesis, which would involve the expression of cell cycle genes. Neurons are still stubby in early postnatal development, and there is extensive dendritogenesis and axonogenesis in this time period. Although we confirmed the presence of perforant path fibers at P2/3 in paper I, the branching density is known to increase until P10 (Deng, Yu et al. 2007), and these arise from EC LII. There is also extensive synaptogenesis in this time period, peaking in week 2 (Semple, Blomgren et al. 2013).

For the miRNAs decreasing in expression from early (P2/P9) to late (P23/P45) time points, the negatively correlated target genes were enriched in neuron differentiation, synaptic transmission, ion channel activity, myelination, learning and plasticity, and locomotory behavior. Neuronal function continues to mature in postnatal development, with synapse specialization and changes in the types of ion channels that are expressed (Moody and Bosma 2005; Semple, Blomgren et al. 2013; Jiang and Nardelli 2016). The different types of oscillations arising from neuronal network activity mature substantially from P8 and on (Wills and Cacucci 2014). Neuronal myelination begins around P10, correlating with the respective drop and sharp rise in the expression levels of miRNAs and genes involved in myelination between P9 and P23 in our data. Eye opening, open field exploration, maturation of spatial neurons, and onset of hippocampal-dependent learning also begins before P23. The high expression levels of miRNAs targeting genes involved in processes related to such functions

at P2/P9 could indicate that the miRNAs function as brakes on the expression levels of these genes in early postnatal development.

Overall, our work in paper II revealed the dynamics of miRNA expression in MEC layers at four postnatal time points, as well as how miRNA expression in neonatal stellate neurons compared to other MEC cells. Bioinformatic analysis of predicted target genes with negatively correlated expression pattern to our miRNAs of interest pointed to likely functions of the miRNAs. Our findings of likely roles of miRNAs in the MEC across the time points measured fit with maturational processes in the rest of the brain, and indicated the regulation of MEC development by miRNAs.

Paper III

Methodological considerations
Paper III provided a transcriptomic study of MEC and LEC LII and LDeep at four different postnatal time points (P2, P9, P23, and P45). Our use of ribosome-depleted RNA sequencing allowed the identification of both polyadenylated and non-polyadenylated RNA species. Although sequencing methods may include most transcripts in a sample, the commonly used analysis pipelines will only yield counts according to the provided annotation file. Here we used rats, and the rat transcriptome is still not as well annotated as that of the mouse (Yu, Fuscoe et al. 2014). Also, our use of the RefSeq annotations for the mRNA data set used in Papers II and III may have caused us to miss some transcripts, especially those that may be more particular to the rat. On the other hand, the RefSeq annotations are of higher quality and include the more widely expressed, conserved genes, increasing the likelihood that our findings also have relevance for other species. LncRNAs are not as well annotated for rats as for humans and mice, organisms thoroughly studied through the GENCODE project (Harrow, Frankish et al. 2012; Mudge and Harrow 2015). We therefore conducted de novo analysis of lncRNAs, and also identified several protein coding genes that are annotated in other species.

As in paper II we used both supervised and unsupervised approaches to analyze the data, but in addition we also used analysis of variance (ANOVA) on gene lists of interest to discern statistically significant global differences in expression levels between ages, layers and regions. The ANOVA test is well-established for gene expression studies when simultaneous comparing of the means of several groups, which was our case. However, ANOVA also assumes independence between genes and between samples, which was not the case for our data, as we used RNA-seq to do parallel gene measurements within samples. Moreover, we used ANOVA to analyze gene lists with varying number of genes. As significance depends on number of observations, the ANOVA p-values were not necessarily directly comparable between different gene lists. We have attempted to alleviate this weakness by choosing the conservative Bonferroni correction method to adjust for the number of lists tested. Moreover, we also reported the estimated expression differences between ages, layers, and regions, which are independent of sample size and therefore can be used to compare these effects between gene lists.

For the main analysis we used the moderated t-test in limma and analyzed differential expression of pairwise contrasts, and found the highest number of differentially expressed protein coding genes between time points, then between layers, and finally between

regions. The higher variation between developmental time points compared to between brain regions have been observed by others (Fertuzinhos, Li et al. 2014), and could be due to the complex mechanisms required for the precise spatiotemporal proliferation, differentiation, and connectivity required for the development of a functional brain. Interestingly, unlike for protein coding genes, the numbers of differentially expressed lncRNAs were similar in the two regional contrasts, indicating an important role in regional differences. There are several examples of lncRNAs participating in neuronal differentiation, synaptogenesis and synaptic plasticity (Briggs, Wolvetang et al. 2015), inviting the possibility of importance for EC functions.

Potential molecular contributions to functional differences between MEC and LEC

Although we found few differences in protein coding gene expression between MEC and LEC, we identified several key genes that could explain the observed differences between the regions, particularly in LII. We also looked into potential drivers of these differences (i.e. transcription factors), of which a majority were involved in dopaminergic signaling. Several of the transcription factors also have effects on spatial and object recognition memory, potentially driving the molecular mechanisms behind the memory dichotomy between MEC and LEC. Few genes have been found to display absolute differences between brain regions (Valor and Barco 2012), which was also the case for the number of genes with absolute expression differences between EC layers and regions. However, we did identify some genes, several of which are currently uncharacterized (e.g. Ccdc129, Cd300e).

The clearest functional difference between MEC and LEC seemed to be in neuropeptide signaling, which was enriched in LEC. Neuropeptides have versatile roles in the brain (Ogren, Kuteeva et al. 2010), including learning and memory and locomotion, which are of relevance to the EC. Neuropeptides generally exert their effect through G-protein coupled receptors, which results in a prolonged effect on neuronal properties, like membrane excitability, transcription, and neurotransmitter release. The neuromodulatory role of neuropeptides on glutamatergic and GABAergic neurons in the hippocampus is well known from physiological and behavioral studies. The lateral perforant path originating in the LEC is regulated by opioid neuropeptides (specifically enkephalin), while the medial perforant path originating in the MEC is regulated by cholecystokinin (Fredens, Stengaard-Pedersen et al. 1984). Each of the two neuropeptide systems is important for LTP induction in the hippocampus (Bramham, Errington et al. 1988; Bramham, Milgram et al. 1991; Bramham, Milgram et al. 1991), which indicates their involvement in memory formation. In addition, neuropeptide S has been hypothesized to contribute to spatial learning and memory due to expression in areas with efferent and afferent hippocampal projections, including the deep layers of the LEC (Xu, Gall et al. 2007).

Our data expands on earlier molecular findings, with one additional neuropeptide type (the CART prepropeptide) and several other types of neuropeptide receptors (glycine, galanin, neuromedin B (aka Bombesin), neuropeptide S, neuropeptide Y and QRFP) being upregulated in LEC compared to MEC. Most of the neuropeptide types in question have established effects on spatial memory, including galanin (Rustay, Wrenn et al. 2005), neuropeptide S (Xu, Gall et al. 2007), neuropeptide Y (although a limited effect, (Borbely, Scheich et al. 2013)), CART (Upadhya, Nakhate et al. 2011), and neuromedin B (Yang, Yao et al. 2017). However,

this does not necessarily mean that the neuropeptide receptors also are directly involved in spatial memory. A mouse knock out of Galr1 did not appear to affect spatial or olfactory memory (Rustay, Wrenn et al. 2005), although it has an effect on aversive memory (Ogren, Kuteeva et al. 2010). Interestingly, the CART peptide, neuropeptide S, and neuropeptide Y also affect object recognition memory in the hippocampus (Redrobe, Dumont et al. 2004; Okamura, Garau et al. 2011; Bharne, Borkar et al. 2016). All neuropeptides are also involved in energy homeostasis and feeding behavior (Beck and Pourie 2013; Primeaux, Barnes et al. 2013; Lau and Herzog 2014; Valsalan and Manoj 2014; Gajjar and Patel 2017).

Since most of these upregulated neuropeptide related genes are receptors, this opens up for modulation of EC neurons by neuropeptides, a plausible scenario due to the widespread roles of neuropeptides in most brain areas and the previously known importance of neuropeptides for the two regions. MEC and LEC neurons would thereby be modulated in different manners due to the likely differences in neuropeptide receptor densities present. The neuromodulation of neuromedin B on EC LIII GABAergic interneurons has already been described (Zhang, Xiao et al. 2014).

Potential molecular contributions to functional differences between layers
With respect to laminar differences, we found it curious that the genes upregulated in LII were not overrepresented among any neuron-related terms, as could be expected according to the laminar phenotype properties. However, the genes upregulated in LDeep were indeed enriched in neuron-related terms. In addition, we found an array of single genes upregulated in LII that could be the basis for the observed differences, including several transcription factors, channel proteins, and synapse-related genes.

Although the most enriched terms for genes upregulated in LII (extracellular matrix and angiogenesis) are not directly brain-specific terms, they are of high importance for brain function. The brain capillary system provides nutrients and oxygen to the brain cells for proper functioning. The EC has a dense vascular network, receiving blood input from both posterior and middle cerebral arteries (Stranahan and Mattson 2010). A few weeks after birth a phenomenon of increased cerebral blood flow following neural activity matures in the brain (Lacoste and Gu 2015), with possible implications for EC LII neurons due to the seemingly higher density of vascular cells present in this layer according to our data. Our findings in paper II also showed enrichment of ontology terms related to blood vessel development for conserved, predicted target genes of laminar miRNAs (Olsen, O'Reilly et al. 2017). Laminar differences in vascularization is supported by the findings of Michaeloudi et al. (2005) (Michaloudi, Grivas et al. 2005), who reported interlaminar differences in maturity and density of capillaries in the LEC. Solodkin and Van Hoesen (1996) also reported a "uniquely arranged blood supply" in EC LII (Solodkin and Van Hoesen 1996). They and others have speculated as to whether LII cells have higher energy demands (Ramsden, Surmeli et al. 2015), which could potentially require increased vascular nutrient supply. A higher density of vascular cells could also contribute to the vulnerability of LII neurons to neurodegenerative disease, as this has been linked to vascular dysfunction (Zhao, Nelson et al. 2015). The role of pericytes, whose marker genes were overall highly upregulated in LII in our data, may be of particular importance for Alzheimer's disease pathogenesis (Winkler, Sagare et al. 2014).

The extracellular matrix is more than just support structure for brain cells, as it has important roles in development and plasticity, including proliferation, migration, axon guidance, and synapse formation and function (Barros, Franco et al. 2011). A special part of the extracellular matrix, the perineuronal net (PNN), has even been hypothesized to be the substance for long term memory storage (Tsien 2013). Several of the genes we found upregulated in LII that were enriched in the extracellular matrix category are involved in linking (Hapln genes) and modifying (matrix metalloproteinases and ADAMTS proteoglycanases) the PNNs (Wang and Fawcett 2012), indicating differences in PNN structures between layers. MEC LII stellate neurons are interconnected by parvalbumin positive (PV+) GABAergic interneurons, a network model that has been proposed as a mechanism for grid cell function (Beed, Gundlfinger et al. 2013; Couey, Witoelar et al. 2013). The PNNs have been found to colocalize largely with PV+ interneurons in other brain areas (Kwok, Dick et al. 2011), which opens the possibility for importance in grid cell function. PNN has also been found to surround highly active neurons.

Interestingly, the extracellular matrix, in particular the PNN, has been implicated in Schizophrenia, epilepsy, and Alzheimer's disease (Bonneh-Barkay and Wiley 2009; McRae and Porter 2012), and could contribute to the laminar effects seen in these diseases in the EC. Inflammatory genes were also enriched amongst genes upregulated in LII, and inflammation has been shown to be an important factor in schizophrenia and Alzheimer's disease (Wyss-Coray and Rogers 2012). Another potential contribution is the LII enrichment of marker genes for microglia, astrocytes and pericytes – cell types important for Alzheimer's pathologenesis (De Strooper and Karran 2016).

To further explore molecular aspects that could underlie the laminar differences in susceptibility to Alzheimer's disease and schizophrenia, we looked into gene expression patterns of genes differentially expressed between brains of healthy and diseased individuals. These lists were obtained from human studies, and are thereby not necessarily relevant for rat brain function. In addition, the differences in gene expression levels do likely not point to any cause, but could very well be due to a disruption of molecular equilibrium or the effect of some other causal aspect. Nevertheless, we found that genes upregulated in Alzheimer's disease and schizophrenia tended to be upregulated in LII, and genes downregulated in Alzheimer's disease tended to be downregulated in LII. Whether these laminar genes indeed are involved in EC vulnerability to disease remains to be seen, but based on these results as well as differential laminar expression for genes involved in processes known to be involved in disease pathogenesis, there does seem to be a molecular basis for the susceptibility of the EC to these diseases.

Potential molecular contributions to the development of EC functions
The expression of all classes of RNAs studied in the hippocampus and the entorhinal cortex was most dynamic between P9 and P18/P23, corresponding with the great strides in development during this time span. Our findings using GO enrichment analyses of genes differentially expressed between early and late time points and ANOVA analyses of cell type markers and GO categories indicate that the postnatal development of the EC is largely similar to the development of the rest of the brain. Genes involved in gliogenesis, myelination, neuron projection formation, ion transport, synaptic plasticity and potentiation, and memory formation displayed great increases in expression levels between P9 and P23,

correlating with the maturation of these processes. However, the time points we measured were limited, so we could not determine whether developmental processes occurred at different ages compared to the rest of the brain.

Grid cell maturation also occurs during the time span measured. Interestingly, we noted the largest number of genes differentially expressed between MEC layers at P23, perhaps pointing to highly dynamic processes in LII at this time point. In addition, genes involved in locomotory behavior showed a significant increase in expression from early to late time points, plateauing at P23. These genes could therefore contribute to maturation of EC spatial memory. However, there was no significant laminar or regional component when the locomotory behavior genes were viewed overall, which could be due to the cancellation effect mentioned above, or because the laminar and regional differences lie in a smaller number of genes. In addition, although locomotory behavior has been used as a measure for spatial memory, the genes in this list are included mostly based on findings elsewhere in the brain, and may also not be of relevance to the EC. However, the presence of many dopaminergic genes in this category point to potential importance for the EC, as the dopaminergic input to the EC has been known for some time (Akil and Lewis 1993). Dopaminergic innervation to the superficial layers of LEC is particularly dense (Cappaert, Strien et al. 2015), and dopamine has been shown to suppress synaptic transmission in LEC LII fan cells (Caruana and Chapman 2008). In addition, the dopaminergic system is important for both spatial and object recognition memory in the hippocampus (McNamara, Tejero-Cantero et al. 2014; Yang, Broussard et al. 2017), and may therefore also be involved in similar functions in the EC.

Looking at the expression of Hcn channels in our data could also provide clues to grid cell maturation. The Hcn1 channel is known to influence grid cell firing, as gene knock out leads to loss of modular spacing along the dorsal-ventral axis of the MEC (Giocomo, Hussaini et al. 2011). Our findings showed that Hcn1 expression increases across time points, reaching a stable level at P23, which coincides with grid cell maturation around P20/P22 (Langston, Ainge et al. 2010). The importance of this gene for MEC LII cells is underscored by the lower expression level in LEC LII. In addition, we also identified a shift in Hcn family expression levels across time points, with Hcn3 and Hcn4 dominating at P2 and P9, and Hcn1 and Hcn2 dominating at P23 and P45, with potential importance to the maturation of firing properties of EC neurons. The shift from Hcn3/4 to Hcn1/2 during postnatal development is also known from the hippocampus (Boehlen, Heinemann et al. 2010).

Less is known about the development of LEC functions, although short term object location memory emerges around P21, with long term retention from P26 (Ramsaran, Sanders et al. 2016; Ramsaran, Westbrook et al. 2016). We found that genes involved in associative memory (of which object location memory is a type) are significantly upregulated at later time points, indicating importance for maturation. In addition, we found several single genes with laminar and regional differential expression belonging to memory and plasticity gene categories that were involved in object recognition memory, including Gpr37, Nr4a2, and Rgs14 (Lopez-Aranda, Lopez-Tellez et al. 2009; McNulty, Barrett et al. 2012; Lopes, Morato et al. 2015). Of these, the Nr4a2 gene may be of particular importance, as it is an immediate early gene and a transcription factor.

Overall, the data set generated in paper III allowed for the exploration of the molecular basis for the differences in functions and phenotypes seen between layers and regions in the EC. In particular, it points to neuromodulation by neuropeptides as a molecular source of difference between LEC and MEC and thus their inputs to the HF.

FUTURE PERSPECTIVES

This work provides a basis for further investigation of the types of molecular differences and their effect on the functional differences between LEC and MEC and between the EC layers, as well as along the dorsal-ventral axis of the HF. Future work should increase the resolution of the profiling, and investigate the expression of RNAs at a single cell level. This is now possible due to the great strides that have been made in the later years with respect to single cell sequencing technology (Ziegenhain, Vieth et al. 2017). Such profiling can be used to arrive at representative profiles for each cell type (i.e. neurons, astrocytes, oligodendrocytes, microglia and their subtypes) using clustering approaches (Zeisel, Munoz-Manchado et al. 2015), and also to investigate how these profiles change during development. The findings can be used further to characterize the molecular properties of the spatially tuned cells, and to investigate whether these cell types correspond to the known morphological cell types in the EC. Another option is to profile cells in litter mates with and without spatial learning (e.g. Morris water maze) or object location learning to identify molecules and pathways important for learning in EC cells. With respect to the molecular basis for grid cell development, it would be useful to profile single LII neurons at closer time intervals, for instance from right before the time the rats begin exploring their environment until the age they display stable grid cell function.

Single cell sequencing has already been done in the hippocampal CA1 region (Zeisel, Munoz-Manchado et al. 2015; Harris, Gonzales et al. 2017), although the analysis of differences in molecular profiles of cell types along the dorsal-ventral axis has yet to be explored. Recently, the technology has also been adapted for single cell sequencing of miRNAs (Faridani, Abdullayev et al. 2016). Previously, profiling of miRNAs in single cells could be accomplished by qPCR, which included the possibility of multiplexing. Traditional single cell sequencing does not provide locational information, but there are new methods allowing RNA sequencing while retaining locational information (e.g. fluorescence *in situ* RNA sequencing, (Lee 2017)). However, further development is required for these methods to yield high quality results. Traditional ISH can be used to obtain locational information on single RNA molecules of interest, and can also be used to validate interesting findings.

In addition to obtaining a cellular resolution of the transcriptome, it would be interesting to zoom in further to profile the synaptosomes. MiRNAs are known to be enriched in at or near synapses, where they have been found to modulate and be modulated by synaptic activity and plasticity (Smalheiser 2014). Profiling of purified synaptosomes, both of smaller and larger RNA species, may provide quite a different picture than the bulk profiling that was done in this work.

Further profiling still only generates new hypotheses as to which molecules are important for EC development and function. For a proper determination of the role of interesting candidate RNA molecules in the entorhinal cortex, functional studies would be required. It would be interesting to test the effect of knock-out (e.g. CRISPR technology) or knock-down (e.g. antagomirs, siRNAs) of candidate RNAs on object-related or spatial memory, or at the more basic level of electrophysiology. Of particular interest is the elucidation of whether our most validated candidate miRNA, miR-143, indeed has a specific function in neurons in addition to its known function in blood vessels, and whether this function entails the

regulation of Lmo4 expression. Determination of function could be accomplished by injecting an antagomir or a miRNA sponge for miR-143 into the entorhinal cortex, and subsequently observing any effects on spatial learning or to examine effects on gene expression levels. A knock-out mouse model of miR-143 already exists (Elia, Quintavalle et al. 2009; Xin, Small et al. 2009), and it would be interesting to examine these mice for phenotypes related to CNS function, particularly for grid cell firing and spatial memory.

Identifying the mRNA targets of a miRNA is also important when deducing its function. There is an array of techniques available for the purpose of finding high confidence targets and the effect of miRNAs on these targets (Steinkraus, Toegel et al. 2016). The identification of real targets could be achieved through CLIPseq methods (Moore, Zhang et al. 2014). The introduction of miRNA sponges or antagomirs *in vivo* across developmental transitions could shed light on the biological function of the miRNAs during the time span tested (Steinkraus, Toegel et al. 2016). Alternatively, the miRNA seed site or the miRNA recognition element in a target gene of interest through CRISPR/Cas9 editing could infer permanent loss of function, and the effect of this loss of function could be studied.

The dataset in paper III has also yielded several candidate lncRNAs with unknown functions. It is likely that several of the lncRNAs are involved in regulating transcription, in particular the ones that are encoded antisense to genes (Quinn and Chang 2016). There are examples of lncRNAs with functions in processes of relevance to laminar and regional EC differences, such as neuron differentiation, synaptogenesis, and plasticity (Briggs, Wolvetang et al. 2015). In addition, there are examples of lncRNAs contributing to the pathology of Alzheimer's disease and Schizophrenia. Potential functions of differentially expressed lncRNAs could be investigated by CRISPR/Cas editing in the lab by *in vitro* or *in vivo* methods. It is also possible that some of these molecules could elicit a sponging effect on miRNAs, as examples of both lncRNAs and circular RNAs with this function exist (Steinkraus, Toegel et al. 2016). In silico work could identify candidate sponges based on the presence of miRNA recognition sequences, and the function of such candidates could be further investigated in the lab.

This work deals only with the transcriptome, and has disregarded the proteome. For interesting protein-coding RNA molecules, immunohistochemistry may be an appropriate alternative to ISH. However, the method requires the existence of a good antibody against the protein in question. An alternative method to study the proteome is mass spectrometry, although it does not provide locational information. Both immunohistochemistry and mass spectrometry could be used to find out whether the differences in extracellular matrix genes between EC layers also can be seen at the protein level (Dauth, Grevesse et al. 2016). Several new methods are arising to study the proteome in the brain, including the very important adhesion and synaptic proteins that are important for the function of individual brain cells as well as the formation and function of brain circuits (Schreiner, Savas et al. 2017). One example of an interesting possibility is the metabolic labeling of newly synthesized proteins in mice through the introduction of stable, heavy isotopes in the diet, combined with methods for fluorescent labeling specific synapse types (e.g. knock in or viral transduction). Synaptosomes can then be purified using fluorescence activated sorting, and the proteome examined with mass spectrometry. Such methodology could be used to examine synapses of interest, for instance whether the proteins in glutamatergic or GABAergic synapses differ between MEC and LEC.

Perhaps one of the most important findings in this work is the discovery that the function and modulation of individual synapses appear to be the most important differences between LEC and MEC. Particularly, the modulatory properties have implications for the circuitry involving LEC and MEC, although the regional differences for some neuropeptides have been known for decades (Loren, Alumets et al. 1979; Stengaard-Pedersen 1983). Antagonists for many of these substances are available, and their effect could be tested on LII principal cell physiology, spatial or object cell physiology, principal cell transcriptome, and perforant path function could be tested.

The transcriptional data provided in this work has generated many new hypotheses, and may be used to generate more hypotheses in the future. We only managed to touch upon a few aspects that may be of interest to EC and HF function and development in this work, but hopefully these resources can be useful for others in the quest to unravel the properties of these important brain regions.

REFERENCES

Abellan, A., E. Desfilis, et al. (2014). "Combinatorial expression of Lef1, Lhx2, Lhx5, Lhx9, Lmo3, Lmo4, and Prox1 helps to identify comparable subdivisions in the developing hippocampal formation of mouse and chicken." Front Neuroanat **8**: 59.

Absalon, S., D. M. Kochanek, et al. (2013). "MiR-26b, upregulated in Alzheimer's disease, activates cell cycle entry, tau-phosphorylation, and apoptosis in postmitotic neurons." J Neurosci **33**(37): 14645-14659.

Agarwal, V., G. W. Bell, et al. (2015). "Predicting effective microRNA target sites in mammalian mRNAs." Elife **4**.

Aird, D., M. G. Ross, et al. (2011). "Analyzing and minimizing PCR amplification bias in Illumina sequencing libraries." Genome Biol **12**(2): R18.

Akil, M. and D. A. Lewis (1993). "The dopaminergic innervation of monkey entorhinal cortex." Cereb Cortex **3**(6): 533-550.

Aksoy-Aksel, A., F. Zampa, et al. (2014). "MicroRNAs and synaptic plasticity--a mutual relationship." Philos Trans R Soc Lond B Biol Sci **369**(1652).

Alliot, F., I. Godin, et al. (1999). "Microglia derive from progenitors, originating from the yolk sac, and which proliferate in the brain." Brain Res Dev Brain Res **117**(2): 145-152.

Allison, S. L., A. M. Fagan, et al. (2016). "Spatial Navigation in Preclinical Alzheimer's Disease." J Alzheimers Dis **52**(1): 77-90.

Allocco, D. J., I. S. Kohane, et al. (2004). "Quantifying the relationship between co-expression, co-regulation and gene function." BMC Bioinformatics **5**: 18.

Almeida, M. I. and G. A. Calin (2016). "The miR-143/miR-145 cluster and the tumor microenvironment: unexpected roles." Genome Med **8**(1): 29.

Amaral, D. G. and P. Lavenex (2007). Hippocampal Neuroanatomy. The Hippocampus Book. A. P., M. R., A. D.G., B. T. and O. K. J. New York, Oxford University Press**:** 37-110.

Ambros, V. (2011). "MicroRNAs and developmental timing." Curr Opin Genet Dev **21**(4): 511-517.

Andersen, P., R. Morris, et al. (2007). Historical Perspective: Proposed Functions, Biological Characteristics and Neurobiological Models of the Hippocampus. The Hippocampus Book. M. R. Andersen P, Amaral D, Bliss T, O'Keefe J, Oxford University Press**:** 9-22.

Annese, J., N. M. Schenker-Ahmed, et al. (2014). "Postmortem examination of patient H.M.'s brain based on histological sectioning and digital 3D reconstruction." Nat Commun **5**: 3122.

Arlotta, P. and O. Hobert (2015). "Homeotic Transformations of Neuronal Cell Identities." Trends Neurosci **38**(12): 751-762.

Arlotta, P., B. J. Molyneaux, et al. (2005). "Neuronal subtype-specific genes that control corticospinal motor neuron development in vivo." Neuron **45**(2): 207-221.

Arnold, S. E. (1999). "Neurodevelopmental abnormalities in schizophrenia: insights from neuropathology." Dev Psychopathol **11**(3): 439-456.

Arnold, S. E. (2000). "Cellular and molecular neuropathology of the parahippocampal region in schizophrenia." Ann N Y Acad Sci **911**: 275-292.

Ashburner, M., C. A. Ball, et al. (2000). "Gene ontology: tool for the unification of biology. The Gene Ontology Consortium." Nat Genet **25**(1): 25-29.

Azim, E., S. J. Shnider, et al. (2009). "Lmo4 and Clim1 progressively delineate cortical projection neuron subtypes during development." Cereb Cortex **19 Suppl 1**: i62-69.

Bae, B. I., D. Jayaraman, et al. (2015). "Genetic changes shaping the human brain." Dev Cell **32**(4): 423-434.

Baiano, M., C. Perlini, et al. (2008). "Decreased entorhinal cortex volumes in schizophrenia." Schizophr Res **102**(1-3): 171-180.

Bakken, T. E., J. A. Miller, et al. (2016). "A comprehensive transcriptional map of primate brain development." Nature **535**(7612): 367-375.

Banerjee, N., H. Kim, et al. (2016). "Plum polyphenols inhibit colorectal aberrant crypt foci formation in rats: potential role of the miR-143/protein kinase B/mammalian target of rapamycin axis." Nutr Res **36**(10): 1105-1113.

Bannerman, D. M., J. N. Rawlins, et al. (2004). "Regional dissociations within the hippocampus--memory and anxiety." Neurosci Biobehav Rev **28**(3): 273-283.

Barca-Mayo, O. and Q. R. Lu (2012). "Fine-Tuning Oligodendrocyte Development by microRNAs." Front Neurosci **6**: 13.

Barros, C. S., S. J. Franco, et al. (2011). "Extracellular matrix: functions in the nervous system." Cold Spring Harb Perspect Biol **3**(1): a005108.

Barucker, C., A. Sommer, et al. (2015). "Alzheimer amyloid peptide abeta42 regulates gene expression of transcription and growth factors." J Alzheimers Dis **44**(2): 613-624.

Bassani, N. P., F. Ambrogi, et al. (2014). "Assessing Agreement between miRNA Microarray Platforms." Microarrays (Basel) **3**(4): 302-321.

Bayer, S. A. (1980). "Development of the hippocampal region in the rat. II. Morphogenesis during embryonic and early postnatal life." J Comp Neurol **190**(1): 115-134.

Beck, B. and G. Pourie (2013). "Ghrelin, neuropeptide Y, and other feeding-regulatory peptides active in the hippocampus: role in learning and memory." Nutr Rev **71**(8): 541-561.

Beed, P., A. Gundlfinger, et al. (2013). "Inhibitory gradient along the dorsoventral axis in the medial entorhinal cortex." Neuron **79**(6): 1197-1207.

Ben-Ari, Y. and N. C. Spitzer (2010). "Phenotypic checkpoints regulate neuronal development." Trends Neurosci **33**(11): 485-492.

Beveridge, N. J. and M. J. Cairns (2012). "MicroRNA dysregulation in schizophrenia." Neurobiol Dis **46**(2): 263-271.

Bharne, A. P., C. D. Borkar, et al. (2016). "Pro-cognitive action of CART is mediated via ERK in the hippocampus." Hippocampus **26**(10): 1313-1327.

Bian, S. and T. Sun (2011). "Functions of noncoding RNAs in neural development and neurological diseases." Mol Neurobiol **44**(3): 359-373.

Bilbo, S. D. and J. M. Schwarz (2012). "The immune system and developmental programming of brain and behavior." Front Neuroendocrinol **33**(3): 267-286.

Bjerknes, T. L., R. F. Langston, et al. (2015). "Coherence among head direction cells before eye opening in rat pups." Curr Biol **25**(1): 103-108.

Bjerknes, T. L., E. I. Moser, et al. (2014). "Representation of geometric borders in the developing rat." Neuron **82**(1): 71-78.

Blankenship, A. G. and M. B. Feller (2010). "Mechanisms underlying spontaneous patterned activity in developing neural circuits." Nat Rev Neurosci **11**(1): 18-29.

Bliss, T. V. and T. Lomo (1973). "Long-lasting potentiation of synaptic transmission in the dentate area of the anaesthetized rabbit following stimulation of the perforant path." J Physiol **232**(2): 331-356.

Boehlen, A., U. Heinemann, et al. (2010). "The range of intrinsic frequencies represented by medial entorhinal cortex stellate cells extends with age." J Neurosci **30**(13): 4585-4589.

Boese, A. S., R. Saba, et al. (2016). "MicroRNA abundance is altered in synaptoneurosomes during prion disease." Mol Cell Neurosci **71**: 13-24.

Bogen, I. L., V. Jensen, et al. (2011). "Glutamatergic neurotransmission in the synapsin I and II double knock-out mouse." Semin Cell Dev Biol **22**(4): 400-407.

Bolstad, B. M., R. A. Irizarry, et al. (2003). "A comparison of normalization methods for high density oligonucleotide array data based on variance and bias." Bioinformatics **19**(2): 185-193.

Bonneh-Barkay, D. and C. A. Wiley (2009). "Brain extracellular matrix in neurodegeneration." Brain Pathol **19**(4): 573-585.

Bonnevie, T., B. Dunn, et al. (2013). "Grid cells require excitatory drive from the hippocampus." Nat Neurosci **16**(3): 309-317.

Borbely, E., B. Scheich, et al. (2013). "Neuropeptides in learning and memory." Neuropeptides **47**(6): 439-450.

Borodinsky, L. N., Y. H. Belgacem, et al. (2015). "Spatiotemporal integration of developmental cues in neural development." Dev Neurobiol **75**(4): 349-359.

Braak, H. and E. Braak (1985). "On areas of transition between entorhinal allocortex and temporal isocortex in the human brain. Normal morphology and lamina-specific pathology in Alzheimer's disease." Acta Neuropathol **68**(4): 325-332.

Braak, H., U. Rub, et al. (2006). "Vulnerability of cortical neurons to Alzheimer's and Parkinson's diseases." J Alzheimers Dis **9**(3 Suppl): 35-44.

Brady, A. M. (2016). "The Neonatal Ventral Hippocampal Lesion (NVHL) Rodent Model of Schizophrenia." Curr Protoc Neurosci **77**: 9 55 51-59 55 17.

Bramham, C. R., M. L. Errington, et al. (1988). "Naloxone blocks the induction of long-term potentiation in the lateral but not in the medial perforant pathway in the anesthetized rat." Brain Res **449**(1-2): 352-356.

Bramham, C. R., N. W. Milgram, et al. (1991). "Activation of AP5-sensitive NMDA Receptors is Not Required to Induce LTP of Synaptic Transmission in the Lateral Perforant Path." Eur J Neurosci **3**(12): 1300-1308.

Bramham, C. R., N. W. Milgram, et al. (1991). "Delta opioid receptor activation is required to induce LTP of synaptic transmission in the lateral perforant path in vivo." Brain Res **567**(1): 42-50.

Brandon, M. P., J. Koenig, et al. (2014). "Parallel and convergent processing in grid cell, head-direction cell, boundary cell, and place cell networks." Wiley Interdiscip Rev Cogn Sci **5**(2): 207-219.

Briggs, J. A., E. J. Wolvetang, et al. (2015). "Mechanisms of Long Non-coding RNAs in Mammalian Nervous System Development, Plasticity, Disease, and Evolution." Neuron **88**(5): 861-877.

Buzsaki, G. (2010). "Neural syntax: cell assemblies, synapsembles, and readers." Neuron **68**(3): 362-385.

Buzsaki, G. and E. I. Moser (2013). "Memory, navigation and theta rhythm in the hippocampal-entorhinal system." Nat Neurosci **16**(2): 130-138.

Campbell, J. D., G. Liu, et al. (2015). "Assessment of microRNA differential expression and detection in multiplexed small RNA sequencing data." RNA **21**(2): 164-171.

Canto, C. B. and M. P. Witter (2012). "Cellular properties of principal neurons in the rat entorhinal cortex. I. The lateral entorhinal cortex." Hippocampus **22**(6): 1256-1276.

Canto, C. B. and M. P. Witter (2012). "Cellular properties of principal neurons in the rat entorhinal cortex. II. The medial entorhinal cortex." Hippocampus **22**(6): 1277-1299.

Canto, C. B., F. G. Wouterlood, et al. (2008). "What does the anatomical organization of the entorhinal cortex tell us?" Neural Plast **2008**: 381243.

Capobianco, E. (2014). "RNA-Seq Data: A Complexity Journey." Comput Struct Biotechnol J **11**(19): 123-130.

Cappaert, N. L. M., N. M. v. Strien, et al. (2015). Hippocampal formation. The rat nervous system Amsterdam: Elsevier, Academic Press**:** 511-573.

Caruana, D. A. and C. A. Chapman (2008). "Dopaminergic suppression of synaptic transmission in the lateral entorhinal cortex." Neural Plast **2008**: 203514.

Cassidy, A. and J. Jones (2014). "Developments in in situ hybridisation." Methods **70**(1): 39-45.

Cayre, M., P. Canoll, et al. (2009). "Cell migration in the normal and pathological postnatal mammalian brain." Prog Neurobiol **88**(1): 41-63.

Cech, T. R. and J. A. Steitz (2014). "The noncoding RNA revolution-trashing old rules to forge new ones." Cell **157**(1): 77-94.

Cederquist, G. Y., E. Azim, et al. (2013). "Lmo4 establishes rostral motor cortex projection neuron subtype diversity." J Neurosci **33**(15): 6321-6332.

Cembrowski, M. S., J. L. Bachman, et al. (2016). "Spatial Gene-Expression Gradients Underlie Prominent Heterogeneity of CA1 Pyramidal Neurons." Neuron **89**(2): 351-368.

Cembrowski, M. S., L. Wang, et al. (2016). "Hipposeq: a comprehensive RNA-seq database of gene expression in hippocampal principal neurons." Elife **5**: e14997.

Chan, W. Y., S. Kohsaka, et al. (2007). "The origin and cell lineage of microglia: new concepts." Brain Res Rev **53**(2): 344-354.

Chen, W. and C. Qin (2015). "General hallmarks of microRNAs in brain evolution and development." RNA Biol **12**(7): 701-708.

Chen, Y., J. A. Gelfond, et al. (2009). "Reproducibility of quantitative RT-PCR array in miRNA expression profiling and comparison with microarray analysis." BMC Genomics **10**: 407.

Chivukula, R. R., G. Shi, et al. (2014). "An essential mesenchymal function for miR-143/145 in intestinal epithelial regeneration." Cell **157**(5): 1104-1116.

Chou, C. H., N. W. Chang, et al. (2016). "miRTarBase 2016: updates to the experimentally validated miRNA-target interactions database." Nucleic Acids Res **44**(D1): D239-247.

Christensen, T., C. F. Bisgaard, et al. (2010). "Transcriptome differentiation along the dorso-ventral axis in laser-captured microdissected rat hippocampal granular cell layer." Neuroscience **170**(3): 731-741.

Chugh, P. and D. P. Dittmer (2012). "Potential pitfalls in microRNA profiling." Wiley Interdiscip Rev RNA **3**(5): 601-616.

Clark, P. M., P. Loher, et al. (2014). "Argonaute CLIP-Seq reveals miRNA targetome diversity across tissue types." Sci Rep **4**: 5947.

Clarke, L. E. and B. A. Barres (2013). "Emerging roles of astrocytes in neural circuit development." Nat Rev Neurosci **14**(5): 311-321.

Clarke, R., H. W. Ressom, et al. (2008). "The properties of high-dimensional data spaces: implications for exploring gene and protein expression data." Nat Rev Cancer **8**(1): 37-49.

Colgin, L. L. (2016). "Rhythms of the hippocampal network." <u>Nat Rev Neurosci</u> **17**(4): 239-249.

Conesa, A., P. Madrigal, et al. (2016). "A survey of best practices for RNA-seq data analysis." <u>Genome Biol</u> **17**: 13.

Costa, R. M., C. Drew, et al. (2005). "Notch to remember." <u>Trends Neurosci</u> **28**(8): 429-435.

Couey, J. J., A. Witoelar, et al. (2013). "Recurrent inhibitory circuitry as a mechanism for grid formation." <u>Nat Neurosci</u> **16**(3): 318-324.

Craig, M. T. and C. J. McBain (2015). "Navigating the circuitry of the brain's GPS system: Future challenges for neurophysiologists." <u>Hippocampus</u> **25**(6): 736-743.

Cui, P., Q. Lin, et al. (2010). "A comparison between ribo-minus RNA-sequencing and polyA-selected RNA-sequencing." <u>Genomics</u> **96**(5): 259-265.

Cui, X. and G. A. Churchill (2003). "Statistical tests for differential expression in cDNA microarray experiments." <u>Genome Biol</u> **4**(4): 210.

Dauth, S., T. Grevesse, et al. (2016). "Extracellular matrix protein expression is brain region dependent." <u>J Comp Neurol</u> **524**(7): 1309-1336.

Davis, T. H., T. L. Cuellar, et al. (2008). "Conditional loss of Dicer disrupts cellular and tissue morphogenesis in the cortex and hippocampus." <u>J Neurosci</u> **28**(17): 4322-4330.

de Andres-Pablo, A., A. Morillon, et al. (2017). "LncRNAs, lost in translation or licence to regulate?" <u>Curr Genet</u> **63**(1): 29-33.

De Strooper, B. and E. Karran (2016). "The Cellular Phase of Alzheimer's Disease." <u>Cell</u> **164**(4): 603-615.

Deng, J. B., D. M. Yu, et al. (2007). "The tracing study of developing entorhino-hippocampal pathway." <u>Int J Dev Neurosci</u> **25**(4): 251-258.

Dent, E. W., S. L. Gupton, et al. (2011). "The growth cone cytoskeleton in axon outgrowth and guidance." <u>Cold Spring Harb Perspect Biol</u> **3**(3).

Derdikman, D. and J. J. Knierim (2014). <u>Space, time and memory in the hippocampal formation</u>. Wien, Springer Verlag Wien.

Derdikman, D. and E. I. Moser (2014). Spatial Maps in the Entorhinal Cortex and Adjacent Structures. <u>Space, Time, and Memory in the Hippocampus</u>. D. Derdikman and J. J. Knierim, Springer**:** pg. 107-126.

Derrien, T., R. Johnson, et al. (2012). "The GENCODE v7 catalog of human long noncoding RNAs: analysis of their gene structure, evolution, and expression." <u>Genome Res</u> **22**(9): 1775-1789.

Deshmukh, S. S. (2014). Spatial and Nonspatial Representations in the Lateral Entorhinal Cortex. <u>Space, Time, and Memory in the Hippocampus</u>. D. Derdikman and J. J. Knierim, Springer**:** pg. 127-152.

Di Liegro, C. M., G. Schiera, et al. (2014). "Regulation of mRNA transport, localization and translation in the nervous system of mammals (Review)." <u>Int J Mol Med</u> **33**(4): 747-762.

Dill, H., B. Linder, et al. (2012). "Intronic miR-26b controls neuronal differentiation by repressing its host transcript, ctdsp2." <u>Genes Dev</u> **26**(1): 25-30.

Dillies, M. A., A. Rau, et al. (2013). "A comprehensive evaluation of normalization methods for Illumina high-throughput RNA sequencing data analysis." <u>Brief Bioinform</u> **14**(6): 671-683.

Dillman, A. A. and M. R. Cookson (2014). "Transcriptomic changes in brain development." <u>Int Rev Neurobiol</u> **116**: 233-250.

Dolorfo, C. L. and D. G. Amaral (1998). "Entorhinal cortex of the rat: organization of intrinsic connections." J Comp Neurol **398**(1): 49-82.

Domnisoru, C., A. A. Kinkhabwala, et al. (2013). "Membrane potential dynamics of grid cells." Nature **495**(7440): 199-204.

Donato, F., R. I. Jacobsen, et al. (2017). "Stellate cells drive maturation of the entorhinal-hippocampal circuit." Science **355**(6330).

Dong, H. W., L. W. Swanson, et al. (2009). "Genomic-anatomic evidence for distinct functional domains in hippocampal field CA1." Proc Natl Acad Sci U S A **106**(28): 11794-11799.

Downes, N. and P. Mullins (2014). "The development of myelin in the brain of the juvenile rat." Toxicol Pathol **42**(5): 913-922.

Du, F., W. O. Whetsell, Jr., et al. (1993). "Preferential neuronal loss in layer III of the entorhinal cortex in patients with temporal lobe epilepsy." Epilepsy Res **16**(3): 223-233.

du Plessis, L., N. Skunca, et al. (2011). "The what, where, how and why of gene ontology--a primer for bioinformaticians." Brief Bioinform **12**(6): 723-735.

Edbauer, D., J. R. Neilson, et al. (2010). "Regulation of synaptic structure and function by FMRP-associated microRNAs miR-125b and miR-132." Neuron **65**(3): 373-384.

Egorov, A. V. and A. Draguhn (2013). "Development of coherent neuronal activity patterns in mammalian cortical networks: common principles and local hetereogeneity." Mech Dev **130**(6-8): 412-423.

Eichenbaum, H. (2014). "Time cells in the hippocampus: a new dimension for mapping memories." Nat Rev Neurosci **15**(11): 732-744.

Eichenbaum, H., D. G. Amaral, et al. (2016). "Hippocampus at 25." Hippocampus **26**(10): 1238-1249.

Elia, L., M. Quintavalle, et al. (2009). "The knockout of miR-143 and -145 alters smooth muscle cell maintenance and vascular homeostasis in mice: correlates with human disease." Cell Death Differ **16**(12): 1590-1598.

Encinas, J. M., A. Sierra, et al. (2013). "A developmental perspective on adult hippocampal neurogenesis." Int J Dev Neurosci **31**(7): 640-645.

ENCODE (2012). "An integrated encyclopedia of DNA elements in the human genome." Nature **489**(7414): 57-74.

Engelhardt, B. and S. Liebner (2014). "Novel insights into the development and maintenance of the blood-brain barrier." Cell Tissue Res **355**(3): 687-699.

Erhard, F., J. Haas, et al. (2014). "Widespread context dependency of microRNA-mediated regulation." Genome Res **24**(6): 906-919.

Fabian, M. R., N. Sonenberg, et al. (2010). "Regulation of mRNA translation and stability by microRNAs." Annu Rev Biochem **79**: 351-379.

Fang, R., T. Xiao, et al. (2012). "MicroRNA-143 (miR-143) regulates cancer glycolysis via targeting hexokinase 2 gene." J Biol Chem **287**(27): 23227-23235.

Fang, Z., J. Martin, et al. (2012). "Statistical methods for identifying differentially expressed genes in RNA-Seq experiments." Cell Biosci **2**(1): 26.

Fanselow, M. S. and H. W. Dong (2010). "Are the dorsal and ventral hippocampus functionally distinct structures?" Neuron **65**(1): 7-19.

Faridani, O. R., I. Abdullayev, et al. (2016). "Single-cell sequencing of the small-RNA transcriptome." Nat Biotechnol **34**(12): 1264-1266.

Femminella, G. D., N. Ferrara, et al. (2015). "The emerging role of microRNAs in Alzheimer's disease." Front Physiol **6**: 40.

Ferrante, M., B. Tahvildari, et al. (2017). "Distinct Functional Groups Emerge from the Intrinsic Properties of Molecularly Identified Entorhinal Interneurons and Principal Cells." Cereb Cortex **27**(6): 3186-3207.

Fertuzinhos, S., M. Li, et al. (2014). "Laminar and temporal expression dynamics of coding and noncoding RNAs in the mouse neocortex." Cell Rep **6**(5): 938-950.

Fiore, R., G. Siegel, et al. (2008). "MicroRNA function in neuronal development, plasticity and disease." Biochim Biophys Acta **1779**(8): 471-478.

Fiorenza, A. and A. Barco (2016). "Role of Dicer and the miRNA system in neuronal plasticity and brain function." Neurobiol Learn Mem **135**: 3-12.

Follert, P., H. Cremer, et al. (2014). "MicroRNAs in brain development and function: a matter of flexibility and stability." Front Mol Neurosci **7**: 5.

Forster, E., S. Zhao, et al. (2006). "Laminating the hippocampus." Nat Rev Neurosci **7**(4): 259-267.

Forstner, A. J., A. Hofmann, et al. (2015). "Genome-wide analysis implicates microRNAs and their target genes in the development of bipolar disorder." Transl Psychiatry **5**: e678.

Fredens, K., K. Stengaard-Pedersen, et al. (1984). "Localization of enkephalin and cholecystokinin immunoreactivities in the perforant path terminal fields of the rat hippocampal formation." Brain Res **304**(2): 255-263.

Fu, H., G. A. Rodriguez, et al. (2017). "Tau Pathology Induces Excitatory Neuron Loss, Grid Cell Dysfunction, and Spatial Memory Deficits Reminiscent of Early Alzheimer's Disease." Neuron **93**(3): 533-541 e535.

Fuchs, E. C., A. Neitz, et al. (2016). "Local and Distant Input Controlling Excitation in Layer II of the Medial Entorhinal Cortex." Neuron **89**(1): 194-208.

Gajjar, S. and B. M. Patel (2017). "Neuromedin: An insight into its types, receptors and therapeutic opportunities." Pharmacol Rep **69**(3): 438-447.

Gallistel, C. R. and L. D. Matzel (2013). "The neuroscience of learning: beyond the Hebbian synapse." Annu Rev Psychol **64**: 169-200.

Gao, F. B. (2010). "Context-dependent functions of specific microRNAs in neuronal development." Neural Dev **5**: 25.

Garber, M., M. G. Grabherr, et al. (2011). "Computational methods for transcriptome annotation and quantification using RNA-seq." Nat Methods **8**(6): 469-477.

Garcia-Campos, M. A., J. Espinal-Enriquez, et al. (2015). "Pathway Analysis: State of the Art." Front Physiol **6**: 383.

Garcia, D. M., D. Baek, et al. (2011). "Weak seed-pairing stability and high target-site abundance decrease the proficiency of lsy-6 and other microRNAs." Nat Struct Mol Biol **18**(10): 1139-1146.

Gatome, C. W., L. Slomianka, et al. (2010). "Number estimates of neuronal phenotypes in layer II of the medial entorhinal cortex of rat and mouse." Neuroscience **170**(1): 156-165.

Geisler, S. and J. Coller (2013). "RNA in unexpected places: long non-coding RNA functions in diverse cellular contexts." Nat Rev Mol Cell Biol **14**(11): 699-712.

Ghanbari, M., M. A. Ikram, et al. (2016). "Genome-wide identification of microRNA-related variants associated with risk of Alzheimer's disease." Sci Rep **6**: 28387.

Giocomo, L. M., S. A. Hussaini, et al. (2011). "Grid cells use HCN1 channels for spatial scaling." Cell **147**(5): 1159-1170.

Giocomo, L. M., M. B. Moser, et al. (2011). "Computational models of grid cells." <u>Neuron</u> **71**(4): 589-603.

Gomez-Pinilla, F., V. So, et al. (2001). "Spatial learning induces neurotrophin receptor and synapsin I in the hippocampus." <u>Brain Res</u> **904**(1): 13-19.

Goncalves, J. T., C. W. Bloyd, et al. (2016). "In vivo imaging of dendritic pruning in dentate granule cells." <u>Nat Neurosci</u> **19**(6): 788-791.

Greene, C. S., J. Tan, et al. (2014). "Big data bioinformatics." <u>J Cell Physiol</u> **229**(12): 1896-1900.

Greenhill, S. D., S. E. Chamberlain, et al. (2014). "Background synaptic activity in rat entorhinal cortex shows a progressively greater dominance of inhibition over excitation from deep to superficial layers." <u>PLoS One</u> **9**(1): e85125.

Greer, P. L. and M. E. Greenberg (2008). "From synapse to nucleus: calcium-dependent gene transcription in the control of synapse development and function." <u>Neuron</u> **59**(6): 846-860.

Grieves, R. M. and K. J. Jeffery (2017). "The representation of space in the brain." <u>Behav Processes</u> **135**: 113-131.

Griffiths-Jones, S., R. J. Grocock, et al. (2006). "miRBase: microRNA sequences, targets and gene nomenclature." <u>Nucleic Acids Res</u> **34**(Database issue): D140-144.

Grimson, A., K. K. Farh, et al. (2007). "MicroRNA targeting specificity in mammals: determinants beyond seed pairing." <u>Mol Cell</u> **27**(1): 91-105.

Grun, D. and A. van Oudenaarden (2015). "Design and Analysis of Single-Cell Sequencing Experiments." <u>Cell</u> **163**(4): 799-810.

Guillemot, F. and C. Zimmer (2011). "From cradle to grave: the multiple roles of fibroblast growth factors in neural development." <u>Neuron</u> **71**(4): 574-588.

Guo, H., N. T. Ingolia, et al. (2010). "Mammalian microRNAs predominantly act to decrease target mRNA levels." <u>Nature</u> **466**(7308): 835-840.

Ha, M. and V. N. Kim (2014). "Regulation of microRNA biogenesis." <u>Nat Rev Mol Cell Biol</u> **15**(8): 509-524.

Hafting, T., M. Fyhn, et al. (2005). "Microstructure of a spatial map in the entorhinal cortex." <u>Nature</u> **436**(7052): 801-806.

Hansen, K. D., R. A. Irizarry, et al. (2012). "Removing technical variability in RNA-seq data using conditional quantile normalization." <u>Biostatistics</u> **13**(2): 204-216.

Harb, K., E. Magrinelli, et al. (2016). "Area-specific development of distinct projection neuron subclasses is regulated by postnatal epigenetic modifications." <u>Elife</u> **5**: e09531.

Harbom, L. J., W. D. Chronister, et al. (2016). "Single neuron transcriptome analysis can reveal more than cell type classification: Does it matter if every neuron is unique?" <u>Bioessays</u> **38**(2): 157-161.

Hargreaves, E. L., G. Rao, et al. (2005). "Major dissociation between medial and lateral entorhinal input to dorsal hippocampus." <u>Science</u> **308**(5729): 1792-1794.

Harris, K. D., C. B. Gonzales, et al. (2017). "Classes and continua of hippocampal CA1 inhibitory neurons revealed by single-cell transcriptomics." <u>bioRxiv</u>.

Harrow, J., A. Frankish, et al. (2012). "GENCODE: the reference human genome annotation for The ENCODE Project." <u>Genome Res</u> **22**(9): 1760-1774.

Hassan, B. A. and P. R. Hiesinger (2015). "Beyond Molecular Codes: Simple Rules to Wire Complex Brains." <u>Cell</u> **163**(2): 285-291.

Hastie, T., R. Tibshirani, et al. (2009). The Elements of Statistical Learning, Springer.

He, M., Y. Liu, et al. (2012). "Cell-type-based analysis of microRNA profiles in the mouse brain." Neuron **73**(1): 35-48.

Head, S. R., H. K. Komori, et al. (2014). "Library construction for next-generation sequencing: overviews and challenges." Biotechniques **56**(2): 61-64, 66, 68, passim.

Hebb, D. O. (1949). The organization of behavior; a neuropsychological theory. New York,, Wiley.

Hemby, S. E., S. D. Ginsberg, et al. (2002). "Gene expression profile for schizophrenia: discrete neuron transcription patterns in the entorhinal cortex." Arch Gen Psychiatry **59**(7): 631-640.

Henriksen, E. J., L. L. Colgin, et al. (2010). "Spatial representation along the proximodistal axis of CA1." Neuron **68**(1): 127-137.

Heppner, F. L., R. M. Ransohoff, et al. (2015). "Immune attack: the role of inflammation in Alzheimer disease." Nat Rev Neurosci **16**(6): 358-372.

Hocine, S., R. H. Singer, et al. (2010). "RNA processing and export." Cold Spring Harb Perspect Biol **2**(12): a000752.

Horii-Hayashi, N., H. Okuda, et al. (2008). "Localization of chondroitin sulfate proteoglycan versican in adult brain with special reference to large projection neurons." Cell Tissue Res **334**(2): 163-177.

Horsham, J. L., C. Ganda, et al. (2015). "MicroRNA-7: A miRNA with expanding roles in development and disease." Int J Biochem Cell Biol **69**: 215-224.

Howdeshell, K. L. (2002). "A model of the development of the brain as a construct of the thyroid system." Environ Health Perspect **110 Suppl 3**: 337-348.

Huang da, W., B. T. Sherman, et al. (2009). "Bioinformatics enrichment tools: paths toward the comprehensive functional analysis of large gene lists." Nucleic Acids Res **37**(1): 1-13.

Huang, R., A. Wallqvist, et al. (2006). "Comprehensive analysis of pathway or functionally related gene expression in the National Cancer Institute's anticancer screen." Genomics **87**(3): 315-328.

Huyck, C. R. and P. J. Passmore (2013). "A review of cell assemblies." Biol Cybern **107**(3): 263-288.

Igarashi, K. M. (2016). "The entorhinal map of space." Brain Res **1637**: 177-187.

Iijima, T., C. Hidaka, et al. (2016). "Spatio-temporal regulations and functions of neuronal alternative RNA splicing in developing and adult brains." Neurosci Res **109**: 1-8.

Insausti, R., M. T. Herrero, et al. (1997). "Entorhinal cortex of the rat: cytoarchitectonic subdivisions and the origin and distribution of cortical efferents." Hippocampus **7**(2): 146-183.

Ito, M. and M. Kano (1982). "Long-lasting depression of parallel fiber-Purkinje cell transmission induced by conjunctive stimulation of parallel fibers and climbing fibers in the cerebellar cortex." Neurosci Lett **33**(3): 253-258.

Jaksik, R., M. Iwanaszko, et al. (2015). "Microarray experiments and factors which affect their reliability." Biol Direct **10**: 46.

Jeanmougin, M., A. de Reynies, et al. (2010). "Should we abandon the t-test in the analysis of gene expression microarray data: a comparison of variance modeling strategies." PLoS One **5**(9): e12336.

Jeffery, I. B., D. G. Higgins, et al. (2006). "Comparison and evaluation of methods for generating differentially expressed gene lists from microarray data." BMC Bioinformatics **7**: 359.

Jiang, X. and J. Nardelli (2016). "Cellular and molecular introduction to brain development." Neurobiol Dis **92**(Pt A): 3-17.

Joshi-Tope, G., M. Gillespie, et al. (2005). "Reactome: a knowledgebase of biological pathways." Nucleic Acids Res **33**(Database issue): D428-432.

Jovicic, A., R. Roshan, et al. (2013). "Comprehensive expression analyses of neural cell-type-specific miRNAs identify new determinants of the specification and maintenance of neuronal phenotypes." J Neurosci **33**(12): 5127-5137.

Kaila, K., T. J. Price, et al. (2014). "Cation-chloride cotransporters in neuronal development, plasticity and disease." Nat Rev Neurosci **15**(10): 637-654.

Kandel, E. R., Y. Dudai, et al. (2014). "The molecular and systems biology of memory." Cell **157**(1): 163-186.

Kerr, G., H. J. Ruskin, et al. (2008). "Techniques for clustering gene expression data." Comput Biol Med **38**(3): 283-293.

Kerr, K. M., K. L. Agster, et al. (2007). "Functional neuroanatomy of the parahippocampal region: the lateral and medial entorhinal areas." Hippocampus **17**(9): 697-708.

Kesner, R. P. and E. T. Rolls (2015). "A computational theory of hippocampal function, and tests of the theory: new developments." Neurosci Biobehav Rev **48**: 92-147.

Khalaf-Nazzal, R. and F. Francis (2013). "Hippocampal development - old and new findings." Neuroscience **248**: 225-242.

Khatri, P., M. Sirota, et al. (2012). "Ten years of pathway analysis: current approaches and outstanding challenges." PLoS Comput Biol **8**(2): e1002375.

Kim, J. J. and M. S. Fanselow (1992). "Modality-specific retrograde amnesia of fear." Science **256**(5057): 675-677.

Kim, W., H. Noh, et al. (2016). "MiR-126 Regulates Growth Factor Activities and Vulnerability to Toxic Insult in Neurons." Mol Neurobiol **53**(1): 95-108.

Kishi, T., T. Tsumori, et al. (2006). "Topographical projection from the hippocampal formation to the amygdala: a combined anterograde and retrograde tracing study in the rat." J Comp Neurol **496**(3): 349-368.

Klink, R. and A. Alonso (1997). "Morphological characteristics of layer II projection neurons in the rat medial entorhinal cortex." Hippocampus **7**(5): 571-583.

Knierim, J. J. (2015). "The hippocampus." Curr Biol **25**(23): R1116-1121.

Kobro-Flatmoen, A., A. Nagelhus, et al. (2016). "Reelin-immunoreactive neurons in entorhinal cortex layer II selectively express intracellular amyloid in early Alzheimer's disease." Neurobiol Dis **93**: 172-183.

Kolodkin, A. L. and M. Tessier-Lavigne (2011). "Mechanisms and molecules of neuronal wiring: a primer." Cold Spring Harb Perspect Biol **3**(6).

Koltai, H. and C. Weingarten-Baror (2008). "Specificity of DNA microarray hybridization: characterization, effectors and approaches for data correction." Nucleic Acids Res **36**(7): 2395-2405.

Kozomara, A. and S. Griffiths-Jones (2014). "miRBase: annotating high confidence microRNAs using deep sequencing data." Nucleic Acids Res **42**(Database issue): D68-73.

Kozomara, A., S. Hunt, et al. (2014). "Target repression induced by endogenous microRNAs: large differences, small effects." PLoS One **9**(8): e104286.

Krol, J., I. Loedige, et al. (2010). "The widespread regulation of microRNA biogenesis, function and decay." Nat Rev Genet **11**(9): 597-610.

Kropff, E., J. E. Carmichael, et al. (2015). "Speed cells in the medial entorhinal cortex." Nature **523**(7561): 419-424.

Kutlu, M. G. and T. J. Gould (2016). "Nicotinic modulation of hippocampal cell signaling and associated effects on learning and memory." Physiol Behav **155**: 162-171.

Kwok, J. C., G. Dick, et al. (2011). "Extracellular matrix and perineuronal nets in CNS repair." Dev Neurobiol **71**(11): 1073-1089.

Lacoste, B. and C. Gu (2015). "Control of cerebrovascular patterning by neural activity during postnatal development." Mech Dev **138 Pt 1**: 43-49.

Lahens, N. F., I. H. Kavakli, et al. (2014). "IVT-seq reveals extreme bias in RNA sequencing." Genome Biol **15**(6): R86.

Lambert de Rouvroit, C. and A. M. Goffinet (2001). "Neuronal migration." Mech Dev **105**(1-2): 47-56.

Langston, R. F., J. A. Ainge, et al. (2010). "Development of the spatial representation system in the rat." Science **328**(5985): 1576-1580.

Lau, J. and H. Herzog (2014). "CART in the regulation of appetite and energy homeostasis." Front Neurosci **8**: 313.

Law, C. W., Y. Chen, et al. (2014). "voom: Precision weights unlock linear model analysis tools for RNA-seq read counts." Genome Biol **15**(2): R29.

Le Magueresse, C. and H. Monyer (2013). "GABAergic interneurons shape the functional maturation of the cortex." Neuron **77**(3): 388-405.

Lee, J. H. (2017). "Quantitative approaches for investigating the spatial context of gene expression." Wiley Interdiscip Rev Syst Biol Med **9**(2).

Lee, Y. J., V. Kim, et al. (2015). "Validated MicroRNA Target Databases: An Evaluation." Drug Dev Res **76**(7): 389-396.

Lein, E. S., M. J. Hawrylycz, et al. (2007). "Genome-wide atlas of gene expression in the adult mouse brain." Nature **445**(7124): 168-176.

Lelli, K. M., M. Slattery, et al. (2012). "Disentangling the many layers of eukaryotic transcriptional regulation." Annu Rev Genet **46**: 43-68.

Leonardo, E. D., J. W. Richardson-Jones, et al. (2006). "Molecular heterogeneity along the dorsal-ventral axis of the murine hippocampal CA1 field: a microarray analysis of gene expression." Neuroscience **137**(1): 177-186.

Levin, J. Z., M. Yassour, et al. (2010). "Comprehensive comparative analysis of strand-specific RNA sequencing methods." Nat Methods **7**(9): 709-715.

Li, F., S. Li, et al. (2014). "TGF-beta1 promotes osteosarcoma cell migration and invasion through the miR-143-versican pathway." Cell Physiol Biochem **34**(6): 2169-2179.

Li, P., Y. Piao, et al. (2015). "Comparing the normalization methods for the differential analysis of Illumina high-throughput RNA-Seq data." BMC Bioinformatics **16**: 347.

Li, R., L. Zhang, et al. (2014). "MicroRNA-143 targets Syndecan-1 to repress cell growth in melanoma." PLoS One **9**(4): e94855.

Li, X. and P. Jin (2010). "Roles of small regulatory RNAs in determining neuronal identity." Nat Rev Neurosci **11**(5): 329-338.

Liu, B., J. Li, et al. (2014). "Identifying miRNAs, targets and functions." Brief Bioinform **15**(1): 1-19.

Lobo, M. K., S. L. Karsten, et al. (2006). "FACS-array profiling of striatal projection neuron subtypes in juvenile and adult mouse brains." Nat Neurosci **9**(3): 443-452.

Lodato, S., A. S. Shetty, et al. (2015). "Cerebral cortex assembly: generating and reprogramming projection neuron diversity." Trends Neurosci **38**(2): 117-125.

Lohmann, C. and H. W. Kessels (2014). "The developmental stages of synaptic plasticity." J Physiol **592**(1): 13-31.

Lopes, J. P., X. Morato, et al. (2015). "The role of parkinson's disease-associated receptor GPR37 in the hippocampus: functional interplay with the adenosinergic system." J Neurochem **134**(1): 135-146.

Lopez-Aranda, M. F., J. F. Lopez-Tellez, et al. (2009). "Role of layer 6 of V2 visual cortex in object-recognition memory." Science **325**(5936): 87-89.

Loren, I., J. Alumets, et al. (1979). "Distribution of gastrin and CCK-like peptides in rat brain. An immunocytochemical study." Histochemistry **59**(4): 249-257.

Low, L. K. and H. J. Cheng (2006). "Axon pruning: an essential step underlying the developmental plasticity of neuronal connections." Philos Trans R Soc Lond B Biol Sci **361**(1473): 1531-1544.

Lu, L., K. M. Igarashi, et al. (2015). "Topography of Place Maps along the CA3-to-CA2 Axis of the Hippocampus." Neuron **87**(5): 1078-1092.

Luhmann, H. J., A. Sinning, et al. (2016). "Spontaneous Neuronal Activity in Developing Neocortical Networks: From Single Cells to Large-Scale Interactions." Front Neural Circuits **10**: 40.

Luo, Q. and Y. Chen (2016). "Long noncoding RNAs and Alzheimer's disease." Clin Interv Aging **11**: 867-872.

Luoni, A. and M. A. Riva (2016). "MicroRNAs and psychiatric disorders: From aetiology to treatment." Pharmacol Ther **167**: 13-27.

Luscher, C. and R. C. Malenka (2012). "NMDA receptor-dependent long-term potentiation and long-term depression (LTP/LTD)." Cold Spring Harb Perspect Biol **4**(6).

Maeder, C. I. and K. Shen (2011). "Genetic dissection of synaptic specificity." Curr Opin Neurobiol **21**(1): 93-99.

Malone, J. H. and B. Oliver (2011). "Microarrays, deep sequencing and the true measure of the transcriptome." BMC Biol **9**: 34.

Marin, I. and J. Kipnis (2013). "Learning and memory ... and the immune system." Learn Mem **20**(10): 601-606.

Marin, O., M. Valiente, et al. (2010). "Guiding neuronal cell migrations." Cold Spring Harb Perspect Biol **2**(2): a001834.

McKee, A. E. and P. A. Silver (2007). "Systems perspectives on mRNA processing." Cell Res **17**(7): 581-590.

McNamara, C. G., A. Tejero-Cantero, et al. (2014). "Dopaminergic neurons promote hippocampal reactivation and spatial memory persistence." Nat Neurosci **17**(12): 1658-1660.

McNeill, E. and D. Van Vactor (2012). "MicroRNAs shape the neuronal landscape." Neuron **75**(3): 363-379.

McNulty, S. E., R. M. Barrett, et al. (2012). "Differential roles for Nr4a1 and Nr4a2 in object location vs. object recognition long-term memory." Learn Mem **19**(12): 588-592.

McRae, P. A. and B. E. Porter (2012). "The perineuronal net component of the extracellular matrix in plasticity and epilepsy." Neurochem Int **61**(7): 963-972.

Meier, S., A. U. Brauer, et al. (2004). "Myelination in the hippocampus during development and following lesion." Cell Mol Life Sci **61**(9): 1082-1094.

Mercer, T. R., M. E. Dinger, et al. (2009). "Long non-coding RNAs: insights into functions." Nat Rev Genet **10**(3): 155-159.

Mestdagh, P., N. Hartmann, et al. (2014). "Evaluation of quantitative miRNA expression platforms in the microRNA quality control (miRQC) study." Nat Methods **11**(8): 809-815.

Michaloudi, H., I. Grivas, et al. (2005). "Areal and laminar variations in the vascularity of the visual, auditory, and entorhinal cortices of the developing rat brain." Brain Res Dev Brain Res **155**(1): 60-70.

Miettinen, M., E. Koivisto, et al. (1996). "Coexistence of parvalbumin and GABA in nonpyramidal neurons of the rat entorhinal cortex." Brain Res **706**(1): 113-122.

Miura, P., S. Shenker, et al. (2013). "Widespread and extensive lengthening of 3' UTRs in the mammalian brain." Genome Res **23**(5): 812-825.

Mody, M., Y. Cao, et al. (2001). "Genome-wide gene expression profiles of the developing mouse hippocampus." Proc Natl Acad Sci U S A **98**(15): 8862-8867.

Molyneaux, B. J., L. A. Goff, et al. (2015). "DeCoN: genome-wide analysis of in vivo transcriptional dynamics during pyramidal neuron fate selection in neocortex." Neuron **85**(2): 275-288.

Moody, W. J. and M. M. Bosma (2005). "Ion channel development, spontaneous activity, and activity-dependent development in nerve and muscle cells." Physiol Rev **85**(3): 883-941.

Moore, M. J., C. Zhang, et al. (2014). "Mapping Argonaute and conventional RNA-binding protein interactions with RNA at single-nucleotide resolution using HITS-CLIP and CIMS analysis." Nat Protoc **9**(2): 263-293.

Moser, E. I. and M. B. Moser (2013). "Grid cells and neural coding in high-end cortices." Neuron **80**(3): 765-774.

Moser, E. I., M. B. Moser, et al. (2014). "Network mechanisms of grid cells." Philos Trans R Soc Lond B Biol Sci **369**(1635): 20120511.

Moser, M. B. and E. I. Moser (1998). "Functional differentiation in the hippocampus." Hippocampus **8**(6): 608-619.

Motameny, S., S. Wolters, et al. (2010). "Next Generation Sequencing of miRNAs - Strategies, Resources and Methods." Genes (Basel) **1**(1): 70-84.

Mudge, J. M. and J. Harrow (2015). "Creating reference gene annotation for the mouse C57BL6/J genome assembly." Mamm Genome **26**(9-10): 366-378.

Mulligan, K. A. and B. N. Cheyette (2012). "Wnt signaling in vertebrate neural development and function." J Neuroimmune Pharmacol **7**(4): 774-787.

Murai, K., G. Sun, et al. (2016). "The TLX-miR-219 cascade regulates neural stem cell proliferation in neurodevelopment and schizophrenia iPSC model." Nat Commun **7**: 10965.

Nadon, R. and J. Shoemaker (2002). "Statistical issues with microarrays: processing and analysis." Trends Genet **18**(5): 265-271.

Navarro, A. I. and B. Rico (2014). "Focal adhesion kinase function in neuronal development." Curr Opin Neurobiol **27**: 89-95.

Nikolic, M., H. A. Gardner, et al. (2013). "Postnatal neuronal apoptosis in the cerebral cortex: physiological and pathophysiological mechanisms." Neuroscience **254**: 369-378.

Noble, W. S. (2009). "How does multiple testing correction work?" Nat Biotechnol **27**(12): 1135-1137.

Nowak, J. S. and G. Michlewski (2013). "miRNAs in development and pathogenesis of the nervous system." Biochem Soc Trans **41**(4): 815-820.

Nuovo, G. J. (2008). "In situ detection of precursor and mature microRNAs in paraffin embedded, formalin fixed tissues and cell preparations." Methods **44**(1): 39-46.

O'Keefe, J. and J. Dostrovsky (1971). "The hippocampus as a spatial map. Preliminary evidence from unit activity in the freely-moving rat." Brain Res **34**(1): 171-175.

O'Rourke, N. A., N. C. Weiler, et al. (2012). "Deep molecular diversity of mammalian synapses: why it matters and how to measure it." Nat Rev Neurosci **13**(6): 365-379.

Ogata, H., S. Goto, et al. (1999). "KEGG: Kyoto Encyclopedia of Genes and Genomes." Nucleic Acids Res **27**(1): 29-34.

Ogren, S. O., E. Kuteeva, et al. (2010). "Neuropeptides in learning and memory processes with focus on galanin." Eur J Pharmacol **626**(1): 9-17.

Ohtaka-Maruyama, C. and H. Okado (2015). "Molecular Pathways Underlying Projection Neuron Production and Migration during Cerebral Cortical Development." Front Neurosci **9**: 447.

Okamura, N., C. Garau, et al. (2011). "Neuropeptide S enhances memory during the consolidation phase and interacts with noradrenergic systems in the brain." Neuropsychopharmacology **36**(4): 744-752.

Okaty, B. W., K. Sugino, et al. (2011). "Cell type-specific transcriptomics in the brain." J Neurosci **31**(19): 6939-6943.

Olsen, L. C., K. C. O'Reilly, et al. (2017). "MicroRNAs contribute to postnatal development of laminar differences and neuronal subtypes in the rat medial entorhinal cortex." Brain Struct Funct.

Oshlack, A., M. D. Robinson, et al. (2010). "From RNA-seq reads to differential expression results." Genome Biol **11**(12): 220.

Pandey, A. K., L. Lu, et al. (2014). "Functionally enigmatic genes: a case study of the brain ignorome." PLoS One **9**(2): e88889.

Pasquinelli, A. E. (2012). "MicroRNAs and their targets: recognition, regulation and an emerging reciprocal relationship." Nat Rev Genet **13**(4): 271-282.

Pastoll, H., H. L. Ramsden, et al. (2012). "Intrinsic electrophysiological properties of entorhinal cortex stellate cells and their contribution to grid cell firing fields." Front Neural Circuits **6**: 17.

Pereda, A. E. (2014). "Electrical synapses and their functional interactions with chemical synapses." Nat Rev Neurosci **15**(4): 250-263.

Petersen, M., C. B. Nielsen, et al. (2000). "The conformations of locked nucleic acids (LNA)." J Mol Recognit **13**(1): 44-53.

Pressler, R. and S. Auvin (2013). "Comparison of Brain Maturation among Species: An Example in Translational Research Suggesting the Possible Use of Bumetanide in Newborn." Front Neurol **4**: 36.

Primeaux, S. D., M. J. Barnes, et al. (2013). "Hypothalamic QRFP: regulation of food intake and fat selection." Horm Metab Res **45**(13): 967-974.

Prinz, M. and J. Priller (2014). "Microglia and brain macrophages in the molecular age: from origin to neuropsychiatric disease." Nat Rev Neurosci **15**(5): 300-312.

Pritchard, C. C., H. H. Cheng, et al. (2012). "MicroRNA profiling: approaches and considerations." Nat Rev Genet **13**(5): 358-369.

Puelles, L. and J. L. Ferran (2012). "Concept of neural genoarchitecture and its genomic fundament." Front Neuroanat **6**: 47.

Qiao, S., R. Peng, et al. (2014). "Reduction of phosphorylated synapsin I (ser-553) leads to spatial memory impairment by attenuating GABA release after microwave exposure in Wistar rats." PLoS One **9**(4): e95503.

Qin, Z., X. Zhou, et al. (2012). "LIM domain only 4 (LMO4) regulates calcium-induced calcium release and synaptic plasticity in the hippocampus." J Neurosci **32**(12): 4271-4283.

Quackenbush, J. (2002). "Microarray data normalization and transformation." <u>Nat Genet</u> **32 Suppl**: 496-501.

Quaranta, M. T., I. Spinello, et al. (2016). "Identification of beta-Dystrobrevin as a Direct Target of miR-143: Involvement in Early Stages of Neural Differentiation." <u>PLoS One</u> **11**(5): e0156325.

Quinn, J. J. and H. Y. Chang (2016). "Unique features of long non-coding RNA biogenesis and function." <u>Nat Rev Genet</u> **17**(1): 47-62.

Radic, T., T. Jungenitz, et al. (2017). "Time-lapse imaging reveals highly dynamic structural maturation of postnatally born dentate granule cells in organotypic entorhino-hippocampal slice cultures." <u>Sci Rep</u> **7**: 43724.

Ramos, A. D., F. J. Attenello, et al. (2016). "Uncovering the roles of long noncoding RNAs in neural development and glioma progression." <u>Neurosci Lett</u> **625**: 70-79.

Ramsaran, A. I., H. R. Sanders, et al. (2016). "Determinants of object-in-context and object-place-context recognition in the developing rat." <u>Dev Psychobiol</u> **58**(7): 883-895.

Ramsaran, A. I., S. R. Westbrook, et al. (2016). "Ontogeny of object-in-context recognition in the rat." <u>Behav Brain Res</u> **298**(Pt A): 37-47.

Ramsden, H. L., G. Surmeli, et al. (2015). "Laminar and dorsoventral molecular organization of the medial entorhinal cortex revealed by large-scale anatomical analysis of gene expression." <u>PLoS Comput Biol</u> **11**(1): e1004032.

Rani, N., T. J. Nowakowski, et al. (2016). "A Primate lncRNA Mediates Notch Signaling during Neuronal Development by Sequestering miRNA." <u>Neuron</u> **90**(6): 1174-1188.

Ray, S. and M. Brecht (2016). "Structural development and dorsoventral maturation of the medial entorhinal cortex." <u>Elife</u> **5**: e13343.

Razanau, A. and J. Xie (2013). "Emerging mechanisms and consequences of calcium regulation of alternative splicing in neurons and endocrine cells." <u>Cell Mol Life Sci</u> **70**(23): 4527-4536.

Redrobe, J. P., Y. Dumont, et al. (2004). "Characterization of neuropeptide Y, Y(2) receptor knockout mice in two animal models of learning and memory processing." <u>J Mol Neurosci</u> **22**(3): 159-166.

Reuter, J. A., D. V. Spacek, et al. (2015). "High-throughput sequencing technologies." <u>Mol Cell</u> **58**(4): 586-597.

Reyes-Herrera, P. H. and E. Ficarra (2012). "One decade of development and evolution of microRNA target prediction algorithms." <u>Genomics Proteomics Bioinformatics</u> **10**(5): 254-263.

Rice, D. and S. Barone, Jr. (2000). "Critical periods of vulnerability for the developing nervous system: evidence from humans and animal models." <u>Environ Health Perspect</u> **108 Suppl 3**: 511-533.

Richardson, G. M., J. Lannigan, et al. (2015). "Does FACS perturb gene expression?" <u>Cytometry A</u> **87**(2): 166-175.

Ringner, M. (2008). "What is principal component analysis?" <u>Nat Biotechnol</u> **26**(3): 303-304.

Ripke, S., C. O'Dushlaine, et al. (2013). "Genome-wide association analysis identifies 13 new risk loci for schizophrenia." <u>Nat Genet</u> **45**(10): 1150-1159.

Risso, D., J. Ngai, et al. (2014). "Normalization of RNA-seq data using factor analysis of control genes or samples." <u>Nat Biotechnol</u> **32**(9): 896-902.

Ritchie, M. E., B. Phipson, et al. (2015). "limma powers differential expression analyses for RNA-sequencing and microarray studies." <u>Nucleic Acids Res</u> **43**(7): e47.

Rosenberg, S. S. and N. C. Spitzer (2011). "Calcium signaling in neuronal development." Cold Spring Harb Perspect Biol **3**(10): a004259.

Rosenberg, T., S. Gal-Ben-Ari, et al. (2014). "The roles of protein expression in synaptic plasticity and memory consolidation." Front Mol Neurosci **7**: 86.

Rowitch, D. H. and A. R. Kriegstein (2010). "Developmental genetics of vertebrate glial-cell specification." Nature **468**(7321): 214-222.

Roy, N. C., E. Altermann, et al. (2011). "A comparison of analog and Next-Generation transcriptomic tools for mammalian studies." Brief Funct Genomics **10**(3): 135-150.

Rustay, N. R., C. C. Wrenn, et al. (2005). "Galanin impairs performance on learning and memory tasks: findings from galanin transgenic and GAL-R1 knockout mice." Neuropeptides **39**(3): 239-243.

Saba, R. and G. M. Schratt (2010). "MicroRNAs in neuronal development, function and dysfunction." Brain Res **1338**: 3-13.

Saito, T. and P. Saetrom (2010). "MicroRNAs--targeting and target prediction." N Biotechnol **27**(3): 243-249.

Sargolini, F., M. Fyhn, et al. (2006). "Conjunctive representation of position, direction, and velocity in entorhinal cortex." Science **312**(5774): 758-762.

Sato, F., S. Tsuchiya, et al. (2009). "Intra-platform repeatability and inter-platform comparability of microRNA microarray technology." PLoS One **4**(5): e5540.

Savelli, F., D. Yoganarasimha, et al. (2008). "Influence of boundary removal on the spatial representations of the medial entorhinal cortex." Hippocampus **18**(12): 1270-1282.

Sayed, D. and M. Abdellatif (2011). "MicroRNAs in development and disease." Physiol Rev **91**(3): 827-887.

Schevzov, G., N. S. Bryce, et al. (2005). "Specific features of neuronal size and shape are regulated by tropomyosin isoforms." Mol Biol Cell **16**(7): 3425-3437.

Schmidt-Hieber, C. and M. Hausser (2013). "Cellular mechanisms of spatial navigation in the medial entorhinal cortex." Nat Neurosci **16**(3): 325-331.

Scholtens, D. and A. von Heydebreck (2005). Analysis of Differential Gene Expression Studies. Bioinformatics and Computational Biology Solutions Using R and Bioconductor. R. Gentleman, V. J. Carey, W. Huber, R. A. Irizarry and S. Dudoit, Springer**:** pp 229-248.

Schreiner, D., J. N. Savas, et al. (2017). "Synapse biology in the 'circuit-age'-paths toward molecular connectomics." Curr Opin Neurobiol **42**: 102-110.

Schuldiner, O. and A. Yaron (2015). "Mechanisms of developmental neurite pruning." Cell Mol Life Sci **72**(1): 101-119.

Schwarcz, R., T. Eid, et al. (2000). "Neurons in layer III of the entorhinal cortex. A role in epileptogenesis and epilepsy?" Ann N Y Acad Sci **911**: 328-342.

Scoville, W. B. and B. Milner (1957). "Loss of recent memory after bilateral hippocampal lesions." J Neurol Neurosurg Psychiatry **20**(1): 11-21.

Semple, B. D., K. Blomgren, et al. (2013). "Brain development in rodents and humans: Identifying benchmarks of maturation and vulnerability to injury across species." Prog Neurobiol **106-107**: 1-16.

Sengupta, P. (2013). "The Laboratory Rat: Relating Its Age With Human's." Int J Prev Med **4**(6): 624-630.

Seok, H., J. Ham, et al. (2016). "MicroRNA Target Recognition: Insights from Transcriptome-Wide Non-Canonical Interactions." Mol Cells **39**(5): 375-381.

SeqQC (2014). "A comprehensive assessment of RNA-seq accuracy, reproducibility and information content by the Sequencing Quality Control Consortium." Nat Biotechnol **32**(9): 903-914.

Shah, S., E. Lubeck, et al. (2016). "In Situ Transcription Profiling of Single Cells Reveals Spatial Organization of Cells in the Mouse Hippocampus." Neuron **92**(2): 342-357.

Shapiro, M. (2015). "A limited positioning system for memory." Hippocampus **25**(6): 690-696.

Simon, C. M., S. Rauskolb, et al. (2015). "Dysregulated IGFBP5 expression causes axon degeneration and motoneuron loss in diabetic neuropathy." Acta Neuropathol **130**(3): 373-387.

Slonim, D. K. and I. Yanai (2009). "Getting started in gene expression microarray analysis." PLoS Comput Biol **5**(10): e1000543.

Smalheiser, N. R. (2014). "The RNA-centred view of the synapse: non-coding RNAs and synaptic plasticity." Philos Trans R Soc Lond B Biol Sci **369**(1652).

Small, S. A., S. A. Schobel, et al. (2011). "A pathophysiological framework of hippocampal dysfunction in ageing and disease." Nat Rev Neurosci **12**(10): 585-601.

Smyth, G. K. (2004). "Linear models and empirical bayes methods for assessing differential expression in microarray experiments." Stat Appl Genet Mol Biol **3**: Article3.

Smyth, G. K. (2005). Limma: linear models for microarray data. Bioinformatics and Computational Biology Solutions using R and Bioconductor. R. Gentleman, V. J. Carey, S. Dudoit, R. Irizarry and W. Huber. New York, Springer**:** pages 397-420.

Solodkin, A. and G. W. Van Hoesen (1996). "Entorhinal cortex modules of the human brain." J Comp Neurol **365**(4): 610-617.

Solstad, T., C. N. Boccara, et al. (2008). "Representation of geometric borders in the entorhinal cortex." Science **322**(5909): 1865-1868.

Solstad, T., E. I. Moser, et al. (2006). "From grid cells to place cells: a mathematical model." Hippocampus **16**(12): 1026-1031.

Soneson, C. and M. Delorenzi (2013). "A comparison of methods for differential expression analysis of RNA-seq data." BMC Bioinformatics **14**: 91.

Southwell, D. G., C. R. Nicholas, et al. (2014). "Interneurons from embryonic development to cell-based therapy." Science **344**(6180): 1240622.

Squire, L. R., C. E. Stark, et al. (2004). "The medial temporal lobe." Annu Rev Neurosci **27**: 279-306.

Stansberg, C., K. M. Ersland, et al. (2011). "Gene expression in the rat brain: high similarity but unique differences between frontomedial-, temporal- and occipital cortex." BMC Neurosci **12**: 15.

Stappert, L., B. Roese-Koerner, et al. (2015). "The role of microRNAs in human neural stem cells, neuronal differentiation and subtype specification." Cell Tissue Res **359**(1): 47-64.

Stead, J. D., C. Neal, et al. (2006). "Transcriptional profiling of the developing rat brain reveals that the most dramatic regional differentiation in gene expression occurs postpartum." J Neurosci **26**(1): 345-353.

Steinkraus, B. R., M. Toegel, et al. (2016). "Tiny giants of gene regulation: experimental strategies for microRNA functional studies." Wiley Interdiscip Rev Dev Biol **5**(3): 311-362.

Stengaard-Pedersen, K. (1983). "Comparative mapping of opioid receptors and enkephalin immunoreactive nerve terminals in the rat hippocampus. A radiohistochemical and immunocytochemical study." Histochemistry **79**(3): 311-333.

Stensola, H., T. Stensola, et al. (2012). "The entorhinal grid map is discretized." <u>Nature</u> **492**(7427): 72-78.

Stranahan, A. M., J. R. Erion, et al. (2013). "Reelin signaling in development, maintenance, and plasticity of neural networks." <u>Ageing Res Rev</u> **12**(3): 815-822.

Stranahan, A. M. and M. P. Mattson (2010). "Selective vulnerability of neurons in layer II of the entorhinal cortex during aging and Alzheimer's disease." <u>Neural Plast</u> **2010**: 108190.

Strange, B. A., M. P. Witter, et al. (2014). "Functional organization of the hippocampal longitudinal axis." <u>Nat Rev Neurosci</u> **15**(10): 655-669.

Sun, C., T. Kitamura, et al. (2015). "Distinct speed dependence of entorhinal island and ocean cells, including respective grid cells." <u>Proc Natl Acad Sci U S A</u> **112**(30): 9466-9471.

Sun, T. and R. F. Hevner (2014). "Growth and folding of the mammalian cerebral cortex: from molecules to malformations." <u>Nat Rev Neurosci</u> **15**(4): 217-232.

Sweatt, J. D. (2016). "Neural plasticity and behavior - sixty years of conceptual advances." <u>J Neurochem</u> **139 Suppl 2**: 179-199.

Tahvildari, B. and A. Alonso (2005). "Morphological and electrophysiological properties of lateral entorhinal cortex layers II and III principal neurons." <u>J Comp Neurol</u> **491**(2): 123-140.

Tam Tam, S., I. Bastian, et al. (2011). "MicroRNA-143 expression in dorsal root ganglion neurons." <u>Cell Tissue Res</u> **346**(2): 163-173.

Tang, Q., A. Burgalossi, et al. (2014). "Pyramidal and stellate cell specificity of grid and border representations in layer 2 of medial entorhinal cortex." <u>Neuron</u> **84**(6): 1191-1197.

Tao, J., H. Wu, et al. (2011). "Deletion of astroglial Dicer causes non-cell-autonomous neuronal dysfunction and degeneration." <u>J Neurosci</u> **31**(22): 8306-8319.

Taube, J. S. (2007). "The head direction signal: origins and sensory-motor integration." <u>Annu Rev Neurosci</u> **30**: 181-207.

Taube, J. S., R. U. Muller, et al. (1990). "Head-direction cells recorded from the postsubiculum in freely moving rats. I. Description and quantitative analysis." <u>J Neurosci</u> **10**(2): 420-435.

Thompson, C. L., S. D. Pathak, et al. (2008). "Genomic anatomy of the hippocampus." <u>Neuron</u> **60**(6): 1010-1021.

Thompson, R. F. and J. J. Kim (1996). "Memory systems in the brain and localization of a memory." <u>Proc Natl Acad Sci U S A</u> **93**(24): 13438-13444.

Thomsen, R., P. S. Nielsen, et al. (2005). "Dramatically improved RNA in situ hybridization signals using LNA-modified probes." <u>RNA</u> **11**(11): 1745-1748.

Thomson, D. W., C. P. Bracken, et al. (2011). "Experimental strategies for microRNA target identification." <u>Nucleic Acids Res</u> **39**(16): 6845-6853.

Tronel, S., A. Fabre, et al. (2010). "Spatial learning sculpts the dendritic arbor of adult-born hippocampal neurons." <u>Proc Natl Acad Sci U S A</u> **107**(17): 7963-7968.

Tsao, A., M. B. Moser, et al. (2013). "Traces of Experience in the Lateral Entorhinal Cortex." <u>Current Biology</u> **23**(5): 399-405.

Tsien, R. Y. (2013). "Very long-term memories may be stored in the pattern of holes in the perineuronal net." <u>Proc Natl Acad Sci U S A</u> **110**(30): 12456-12461.

Upadhya, M. A., K. T. Nakhate, et al. (2011). "Cocaine- and amphetamine-regulated transcript peptide increases spatial learning and memory in rats." <u>Life Sci</u> **88**(7-8): 322-334.

Urbanek, M. O., A. U. Nawrocka, et al. (2015). "Small RNA Detection by in Situ Hybridization Methods." <u>Int J Mol Sci</u> **16**(6): 13259-13286.

Valor, L. M. and A. Barco (2012). "Hippocampal gene profiling: toward a systems biology of the hippocampus." Hippocampus **22**(5): 929-941.

Valsalan, R. and N. Manoj (2014). "Evolutionary history of the neuropeptide S receptor/neuropeptide S system." Gen Comp Endocrinol **209**: 11-20.

van Strien, N. M., N. L. Cappaert, et al. (2009). "The anatomy of memory: an interactive overview of the parahippocampal-hippocampal network." Nat Rev Neurosci **10**(4): 272-282.

Vandesompele, J., K. De Preter, et al. (2002). "Accurate normalization of real-time quantitative RT-PCR data by geometric averaging of multiple internal control genes." Genome Biol **3**(7): RESEARCH0034.

Varga, C., S. Y. Lee, et al. (2010). "Target-selective GABAergic control of entorhinal cortex output." Nat Neurosci **13**(7): 822-824.

Vidigal, J. A. and A. Ventura (2015). "The biological functions of miRNAs: lessons from in vivo studies." Trends Cell Biol **25**(3): 137-147.

Vuong, C. K., D. L. Black, et al. (2016). "The neurogenetics of alternative splicing." Nat Rev Neurosci **17**(5): 265-281.

Wan, H., J. P. Aggleton, et al. (1999). "Different contributions of the hippocampus and perirhinal cortex to recognition memory." J Neurosci **19**(3): 1142-1148.

Wang, B., P. Howel, et al. (2011). "Systematic evaluation of three microRNA profiling platforms: microarray, beads array, and quantitative real-time PCR array." PLoS One **6**(2): e17167.

Wang, D. and J. Fawcett (2012). "The perineuronal net and the control of CNS plasticity." Cell Tissue Res **349**(1): 147-160.

Wang, W. X., B. W. Rajeev, et al. (2008). "The expression of microRNA miR-107 decreases early in Alzheimer's disease and may accelerate disease progression through regulation of beta-site amyloid precursor protein-cleaving enzyme 1." J Neurosci **28**(5): 1213-1223.

Wang, X., G. Hu, et al. (2010). "Repression of versican expression by microRNA-143." J Biol Chem **285**(30): 23241-23250.

Warford, A. (2016). "In situ hybridisation: Technologies and their application to understanding disease." Prog Histochem Cytochem **50**(4): 37-48.

Watson, R. E., J. M. Desesso, et al. (2006). "Postnatal growth and morphological development of the brain: a species comparison." Birth Defects Res B Dev Reprod Toxicol **77**(5): 471-484.

Weedall, G. D., H. Irving, et al. (2015). "Molecular tools for studying the major malaria vector Anopheles funestus: improving the utility of the genome using a comparative poly(A) and Ribo-Zero RNAseq analysis." BMC Genomics **16**: 931.

Wills, T. J., C. Barry, et al. (2012). "The abrupt development of adult-like grid cell firing in the medial entorhinal cortex." Front Neural Circuits **6**: 21.

Wills, T. J. and F. Cacucci (2014). "The development of the hippocampal neural representation of space." Curr Opin Neurobiol **24**(1): 111-119.

Wills, T. J., F. Cacucci, et al. (2010). "Development of the hippocampal cognitive map in preweaning rats." Science **328**(5985): 1573-1576.

Wills, T. J., L. Muessig, et al. (2014). "The development of spatial behaviour and the hippocampal neural representation of space." Philos Trans R Soc Lond B Biol Sci **369**(1635): 20130409.

Winkler, E. A., A. P. Sagare, et al. (2014). "The pericyte: a forgotten cell type with important implications for Alzheimer's disease?" Brain Pathol **24**(4): 371-386.

Winson, J. (1978). "Loss of hippocampal theta rhythm results in spatial memory deficit in the rat." Science **201**(4351): 160-163.

Winter, S. S. and J. S. Taube (2014). Head direction cells: from generation to integration. Space,Time and Memory in the Hippocampal Formation. D. Derdikman and J. J. Knierim, Springer**:** 83–106.

Witkos, T. M., E. Koscianska, et al. (2011). "Practical Aspects of microRNA Target Prediction." Curr Mol Med **11**(2): 93-109.

Witter, M. P., C. B. Canto, et al. (2014). "Architecture of spatial circuits in the hippocampal region." Philos Trans R Soc Lond B Biol Sci **369**(1635): 20120515.

Witter, M. P., T. P. Doan, et al. (2017). "Architecture of the Entorhinal Cortex A Review of Entorhinal Anatomy in Rodents with Some Comparative Notes." Front Syst Neurosci **11**: 46.

Witter, M. P., F. G. Wouterlood, et al. (2000). "Anatomical organization of the parahippocampal-hippocampal network." Ann N Y Acad Sci **911**: 1-24.

Wu, Z., X. Liu, et al. (2014). "Regulation of lncRNA expression." Cell Mol Biol Lett **19**(4): 561-575.

Wyss-Coray, T. and J. Rogers (2012). "Inflammation in Alzheimer disease-a brief review of the basic science and clinical literature." Cold Spring Harb Perspect Med **2**(1): a006346.

Xiao, F., Z. Zuo, et al. (2009). "miRecords: an integrated resource for microRNA-target interactions." Nucleic Acids Res **37**(Database issue): D105-110.

Xin, M., E. M. Small, et al. (2009). "MicroRNAs miR-143 and miR-145 modulate cytoskeletal dynamics and responsiveness of smooth muscle cells to injury." Genes Dev **23**(18): 2166-2178.

Xu, R. H., B. Liu, et al. (2016). "miR-143 is involved in endothelial cell dysfunction through suppression of glycolysis and correlated with atherosclerotic plaques formation." Eur Rev Med Pharmacol Sci **20**(19): 4063-4071.

Xu, W., A. San Lucas, et al. (2014). "Identifying microRNA targets in different gene regions." BMC Bioinformatics **15 Suppl 7**: S4.

Xu, Y. L., C. M. Gall, et al. (2007). "Distribution of neuropeptide S receptor mRNA and neurochemical characteristics of neuropeptide S-expressing neurons in the rat brain." J Comp Neurol **500**(1): 84-102.

Yang, J., Y. Yao, et al. (2017). "Gastrin-releasing peptide facilitates glutamatergic transmission in the hippocampus and effectively prevents vascular dementia induced cognitive and synaptic plasticity deficits." Exp Neurol **287**(Pt 1): 75-83.

Yang, K., J. I. Broussard, et al. (2017). "Dopamine receptor activity participates in hippocampal synaptic plasticity associated with novel object recognition." Eur J Neurosci **45**(1): 138-146.

Yates, L. A., C. J. Norbury, et al. (2013). "The long and short of microRNA." Cell **153**(3): 516-519.

Yoganarasimha, D., G. Rao, et al. (2011). "Lateral entorhinal neurons are not spatially selective in cue-rich environments." Hippocampus **21**(12): 1363-1374.

Young, B. J., T. Otto, et al. (1997). "Memory representation within the parahippocampal region." J Neurosci **17**(13): 5183-5195.

Yu, Y., J. C. Fuscoe, et al. (2014). "A rat RNA-Seq transcriptomic BodyMap across 11 organs and 4 developmental stages." Nat Commun **5**: 3230.

Yuan, J. S., A. Reed, et al. (2006). "Statistical analysis of real-time PCR data." BMC Bioinformatics **7**: 85.

Zeisel, A., A. B. Munoz-Manchado, et al. (2015). "Brain structure. Cell types in the mouse cortex and hippocampus revealed by single-cell RNA-seq." Science **347**(6226): 1138-1142.

Zhang, D., L. Xie, et al. (2015). "In situ Detection of MicroRNAs: The Art of MicroRNA Research in Human Diseases." Journal of cytology & histology **Suppl 3(1):013**.

Zhang, H. P., Z. Xiao, et al. (2014). "Bombesin facilitates GABAergic transmission and depresses epileptiform activity in the entorhinal cortex." Hippocampus **24**(1): 21-31.

Zhang, J., X. Y. Sun, et al. (2015). "MicroRNA-7/Shank3 axis involved in schizophrenia pathogenesis." J Clin Neurosci **22**(8): 1254-1257.

Zhang, S. J., J. Ye, et al. (2013). "Optogenetic dissection of entorhinal-hippocampal functional connectivity." Science **340**(6128): 1232627.

Zhao, S. (2014). "Assessment of the impact of using a reference transcriptome in mapping short RNA-Seq reads." PLoS One **9**(7): e101374.

Zhao, S., W. P. Fung-Leung, et al. (2014). "Comparison of RNA-Seq and microarray in transcriptome profiling of activated T cells." PLoS One **9**(1): e78644.

Zhao, W., X. He, et al. (2014). "Comparison of RNA-Seq by poly (A) capture, ribosomal RNA depletion, and DNA microarray for expression profiling." BMC Genomics **15**: 419.

Zhao, X., X. He, et al. (2010). "MicroRNA-mediated control of oligodendrocyte differentiation." Neuron **65**(5): 612-626.

Zhao, Z., A. R. Nelson, et al. (2015). "Establishment and Dysfunction of the Blood-Brain Barrier." Cell **163**(5): 1064-1078.

Zhu, X. O., M. W. Brown, et al. (1995). "Neuronal signalling of information important to visual recognition memory in rat rhinal and neighbouring cortices." Eur J Neurosci **7**(4): 753-765.

Zhuang, F., R. T. Fuchs, et al. (2012). "Small RNA expression profiling by high-throughput sequencing: implications of enzymatic manipulation." J Nucleic Acids **2012**: 360358.

Ziegenhain, C., B. Vieth, et al. (2017). "Comparative Analysis of Single-Cell RNA Sequencing Methods." Mol Cell **65**(4): 631-643 e634.

PAPER I

PAPER II

CrossMark

ORIGINAL ARTICLE

MicroRNAs contribute to postnatal development of laminar differences and neuronal subtypes in the rat medial entorhinal cortex

Lene C. Olsen[1] · Kally C. O'Reilly[2] · Nina B. Liabakk[1] · Menno P. Witter[2] ·
Pål Sætrom[1,3,4]

Abstract The medial entorhinal cortex (MEC) is important in spatial navigation and memory formation and its layers have distinct neuronal subtypes, connectivity, spatial properties, and disease susceptibility. As little is known about the molecular basis for the development of these laminar differences, we analyzed microRNA (miRNA) and messenger RNA (mRNA) expression differences between rat MEC layer II and layers III–VI during postnatal development. We identified layer and age-specific regulation of gene expression by miRNAs, which included processes related to neuron specialization and locomotor behavior. Further analyses by retrograde labeling and expression profiling of layer II stellate neurons and in situ hybridization revealed that the miRNA most up-regulated in layer II, miR-143, was enriched in stellate neurons, whereas the miRNA most up-regulated in deep layers, miR-219-5p, was expressed in ependymal cells, oligodendrocytes and glia. Bioinformatics analyses of predicted mRNA targets with negatively correlated expression patterns to miR-143 found that miR-143 likely regulates the Lmo4 gene, which is known to influence hippocampal-based spatial learning.

Keywords Medial entorhinal cortex · MiRNA · Brain development · Stellate neurons

✉ Pål Sætrom
pal.satrom@ntnu.no

[1] Department of Cancer Research and Molecular Medicine, Norwegian University of Science and Technology, Trondheim, Norway

[2] Kavli Institute for Systems Neuroscience and Centre for Neural Computation, Norwegian University for Science and Technology, Trondheim, Norway

[3] Department of Computer and Information Science, Norwegian University for Science and Technology, Trondheim, Norway

[4] Bioinformatics core facility-BioCore, Norwegian University of Science and Technology, Trondheim, Norway

Introduction

The entorhinal cortex (EC) is implicated in the formation of memory. In particular, the medial part of the entorhinal cortex (MEC) is important for spatial memory and navigation (Derdikman and Moser 2010; Eichenbaum et al. 2012). The MEC has a laminar structure in which each layer has dominant cell types, differing in physiological properties and connectivity (Canto and Witter 2012; Greenhill et al. 2014). The laminar topography is also evident with regards to gene expression (Ramsden et al. 2015) and in certain pathological conditions; neuronal death and neurofibrillary tangles form in layer II (LII) at early stages of Alzheimer's disease (Gomez-Isla et al. 1996), and LII also displays abnormalities in schizophrenia (Arnold 2000), whereas layer III of MEC has been implicated in temporal lobe epilepsy (Schwarcz et al. 2000). Origins of laminar differences in MEC are therefore important for both normal and pathological MEC functions.

The overall structure of MEC is observable at birth, but there is substantial postnatal development of MEC cells, physiological properties, and projections, continuing at least until postnatal day 28 (P28) (Burton et al. 2008). With respect to cell types, it is established that the adult rat MEC contains several types of spatially tuned neurons, including grid, border, and head direction cells, as well as speed modulated neurons and conjunctive cells that display both

grid and head direction properties (Rowland et al. 2016). Spatially tuned neurons are unevenly distributed across MEC layers, with the majority of grid cells found in LII (Sargolini et al. 2006). The dominant cell type (67%) in LII is the glutamatergic stellate neuron (Gatome et al. 2010), thereby making it likely that this neuron corresponds to the grid cell, although this has been debated by several groups (Domnisoru et al. 2013; Moser and Moser 2013; Tang et al. 2014). General postnatal development in all cortical areas of the rat includes glial cell production and specialization, myelination, and an overproduction of synapses in infancy followed by pruning in juveniles (Downes and Mullins 2014; Semple et al. 2013). Extensive synaptogenesis and dendrite formation also occurs in the MEC, and the stellate neurons double their spine density between P14 and P18 (Burton et al. 2008). The physiological properties of MEC neurons also mature during the first postnatal weeks, with stellate cells exhibiting falling resistance and increasing resonance (Burton et al. 2008; Langston et al. 2010). Whereas grid-like cells are present soon after the eyes open (~P14), the grid cell properties stabilize around 4 weeks of age (Langston et al. 2010). Other spatially tuned cells mature earlier. Head direction cells appear adult-like upon eye opening, and boundary cells display adult-like firing when the rats begin to explore their environment (Bjerknes et al. 2014; Langston et al. 2010). The major projection from MEC to hippocampus already shows adult-like topography within the first postnatal week (Deng et al. 2007; O'Reilly et al. 2015). However, this MEC-to-hippocampus projection density is not considered adult-like until P10 (Deng et al. 2007). Changes through the first few weeks after birth are therefore fundamental for the properties of the adult MEC.

As changes in spatio-temporal gene expression underlie general postnatal development, layer-specific gene expression likely guides the cellular, physiological, and structural changes occurring postnatally in each MEC layer. Reelin (Reln, see Supplementary Table 1 for full gene names) plays a role in the development of neuron morphology and layer-specific connections in both the EC and the rest of the cortex (Borrell et al. 1999; Stranahan et al. 2013), but little is known about other molecular changes orchestrating laminar specialization.

MicroRNAs (miRNAs) are small non-coding RNA molecules that regulate gene expression after transcription and are important in many aspects of central nervous system development (Olde Loohuis et al. 2012). Many miRNAs are differentially expressed in various brain regions (Olsen et al. 2009), reflecting the brain region specific regulation of messenger RNAs (mRNAs). Some miRNAs also regulate mRNAs locally at the synapse and play a role in the development of neuronal morphology and regulation of synaptic plasticity (Olde Loohuis et al. 2012), whereas

other miRNAs are involved in specifying neuronal subtypes (Stappert et al. 2015).

Knowing the importance of miRNAs in orchestrating neuronal development and most other cellular processes, we hypothesized that miRNAs contribute to the laminar and neuronal subtype specialization within the MEC in general, and the stellate cells in particular. We therefore measured miRNA expression in LII, where the stellate cells are abundant, and the deeper layers (layers III–VI, LDeep) of the MEC of rats during postnatal development. We sampled at P2, P9, P23, and P45, as these ages represent early, intermediate, late, and completed postnatal developmental time points, respectively, and thereby cover major developmental events, including maturation of grid cells and onset of hippocampal spatial learning (Fig. 1a). In addition, we examined the miRNA profile of the stellate cells compared to the rest of the MEC at an early postnatal age (P4/5). We found several miRNAs to be differentially expressed between layers and cell types (stellate vs. non-stellate cells). To identify more likely target gene candidates for interesting miRNAs in the MEC, we measured ribosomal RNA-depleted total RNA gene expression in LII and LDeep at the same time points. MicroRNAs with increased expression level in older rats compared to younger rats appear to play a role in the cell cycle and early developmental events such as axon guidance, whereas miRNAs with opposite expression patterns seem to have important roles in synaptic transmission, plasticity and myelination. Important for navigation, miRNAs with decreased expression in older rats also appear to regulate locomotor behavior. Two miRNAs, miR-143 and miR-150, were up-regulated both in LII and in stellate neurons. The most significant up- and down-regulated miRNAs in LII (miR-143 and miR-219-5p, respectively) were validated by in situ hybridization. By analyzing for enriched ontology terms for their predicted, negatively correlated target genes, we found that miR-219-5p appears to regulate myelination, while miR-143 likely contributes to the specification of neuronal subtypes.

Methods

Animals

Long Evans pups were used for the studies presented here. Breeding harems consisted of one male rat and up to three female rats. The harems were housed in an enriched environment with toys and access to food and water ad libitum. The rats were maintained on a 12 h reversed light/dark schedule. Cages were examined morning and evening, and the day pups were observed was considered P0. Litters were culled to approximately ten pups by P3. Pups were allowed to remain with the mother in the nest until weaning at P21.
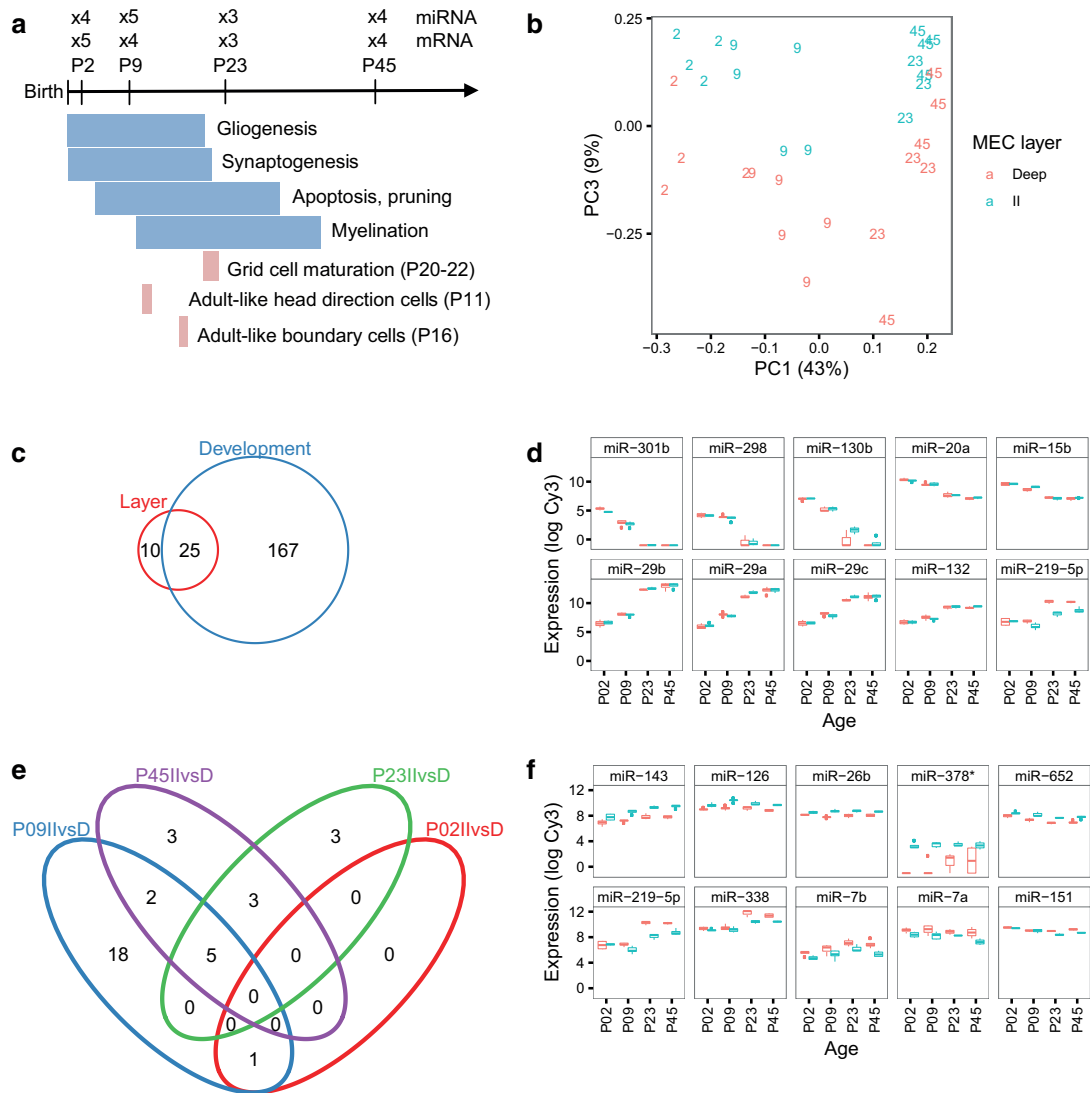
Fig. 1 Analysis of miRNA expression in MEC. **a** Overview of the laminar gene expression experiment. Time points and number of biological replicates used for miRNA and mRNA expression analysis in relation to the timing of major maturation events (*blue*) and the known maturation time points of navigational cell types in MEC (*tan*). **b** Principal component analysis of the miRNA expression samples. The *x* and *y axes* show the first and third principle components (PC1 and PC3); the axes text specify the percentage of expression variation explained by the respective PCs. PC2 depicted a mixture between age and layers, whereas PC3 clearly reflected laminar differences. Each *character string* represents the age of the animal and an age-specific number identifying LII (*turquoise*) and LDeep (*red*) samples from the same animal. **c** *Venn diagram* showing the number of differentially expressed miRNAs between layers (*red*) and between ages (*blue*, P2/P9 vs. P23/P45, LFC = 0, BH < 0.05), and their overlap. **d** Expression of the five most significant down-regulated (*top*) and up-regulated (*bottom*) miRNAs between ages. **e** *Venn diagram* showing the number of miRNAs DE between layers at P2 (*red*), P9 (*blue*), P23 (*green*), and P45 (*purple*), and their overlap. **f** Expression patterns of the five most significant miRNAs up-regulated in LII (*top*) and up-regulated in LDeep (*bottom*) across development

All procedures were approved by a local ethics committee according to Norwegian and EU regulations.

Collection and dissection of laminar tissue samples

Rats aged P2, P9, P23, and P45 were anesthetized with isoflurane and decapitated. The brains were quickly harvested and kept in ice cold artificial spinal fluid. Horizontal 400 μm sections were cut on a Leica VT 1000 S microtome and put in RNA*later*® (AM7020, Ambion, Austin, TX, USA). The tissue sections were kept at 4 °C until dissection. Bilateral dissection of layer II and layers III-VI (LDeep) of MEC was performed, while watching the tissue through a dissection microscope (Zeiss Discovery V8 stereomicroscope) applying architectonic criteria (Boccara et al. 2015; O'Reilly et al. 2015; Paxinos and Watson 2007) to unstained tissue. In horizontal sections, MEC is easily recognized using transmitted and reflected white light by the marked shape of the cortex, the prominent white, opaque lamina dissecans and the radial organization of the layers deep to the latter. Layer II neurons are large spherical neurons, which differ markedly in level of opacity from those in layer III. The medial border between MEC and parasubiculum is characterized by the loss of the differences between layers II and III, while the border with the laterally adjacent postrhinal cortex is characterized by the loss of the large spherical neurons in layer II. All dissections avoided border regions, i.e., were taken centered in the identified MEC and specific layers. The dissected MEC tissue was transferred into fresh RNA*later*® and kept at −20 °C until RNA purification.

RNA purification and quality control

Total RNA was purified using the RNAqueous®-Micro kit (AM1931, Ambion, Austin, TX, USA). The manufacturer's instructions were followed, except that wash steps 2 and 3 were modified to include rolling of the tubes and incubation with the wash buffer for 1 min, and the ethanol added for precipitation was increased to 1.25× lysis buffer volume to include small RNAs. The RNA was eluted in 2×10 μl RNAqueous Elution Buffer. In the layer samples for miRNA microarray analysis, four of the tissue samples were extracted using the mirVana™ kit (Ambion, Austin, TX, USA). The RNA was eluted in 2×50 μl mirVana Elution Buffer. We used the Norgen Total RNA purification kit (Norgen Biotek, Canada) to purify RNA from whole medial entorhinal tissue.

RNA yield was determined using the NanoDrop 1000 spectrophotometer or the Qubit® 2.0 Fluorometer (Life Technologies, Carlsbad, CA), and the quality was assessed with the Agilent BioAnalyzer 2100 Nano chip. Only samples with a RIN value of 8.5 or above were included for further analysis. Isolated RNA samples were stored at −80 °C until further use.

Microarray analysis

The total RNA from the laminar samples were shipped on dry ice to IMGM® Laboratories in Martinsried, Germany, for microarray analysis. 100 ng total RNA per sample were introduced into the labeling reaction. Prior to this, the total RNA samples were spiked with in vitro synthesized oligonucleotides (MicroRNA Spike-In Kit, Agilent Technologies), which serve as an internal labeling control for linearity, sensitivity and accuracy. Microarray analyses were done on Rat miRNA Microarrays, Release 15.0 (Agilent Technologies, AMADID 029200, 8×15 K format), according to the manufacturer's instructions. The miRNA expression data has been submitted to the Gene Expression Omnibus (GEO) database with accession number GSE85753.

Retrograde labeling of stellate cells

On P2, Long Evans rats were anesthetized with isoflurane in an induction chamber and then moved to a stereotaxic frame. Rats were placed in a neonatal mask (Kopf, model 973-B, Tujunga, CA, USA), head fixed using zygoma ear cups (Kopf, model 921, Tujunga, CA, USA), while isoflurane anesthesia was maintained for the duration of the surgery. Saline was administered subcutaneously during the course of the surgery (up to 50 μl/g body weight). Rats were also administered 5 μg/g body weight of rimadyl as an analgesic. The retrograde tracer dioctadecyloxacarbocyanine (DiO, cat# D275, Invitrogen, Molecular Probes, Eugene, OR, USA) dissolved in ethanol:dimethyl sulfoxide (9:1 EtOH:DMSO) at a concentration of 3 mg/mL was iontophoretically injected into the dentate gyrus through glass micropipettes (outer diameter of ~30 μm). We used a 5- to 7-μA alternating positive current (6 s on/6 s off for 15 min) delivered by a digital current source (Stoelting Europe, Dublin, Ireland). After recovery under a heat lamp, rat pups were returned to maternal care for 24–48 h.

At P4/5, the animal was decapitated while under deep isoflurane anesthesia. Retrogradely labeled and non-labeled MEC was dissected from both hemispheres, minced into smaller pieces in a bath of ice cold Hibernate A (no phenol red, Brain Bits) containing 0.5 mM Glutamine and B27 supplement (17504-044, Invitrogen, Carlsbad, CA, USA) to support neuronal viability. The pieces were aspirated into a tube containing Hibernate A at 4 °C using a wide bore pipette.

P4/5 was chosen to ensure easier dissociation in the absence of myelin, and also to allow shorter transportation times for the dye.

Cell dissociation

The dissected entorhinal tissue was dissociated using a protocol adapted from Brewer (Brewer 1997). Briefly, the tube containing the pieces of entorhinal cortex in Hibernate A was kept at 30 °C for 5 min with occasional resuspension of the pieces. The Hibernate A was then aspirated and replaced by 1 ml of pre-warmed Hibernate A with 2 mg/ml papain (LS003119, 26.1 U/mg, 79% protein, Worthington Biochemical Corporation, Lakewood, NJ, USA). The tube was incubated at 30 °C for 30 min with resuspension of pieces every 5 min, after which the enzyme solution was replaced with 0.5 ml Hibernate A/B27 at 30 °C. DNase (D4527-10KU, Sigma–Aldrich Co. LLC, St. Louis, MO, USA) was added to the suspension solution (0.3 U/ml), followed by a 5 min incubation at room temperature before gentle trituration with a Pasteur pipette. The suspension was allowed to settle for 2 min before the supernatant was transferred to a fresh tube and the pellet resuspended in 0.5 ml Hibernate/B27. This trituration procedure was repeated twice more using Pasteur pipettes with consecutively smaller openings.

The resulting cell suspension was centrifuged on an Optiprep gradient (1114542, Axis-Shield PoC, Oslo, Norway) according to the manufacturer's application sheet C29. The top two ml and the densest layer of debris were removed, before diluting the resulting suspension 1:2 with Hibernate A/B27.

Fluorescence activated cell sorting (FACS)

The retrogradely labeled cells were separated from the non-labeled cells using a FACS Diva cell sorter (BD Biosciences). Cells were first gated based on forward and side scatter using Calcein Blue AM fluorescence (final concentration 2 μM, C1429, Invitrogen, Carlsbad, CA, USA) on a small portion of the cell suspension to determine the viable cell population. Propidium iodide (final concentration 1 μg/ml, Invitrogen, Carlsbad, CA, USA) was used to exclude apoptotic/dead cells, and fluorescence in the green channel was used to select retrogradely labeled DiO positive cells. 10,000–100,000 cells were sorted directly into RNAqueous®-Micro lysis buffer and stored at −80 °C before RNA purification. Cells from both hemispheres were pooled.

Taqman qPCR array analysis

The total RNA purified from the FACS sorted samples was shipped on dry ice to IMGM® Laboratories in Martinsried, Germany, for TaqMan array analysis. The TaqMan®MicroRNA Reverse Transcription Kit (Applied Biosystems) in combination with the Megaplex™ RT Primers, Rodent Pool Set v3.0 for TaqMan®MicroRNA Assays (Applied Biosystems) was used in a multiplex reverse transcription of miRNA into single stranded cDNA. In total, two (A+B) separate RT reactions were carried out for each sample with >1 ng of total RNA per reaction according to the manufacturer's instructions. 2.5 μl of each cDNA (A+B) were amplified using the TaqMan® PreAmp Master Mix together with the Megaplex™ PreAmp Primers, Rodent Pool Set v3.0 according to manufacturer's instructions. The software ViiA7 Software v1.2 (Applied Biosystems) was used for instrument control and raw data control. For each well, cycle threshold (Ct) values, i.e., the cycle number where the amplification curve clearly exceeds the background, were calculated in the software ViiA7 Software v1.2 using the default analysis settings. The TaqMan miRNA array data has been submitted to the GEO database with accession number GSE85752.

Deep sequencing

The Illumina TruSeq® Stranded Total RNA HT with Ribo-Zero Gold was used for library preparation according to the manufacturer's recommendations, and the resulting libraries were sequenced on the Illumina HiSeq 2500 (Illumina, San Diego, CA) using 2×100 bp paired end sequencing by the Genomics Core Facility at NTNU, Trondheim, Norway. The use of multiplex adapters allowed all samples to be run across all lanes. The RNA-seq data has been submitted to the GEO database with accession number GSE85789.

The sample for small RNA sequencing was prepared according to Illumina's small RNA TruSeq protocol, and sequenced using 50 bp single read on one lane on the Illumina HiSeq 2000 at the Norwegian High Throughput Sequencing Centre at Oslo University Hospital, Oslo, Norway. The small RNA-seq data has been submitted to the GEO database with accession number GSE85788.

In situ hybridization

We perfused two rats aged P23 intracardially with Ringers solution followed by 4% paraformaldehyde/PBS. The brains were extracted and postfixed for 24 h in 4% paraformaldehyde followed by cryoprotection in 0.5 M sucrose/PBS solution for 48 h (both at 4 °C). The brains were snap frozen in TissueTek OCT (Sakura, Japan) by immersion in an isopentane/dry ice slurry. 14 μm sagittal sections were cut by cryostat (Microm HM 560, Thermo Scientific) and mounted on SuperFrost® Plus slides (Thermo Scientific). The sections were dried for 45 min, and kept at −20 °C until further use.

In situ hybridization was performed with locked nucleic acid probes from Exiqon (Vedbaek, Denmark). The slides were removed from the freezer and allowed to thaw and

dry at room temperature for 15 min, before incubation with 1.25 or 1.5 μg/ml Proteinase K for 10 min at 37 °C. The rest of the procedure was according to Exiqon's miRCURY LNA™ microRNA ISH Optimization Kit (FFPE) Instruction manual v2, except that we used 40 μl of probe solution and covered with RNAseAWAY-treated parafilm. A Dako Hybridizer (Dako, Denmark) was used for all incubations. Imaging of sections was performed with a Zeiss Axio Imager M2 microscope, with a 5× magnification objective.

Data analysis

Statistical and other analyses were performed in R, unless otherwise stated. The miRNA microarray results were analyzed using the AgiMicroRna package (Lopez-Romero 2011) with the filterMicroRna function and quantile normalization of the total gene signal calculated by the Agilent Feature Extraction software. Limma with empirical Bayes correction was used to ascertain differential expression (v.3.18.13) (Smyth 2004).

We used the HTqPCR package (Dvinge and Bertone 2009) to analyze the TaqMan array data, with deltaCt normalization, and the filterCtData function to filter out "Undetermined" and "Unreliable" results. Differential expression was determined using the limmaCtData function.

For the Illumina small RNA sequencing data, raw reads were processed using CASAVA (v. 1.8.2 Illumina), and the quality of the reads assessed by FastQC (v0.11.2, http://www.bioinformatics.babraham.ac.uk/projects/fastqc/). We used Cutadapt v.1.0 (Martin 2011) to remove all reads below 15 nt and adapter sequences, as well as trimming low quality ends (Phred < 20). We also removed all reads with an average Phred quality score below 20 using FastQ Quality Filter (Fastx tool kit v.0.0.13, http://hannonlab.cshl.edu/fastx_toolkit/). The resulting reads were aligned to the Rn4 genome with Bowtie v.0.12.7 (Langmead et al. 2009), allowing up to ten alignments per read. The mapped reads were annotated and counted using HTSeqCount v.0.5.4p3 (Anders et al. 2015) with annotation data from miRBase v. 20.

For the Illumina paired end RNA sequencing analysis, raw reads were processed using bcl2fastq (v.1.8.4, Illumina). We removed adapter sequences, reads below 20 nt, and low quality bases at the ends using Trimmomatic (v.0.33) (Bolger et al. 2014). The sequences were aligned to the rat reference genome (Rn6) using STAR [v2.4.0, (Dobin et al. 2013)]. Annotation and gene counts were obtained using featureCounts of the Subread package (v1.4.6-p1) (Liao et al. 2014), using RefSeq gene annotations for Rn6 downloaded from UCSC on April 8, 2015. The counts were transformed with the Limma voom function (Law et al. 2014), and normalized by TMM

(Robinson and Oshlack 2010) and quantile normalization (Bolstad et al. 2003). We used Limma with empirical Bayes to identify differentially expressed genes (v.3.26.9) (Ritchie et al. 2015; Smyth 2004).

Overlaps between differentially expressed genes and miRNAs in different contrasts were visualized with the Vennerable package (https://github.com/js229/Vennerable), and overlaps between miRNA expression technologies were visualized with the Venneuler package (http://www.rforge.net/venneuler/). We grouped DE miRNAs into co-expression modules based on Pearson correlation, and groups were identified using the Partitioning Algorithm and the Recursive Thresholding (PART) method in the CRAN package clusterGenomics (Nilsen et al. 2013).

We downloaded validated targets for miRNAs of interest from miRTarBase (Hsu et al. 2014). Predicted, conserved targets for the same miRNAs were obtained from TargetScan v.6.2 (Grimson et al. 2007). We downloaded the "Conserved_Site_Context_Scores.txt" file, and selected rat genes with a context + score below −0.1. The most important target predictions were later examined against TargetScan v.7. MirbaseTracker (Van Peer et al. 2014) allowed miRNA naming conversions between different versions of miRBase.

To identify negatively correlated potential and validated targets of the differentially expressed miRNAs, we set three requirements. First, the mRNA had to be listed as a predicted, conserved target in TargetScan or as a validated target in miRTarBase. Second, both the miRNA and the mRNA had to be differentially expressed between LII and LDeep, or between younger (P2/P9) and older (P23/P45) animals. Third, the expression pattern of the miRNA had to be significantly negatively correlated with that of its mRNA target (Spearman's rho < −0.5).

Gene ontology analysis

GO, KEGG pathway, and REACTOME pathway enrichment analyses for *Rattus norvegicus* genes were performed using the Bioconductor package gProfileR (Reimand et al. 2007). Only genes displaying a log fold change (LFC) of more than 0.5 were included for the analysis. We also performed this analysis on predicted, conserved target genes of differentially expressed miRNAs that were expressed in the MEC. The p values for the enriched terms were adjusted with the FDR method, and only terms with an adjusted p value below 0.05 were included. We calculated the odds ratio for each enriched term using the Fisher's exact test. After removing terms containing more than 2500 genes, the results were curated manually to remove redundant and/or uninformative terms.

miRNA cluster analysis

We downloaded genomic coordinates of the different miR-NAs from miRBase, and defined a miRNA cluster as a minimum of two miRNAs, where each miRNA was located within 10 kb of the next miRNA member of the cluster.

Results

miRNA expression in MEC layers during postnatal development

To identify miRNAs that are important for postnatal development of the entorhinal cortex in general, and for laminar development within the MEC in particular, we performed miRNA microarray analysis on total RNA from LII and LDeep of rats at four different postnatal ages (P2, P9, P23, and P45; Fig. 1a, Supplementary Fig. 1). Because stellate cells are enriched in LII, we hypothesized that the results for LII would include findings relevant for this neuronal subtype.

Principal component analyses of the miRNA expression data showed that the main variation in the data separated the early (P2) and intermediate (P9) ages from the late (P23/P45) ages (Fig. 1b, component 1). To identify miRNAs that showed robust expression differences during development, we grouped the younger (P2/P9) and older (P23/P45) animals. After filtering and normalization (see methods), we found 192 miRNAs to be differentially expressed between ages (Fig. 1c; Supplementary Table 2; Benjamini-Hochberg (BH) adjusted p value < 0.05), of which 88 were down-regulated in older compared to younger animals (with higher expression at P2/P9 compared to P23/P45 rats), and 104 were up-regulated in older compared to younger animals (higher expression at P23/P45 than at P2/P9). The members of the miR-29 family showed the highest increase in expression level from younger to older animals (Fig. 1d; log fold-change (LFC) of up to 5.5 from P2/P9 to P23/P45).

Fewer miRNAs displayed differential expression between LII and LDeep, with only one miRNA being differentially expressed at P2, 26 differentially expressed at P9, 11 at P23, and 13 at P45 (35 unique miRNAs, Fig. 1c, e, f, Supplementary Table 2). This was also evident from the principal component analysis, where only nine percent of the variability in the data was explained by laminar differences (PC3) (Fig. 1b). When all ages were combined, 44 miRNAs were differentially expressed between layers (Supplementary Table 2). Of these 44, 27 miRNAs showed higher expression in LII than in LDeep, and 17 showed higher expression in LDeep than in LII. Most miRNAs that showed expression differences between layers also displayed differential expression levels between ages.

In summary, these results point to radical changes in miRNA expression during postnatal development of the MEC and identify several miRNAs that have different expression patterns in MEC LII compared with deep layers.

Functional analysis of laminar genes and predicted targets of laminar miRNAs

As miRNA regulation primarily causes mRNA degradation (Guo et al. 2010), we expected negatively correlated expression patterns for many miRNAs and their target genes (Wang and Li 2009). To identify potential target genes of our differentially expressed miRNAs, we used ribosome-depleted total RNA sequencing to measure mRNA expression at the same time points and layers as for the miRNA expression analysis (Fig. 2a, b, Supplementary Table 3). This analysis also detected preliminary miRNA molecules (pre-mirs), and the expression of these correlated well with the corresponding mature miRNAs measured by microarrays, corroborating the findings from our microarray analyses (Supplementary Analyses SA1, Supplementary Fig. 2).

We used the gProfileR tool to identify common functions of the mRNAs differentially expressed between layers at each postnatal age tested (Fig. 2c). The same was done for predicted and validated targets of miRNAs differentially expressed at the different time points, except for P2. The only miRNA differentially expressed at P2 had neither predicted, nor validated targets in the databases we used for the analyses (see "Methods").

Because morphology, connectivity, and physiological properties differ between the MEC layers, and because these properties develop in the time period tested, we expected to find GO terms and pathways involved in neural cell development, axon guidance, and ion channels. Indeed, mRNAs differentially expressed between layers were enriched in GO terms related to neuron projection and differentiation, irrespective of whether the mRNAs were up in LII or in LDeep. The mRNAs up-regulated in LII were particularly enriched in extracellular matrix proteins, cell adhesion, and angiogenesis, whereas genes up-regulated in LDeep were enriched in terms linked to neuron projection and synaptic activity. Many of the terms enriched for differentially expressed genes, such as the neuron development, angiogenesis, and adhesion terms, were also enriched for predicted or validated targets of laminar miRNAs. Strikingly, the targets for both up- and down-regulated miRNAs had many significant terms in common. This could reflect fine-tuning of gene expression between layers by miRNAs, which in turn could contribute to the laminar specialization.

We asked if the differentially expressed mRNAs included in the "neuron differentiation" category included miRNA-regulated transcription factors that potentially
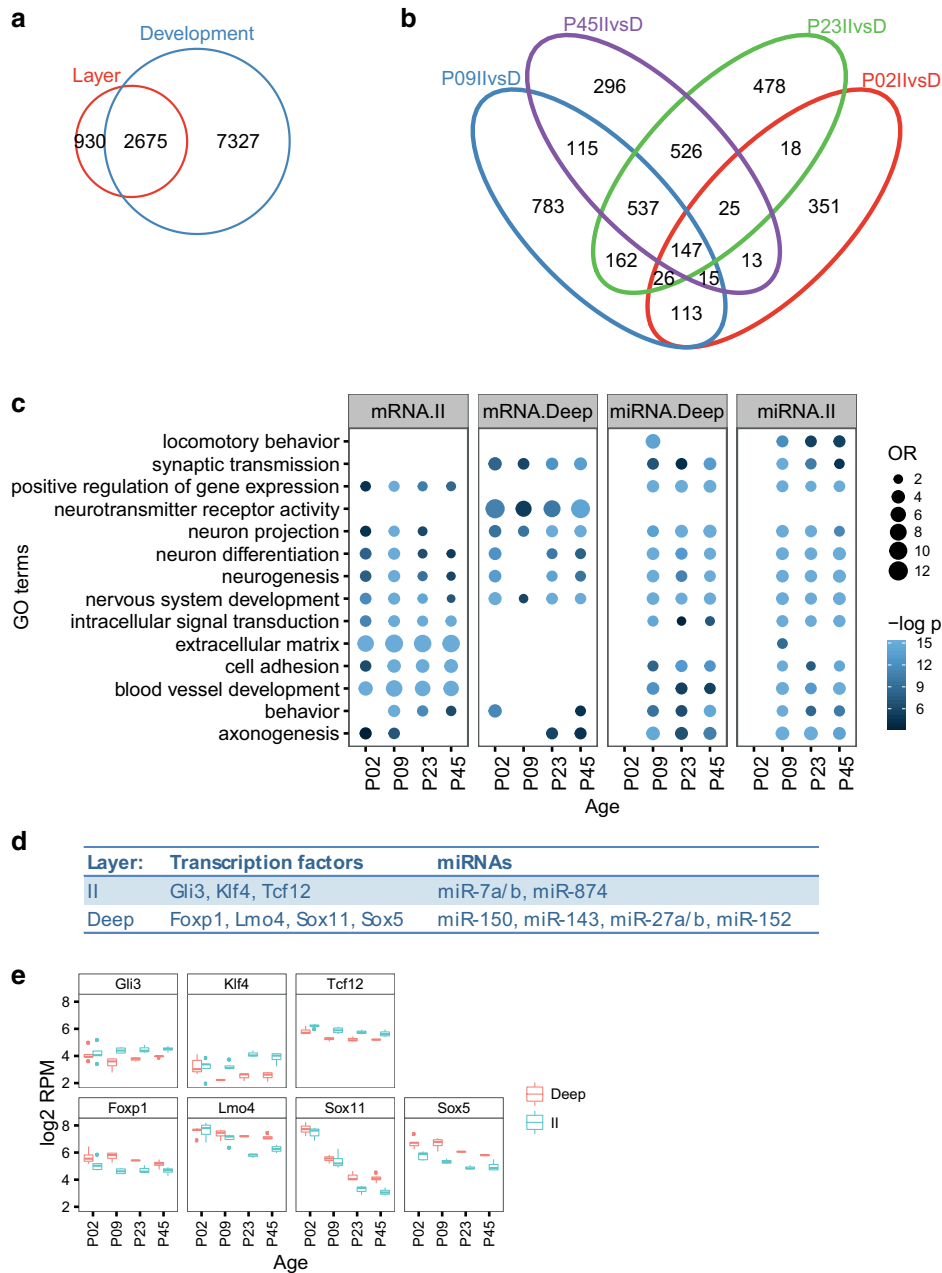
drive the differentiation or maintenance of the laminar neuronal subtypes. We used versions 6 and 7 of TargetScan to determine the context scores—a measure of a miRNA's affinity to its predicted target site—of the differentially expressed mRNAs in the "neuron differentiation" category

(179 mRNAs up-regulated in LII and 134 up-regulated in LDeep). We found that 116 differentially expressed mRNAs were also predicted targets of differentially expressed miRNAs. 11 of these mRNAs were transcription factors displaying negatively correlated expression patterns

◄**Fig. 2** MEC mRNA expression and enrichment terms. **a** *Venn diagram* showing the number of differentially expressed mRNAs between layers (*red*) and between ages (*blue*, P2/P9 vs. P23/P45, LFC = 0, BH < 0.05), and their overlap. **b** *Venn diagram* showing the number of mRNAs differentially expressed between layers at P2 (*red*), P9 (*blue*), P23 (*green*), and P45 (*purple*), and their overlap. **c** Functional characterization of laminarly enriched mRNAs and targets of laminarly enriched miRNAs across development. We used gProfileR to search for enriched ontology terms for mRNAs up-regulated in LDeep (mRNA.Deep) and LII (mRNA.II), and for validated and predicted miRNA targets expressed in MEC for miRNAs up-regulated in LII (miRNA.II) and in LDeep (miRNA.Deep) for each age group. The color intensity reflects the statistical significance (negative log adjusted *p* value), and the size of the circles the odds ratio calculated by Fisher's exact test. For illustration purposes, all OR and negative log *p* values above a maximum value of 12 and 15, respectively, were rounded down to these maximum values. **d** Transcription factors involved in neuron differentiation that are negatively correlated and predicted, conserved targets of miRNAs up-regulated in LII and up-regulated in LDeep. **e** Expression patterns of the transcription factors from d

to the miRNAs predicted to target them, and seven of these eleven transcription factors contained highly conserved target sites with context scores below −0.1 (Fig. 2d, e). Some of these differentially expressed mRNAs, i.e., Sox5, Gli3, and Lmo4, are known to be drivers of laminar subtype specification in other brain areas (Ohtaka-Maruyama and Okado 2015; Woodworth et al. 2012), making these mRNAs and the miRNAs that regulate their expression prime candidates for transcriptional drivers of the laminar differences in neuron properties seen in the MEC.

miRNA co-expression modules

There is increasing evidence that co-expressed miRNAs regulate functionally related genes (Bryan et al. 2014; Chavali et al. 2013; Gennarino et al. 2012; Guo et al. 2016; Wang et al. 2011). As our analyses of the miRNA expression data indicated multiple patterns of expression changes between MEC layers and postnatal ages (Fig. 1c–f), we clustered all miRNAs that were significantly differentially expressed (BH < 0.05) between ages or between layers. This approach identified eight robust co-expression modules that were representative of the 245 differentially expressed miRNAs (Fig. 3a, b, Supplementary Table 4). Consistent with previous observations (Baskerville and Bartel 2005) and with these modules representing co-regulated miRNAs, miRNAs encoded close in the genome tended to belong to the same co-expression module (Supplementary Analyses SA2, Supplementary Fig. 3 a–c).

The predominant patterns (modules 2 and 6) displayed opposing trends across development. Module 2 miRNAs displayed a sharp increase and module 6 a sharp decrease between P9 and P23. Laminar differences in miRNA expression were particularly seen for modules 3 and 7,

which also had opposing trends between young and old animals. P9 had the highest number of miRNAs with laminar differences, and two modules were enriched in miRNAs that showed differential expression primarily at this age (modules 1 and 4). The miRNAs in module 5 were down-regulated in LII at P23 and P45, which makes it likely that the genes they regulate are up-regulated in LII at these time points.

Correlating gene expression with miRNA expression

As most miRNAs either destabilize or repress their targets, we expected a majority of miRNAs and mRNA targets to display negatively correlated expression profiles. Indeed, when comparing the correlation distribution of conserved predicted targets to the control distribution of all predicted targets (including non-conserved), we found a skew towards negatively correlated miRNA-target pairs (Supplementary Fig. 4a). This skew was even more enhanced if we used more stringent criteria, such as increasing the TargetScan threshold, only including the 25% most highly expressed miRNAs, or requiring that an increasing percentage of the predicted miRNA target sites in a given gene were of miRNAs from the same module (Supplementary Fig. 4b–e). Combining all three filters gave a strong shift towards negative correlations compared to all conserved predicted targets (*p* = 6e-24, Mann–Whitney *U* test; Supplementary Fig. 4f). Although some miRNAs are known to increase the translation of their targets (Fabian et al. 2010), we chose to focus on these negatively correlated, conserved miRNA-gene pairs that are more likely to be real miRNA targets.

For the miRNAs in each of the co-expression modules, we identified validated targets from mirTarBase and predicted, conserved targets from TargetScan whose mRNA expression pattern was negatively correlated with that of the miRNA targeting it. The proportion of validated or predicted targets that were negatively correlated to the genes in each module varied from 7 to 50% for the different modules (Supplementary Table 4). Although we cannot exclude that this variation is an artifact of the analyses, we note that the miRNA module with the highest percentage of negatively correlated target genes had a clear developmental expression pattern, consistent with the importance of miRNA regulation of developmental genes (Ambros 2011; Davis et al. 2015).

Functional analysis of the negatively correlated targets of miRNA co-expression modules

Based on the assumption that co-regulated miRNAs will target functionally related genes, we hypothesized that there would be a tendency for the target genes of each
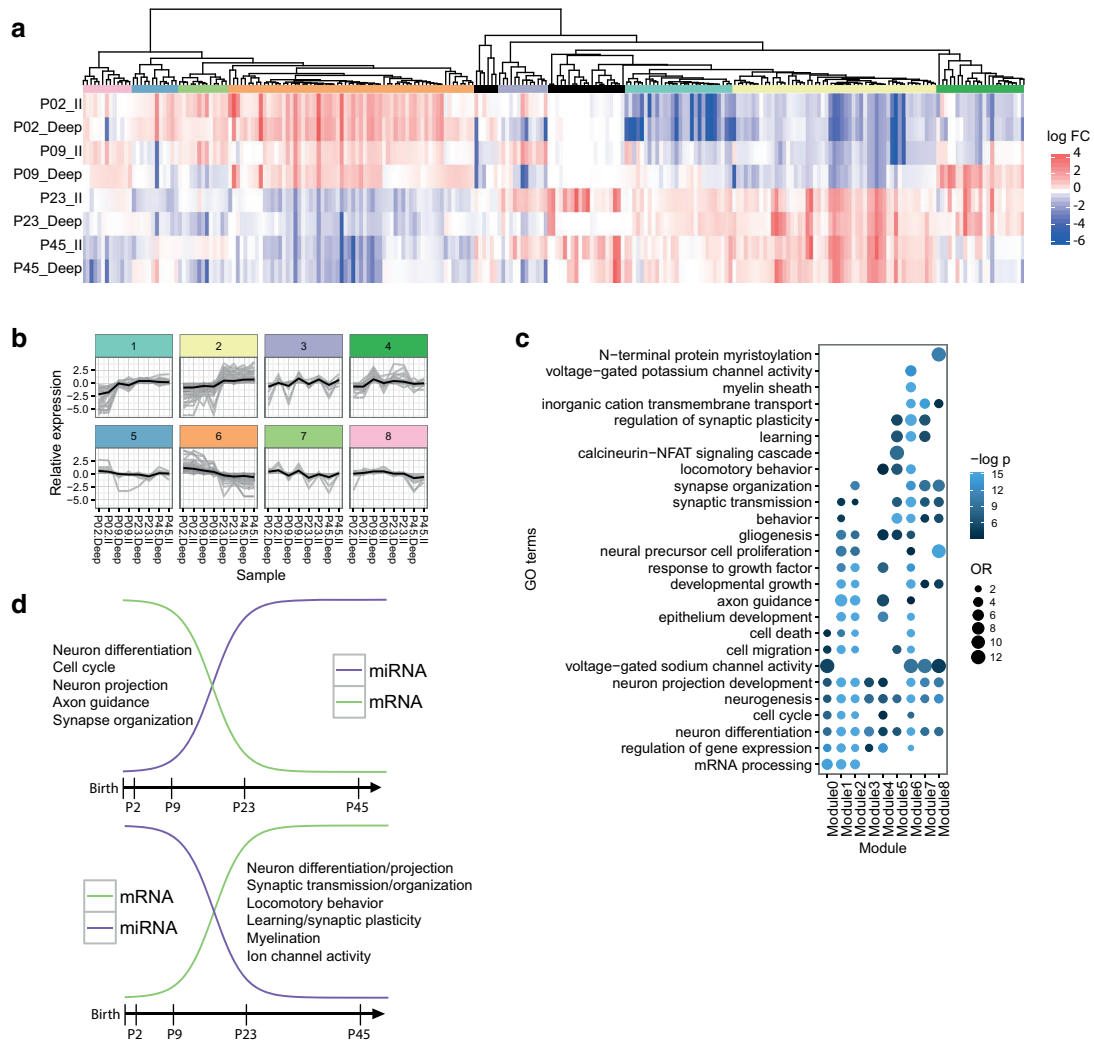
Fig. 3 MicroRNA co-expression modules. **a** Differentially expressed miRNAs clustered according to Pearson correlation in a cluster dendrogram. The tree was cut using the recursive partitioning algorithm (Nilsen et al. 2013), yielding eight co-expression modules, each represented with its own color. Outliers are shown in *black*. **b** Relative expression of the miRNAs in the eight co-expression modules across the samples (*gray*) and the representative expression pattern of each module (*black*). Modules are *color* coded as in **a**. **c** Functional analysis of negatively correlated validated and conserved predicted target genes of the miRNAs in each co-expression module. The color inten-

sity reflects the statistical significance (negative log adjusted *p* value), and the *size of the circles* the odds ratio calculated by Fisher's exact test. For illustration purposes, all OR and negative log *p* values above a maximum value of 12 and 15, respectively, were rounded down to these maximum values. **d** Overview of the main gene ontology enrichment findings for temporally differentially expressed miRNAs. These findings are based on the negatively correlated, predicted targets of miRNAs with increasing (*left*) or decreasing (*right*) expression from the two early (P2/P9) to the two late time points (P23/P45)

co-expression module to be enriched in GO terms that differ from those of the other modules. The functional enrichment analysis for the negatively correlated targets in each module (Fig. 3c) showed several general terms, especially

those pertaining to general nervous system development, which were enriched across the modules. Modules 1 and 2 shared many enriched terms, which probably reflected their similarities in expression pattern. Most of their terms are

linked to events that occur early in nervous system development, such as axon guidance and cell cycle and migration, indicating that the genes regulated by these miRNAs are down-regulated later in development.

Modules 5–8 also shared similarities in both expression patterns and enriched terms, including synaptic transmission, plasticity and locomotory behavior terms. Module 6 miRNAs may also be involved in regulating myelination; indeed, the expression patterns of module 6 miRNAs correspond with the onset of myelination from P10. The pattern of module 6 also corresponds with the maturation of grid cell properties from eye opening until P22 in the MEC. Modules 6–8 are enriched in ion transmembrane transport terms, implying that miRNAs could contribute to the maturation of physiological properties around the third postnatal week. Module 7, which has a clear laminar profile of miRNAs up-regulated in LII, may contribute to the differences in neuronal populations in the MEC layers. Predicted target genes include Hcn1, Scn1a/2a/8a, and Scn4b, but the negative correlation of miRNAs in module 7 with these ion channels seem to be more linked to developmental than laminar differences, as their expression increases across development. Hcn1 is important for grid cell function (Giocomo et al. 2011), and is likely targeted by miR-16 in module 7. In comparison, module 3 shared laminar profile with module 7 but had opposite expression across development. The two modules shared terms related to development and differentiation, but terms related to neuronal function such as sodium channel activity and synaptic transmission, were exclusive to module 7.

Finally, module 4 consisted of miRNAs that mainly were up-regulated in LDeep at P9. Although this module shared functions with other modules (primarily modules 1, 2, and 6), the strong laminar difference at P9 could indicate that the miRNAs in this module may contribute to initiate laminar differences in these functions, such as locomotory behavior, around this age.

In summary, the two predominant patterns (modules 2 and 6), shared functions such as growth, development, and cell migration, but also had distinct terms (Fig. 3d). MicroRNAs up-regulated at P23 and P45 (module 2) were enriched for mRNA processing and had markedly lower *p* values for cell cycle and axon guidance functions. In contrast, miRNAs down-regulated at P23 and P45 (module 6) were enriched for terms related to myelination, ion channel activity, synaptic plasticity, and locomotory behavior. Several of these terms were shared with modules that had similar but less pronounced expression differences between early and late ages (modules 5, 7, and 8). Our results implicate miRNAs in the development of the MEC's navigational functions, as well as the specialized functions of neuronal subpopulations in the different layers.

miRNA expression in retrogradely labeled stellate cells

Although the stellate cells are the dominant cell type in MEC LII, it is possible that miRNAs could be up-regulated in LII without having stellate-specific expression. To identify miRNAs that are differentially expressed in stellate cells vs. the surrounding neurons and non-neuronal tissue, we retrogradely labeled stellate cells through injection of the fluorescent dye DiO into the dentate gyrus, which is a main site of stellate cells' axonal projections (Tamamaki and Nojyo 1993) (Fig. 4a). The labeled cells were separated by FACS from the remaining tissue after tissue dissociation of dissected entorhinal cortex from pups aged P4/P5 (Fig. 4b, c, Supplementary Fig. 5). The young age of the pups allowed for fast diffusion of the dye and easy cell dissociation of young, unmyelinated neurons (Brewer and Torricelli 2007).

After miRNA expression analysis of each cell population by TaqMan miRNA qPCR array, seven miRNAs were found to be up-regulated in the labeled cells, while zero miRNAs were down-regulated (Fig. 4d, see "Methods"). When comparing these findings to those of the laminar sample study, we saw that one of the up-regulated miRNAs, miR-143, was also up-regulated in LII. Another miRNA, miR-150, was significantly up-regulated in LII at P09, and showed the same trend at P23 and P45, although up-regulation did not reach significance at these ages. Two of the other miRNAs, miR-375 and miR-494, also showed the same pattern of up-regulation in LII without reaching statistical significance in the layered samples. In general, we observed good correlation between the different technologies used (Spearman's rank correlation 0.61–0.70, $p < 3.5e\text{-}14$; Supplementary Analyses SA3, Supplementary Fig. 6). Taken together, these results confirm that several of the miRNAs up-regulated in LII also are up-regulated in stellate cells and identify miR-143 as the prime candidate for a stellate-enriched miRNA.

In situ hybridization of miRNAs

Although stellate cells were profiled at an early postnatal time point (P4/5), the results from the laminar samples showed that the expression of miR-143 increased further in LII across development. Due to this increased expression during postnatal development, it is possible that the importance of gene regulation by miR-143 increases with age. Grid cells, which are presumed to be stellate cells, reach maturation around the third postnatal week in rats, making the P23 developmental time point relevant for validation of miR-143 up-regulation. We hypothesized that if miR-143 was important for regulating stellate-specific gene expression, we would observe miR-143 expression in stellate
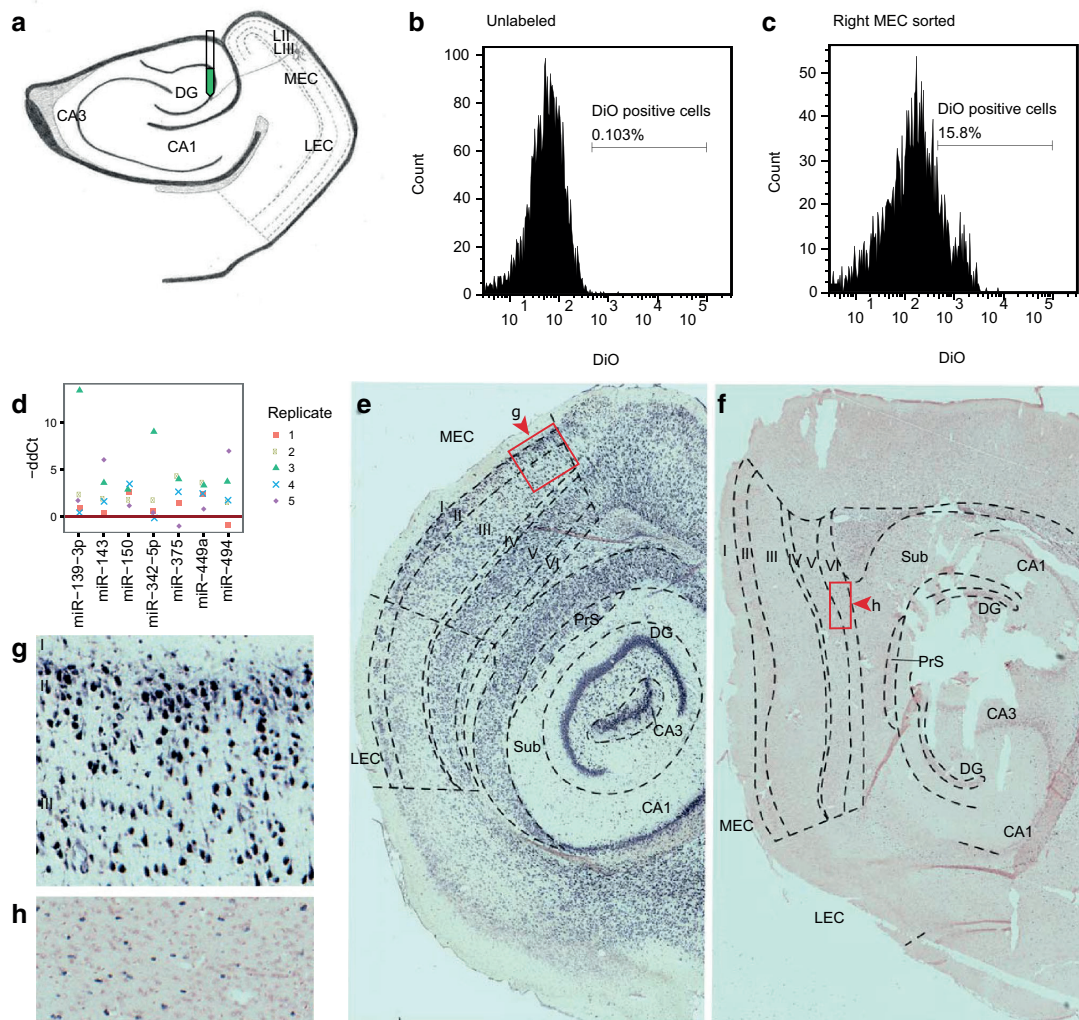
Fig. 4 Differentially expressed miRNAs between FACS sorted retrogradely labeled stellate cells and non-labeled MEC cells, and validation of differentially expressed miRNAs by in situ hybridization. **a** Illustration of the retrograde labeling of the stellate neurons. DiO was injected by iontophoresis into the dentate gyrus, where the stellate neurons project. **b** DiO baseline fluorescence level in live dissociated, unlabeled MEC. This control was used to determine the fluorescence level threshold for the sort. **c** A fluorescence plot of a representative sample of live DiO labeled, dissociated MEC cells. The threshold for the fluorescence level used for the sort is shown. **d** miRNAs differentially expressed between stellate neurons and the rest of MEC. The five biological replicates are color coded and represented with different symbols. **e–h** miRNA *in situ* hybridization on sagittal brain slices from a P23 rat using LNA-probes for miR-143 (**e, g**) and miR-219-5p (**f, h**). Zoomed in areas (**g, h**) correspond to the labeled *boxed areas* in **e** and **f**, with *arrowheads* pointing to the *top* in **g** and **h**. The probe stain is *purple*, and the counter *stain red*

cells of MEC. We therefore performed in situ hybridization using sagittal slices from brains of P23 rats.

The miR-143 signal was indeed strong in LII, with the signal in stellate neurons being very dense but not exclusive to this neuronal subtype (Fig. 4e, g). We noticed additional staining in smaller cells in LII, likely representing pyramidal principle cells and interneurons, as well as pyramidal cells in LIII and LV. miR-143 is known to be involved in differentiation and proliferation of vascular smooth muscle cells (Rangrez et al. 2011), and modulates the angiogenic

and vessel stabilization properties of endothelial cells (Climent et al. 2015). Although we did see some staining in vessels, this signal was not universal across all vascular cells. Consequently, the vascular role of miR-143 appears to be less important in rat MEC, where it instead appears to have roles in stellate and pyramidal cell function. Interestingly, the density of miR-143 seemed to be higher in MEC than in the lateral part of the EC (LEC), and the signal was more homogeneous across layers in LEC. The medial and lateral entorhinal cortices are known to differ in electrophysiology, connectivity, and function, and with differing patterns in the two regions, miR-143 could be involved in regulating these properties.

We also examined miR-219-5p, which was the most significantly up-regulated miRNA of the deeper layers compared to LII, and which was not detected in the FACS-sorted stellate cells. At P2/P9, miR-219-5p had similarly low expression in LII and LDeep compared to the later time points, but its expression increased between P9 and P23, reaching a maximum level at P23/P45 when it also had a distinct laminar profile (Fig. 1f). Examination of this miRNA allowed us to further characterize the cell-specific localization of its expression and thus its role in MEC lamination. Consistent with the microarray data, there was hardly any miR-219-5p signal in LII, a weak signal in LIII, and a much stronger signal in LV and VI (Fig. 4f). The miRNA was expressed in ependymal cells, oligodendrocytes and glia in the tissue, which corroborates the findings of others, who have detected expression of this miRNA in glia and found it to be involved in oligodendrocyte differentiation (Zhao et al. 2010).

Functional analysis of predicted targets of miRNAs differentially expressed in stellate cells indicates that the miRNAs are involved in stellate cell specialization

The stellate cells were extracted from pups aged P4/P5, when there is marked synaptogenesis and neuron differentiation (Semple et al. 2013). Indeed, for the predicted or validated targets of the miRNAs up-regulated in labeled stellate cells, most of the significant terms were related to formation and differentiation of neurons (Fig. 5a). Enriched terms also included cell projection organization, behavior, and terms related to synaptic activity, whereas enriched pathways included PI3K-Akt, MAPK, and NGF signaling (Fig. 5b, c).

Because miR-143 was up-regulated both in stellate cells and in LII in general, we also specifically considered the enriched terms and pathways of its predicted or validated targets (Fig. 5a–c). As this miRNA also was included in the analysis of all the up-regulated stellate miRNAs, many of the same terms were enriched.

However, what differed from the larger analysis was IGF1R activity and assembly of collagens. The IGF signaling pathway has a role in dendrite formation and synaptogenesis (Popken et al. 2005). Although the most characterized role for miR-143 is in vascularization, this miRNA could, by regulating IGF signaling, also have a special role in neurons.

Correlating gene expression with miR-143 expression

To further delineate targets relevant for miR-143 in MEC LII and stellate cells, we combined the expression profile of miR-143 with those of its predicted, conserved targets. We required predicted targets to have negatively correlated expression patterns, a minimum expression level (median normalized $\log_2$ expression ≥ 5), and be significantly differentially expressed both between ages and between layers. Twelve genes satisfied these requirements (Supplementary Table 5). The most likely targets of miR-143 in the MEC, according to these criteria, were the Lmo4, Tpm3, and Cachd1 genes (Fig. 5d). Lmo4 was the gene with highest LFC between MEC layers in gene expression, the best target site as measured by the TargetScan context score, and the second highest negative correlation with miR-143 expression levels.

Correlating gene expression with miR-219-5p expression

Predicted targets of miR-219-5p, irrespective of correlation with miR-219-5p expression, were enriched in neuron development terms (Fig. 5e). However, known targets of miR-219-5p include several genes involved in the process of differentiating neuronal stem cells to myelinating oligodendrocytes (Barca-Mayo and Lu 2012). All of the known targets that are involved in the development of oligodendrocytes from oligodendrocyte precursor cells displayed negatively correlated expression patterns with miR-219-5p, although few were differentially expressed between layers (Supplementary Analyses SA4, Supplementary Fig. 7). However, the gene involved in final maturation and myelin maintenance, Elovl7, had a positively correlated expression pattern with miR-219-5p.

Using the same criteria as for miR-143, we found 16 genes that had opposite expression to miR-219-5p between both ages and layers. Of these, we identified three genes that had both high context scores in TargetScan (v. 6.2 and 7.1) and a high degree of negative correlation, namely Fads2, Pdgfra, and Ubash3b (Supplementary Table 5; Fig. 5f).
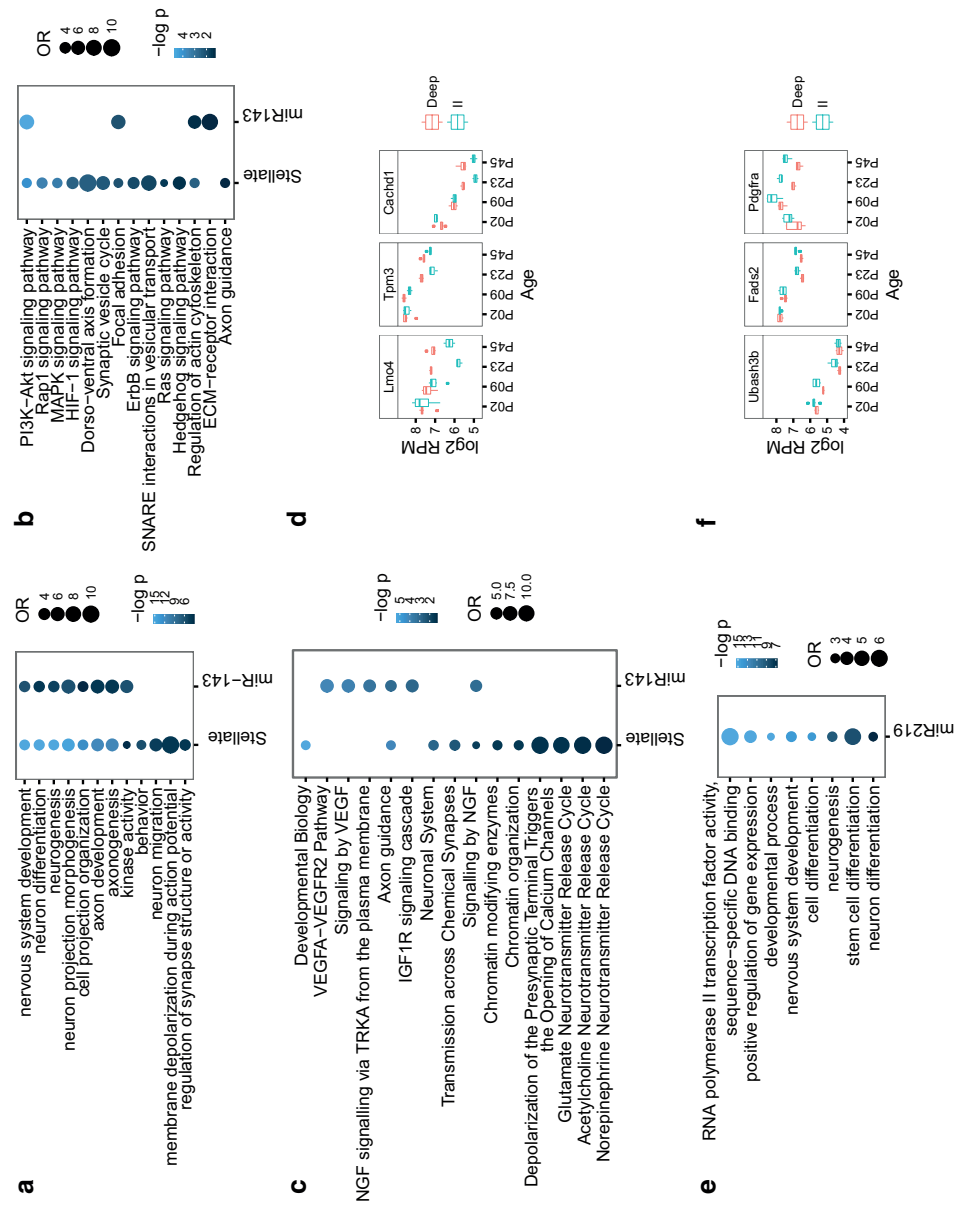
Fig. 5 Analyses of predicted, conserved mRNA targets expressed in the MEC of miR-143 (**a–d**) and miR-219 (**e, f**). **a** Gene ontology, **b** KEGG pathway, and **c** REACTOME pathway enrichment analyses for validated and predicted, conserved targets of miRNAs up-regulated in stellate cells in general and miR-143 in particular. **e** Gene ontology enrichment analysis for validated and predicted, conserved targets of miR-219-5p. The color intensity reflects the statistical significance (negative log adjusted *p* value), and the *size of the circles* the odds ratio calculated by Fisher's exact test. For illustration purposes, all OR and negative log *p* values above a maximum value of 12 and 15, respectively, were rounded down to these maximum values. Expression patterns of mRNAs that are the most likely miR-143 (**d**) and miR-219-5p (**f**) targets (rho < −0.5 and the best TargetScan 6.0 or 7.0 context score). Laminar samples are colored (LDeep *red*, LII *turquoise*)

Discussion

Known functions of MEC miRNAs differentially expressed between early and late postnatal ages or between layer II and deep layers

We found 202 miRNAs to be significantly differentially expressed between early (P2/P9) and late (P23/P45) ages or between LII and LDeep at individual time points. Most (192) of these were differentially expressed between ages (Fig. 1c; Supplementary Table 2). Three of the top five most significant miRNAs that increased from early to late age were members of the miR-29 family. MicroRNA miR-29b is known to increase during neuronal maturation and to inhibit apoptosis in neurons, and miR-29a/b both affect dendritic spine morphology (Kole et al. 2011; Lippi et al. 2011). Other general functions for this family include regulation of the extracellular matrix and cell proliferation and differentiation (Kriegel et al. 2012). miR-29a/b also target several proteins involved in neurodegenerative diseases, including BACE1/β-secretase, of which elevated levels can lead to increased amyloid β-peptides in patients with sporadic Alzheimer's disease (Hebert et al. 2008). One of the miRNAs displaying the greatest decrease in expression between ages, miR-298, also targets the BACE1 mRNA (Boissonneault et al. 2009), suggesting complementary roles between miR-298 and miR-29a/b in regulating this protein. The other highly significant miRNAs displaying a steep decrease from younger to older animals (miR-301b, miR-130b, miR-20a, and miR-15b) are known to be involved in cancers (Attar et al. 2012; Funamizu et al. 2014; O'Donnell et al. 2005; Zhu et al. 2015), suggesting a role for these miRNAs in regulating MEC cell proliferation immediately after birth.

Only 35 miRNAs were significantly differentially expressed between LII and LDeep at individual ages (Fig. 1e; Supplementary Table 2); of these, 25 miRNAs differed significantly between early (P2/P9) and late (P23/P45) ages. The trend of a higher number of miRNAs being differentially expressed across development than between cortical layers, has also been observed in mouse somatosensory cortex (Fertuzinhos et al. 2014), and probably reflects the importance of miRNAs in the processes important for brain development in general. Between P2 and P23, there is extensive spine formation, synaptic pruning and myelination in the brain, all known to be regulated by miRNAs (Schratt 2009).

The two miRNAs with the lowest p value up-regulated in LII (miR-143 and miR-126; Fig. 1f) are involved in angiogenesis (Climent et al. 2015; Sonntag et al. 2012). Uneven laminar distribution of capillaries has been observed in the lateral part of the EC (Michaloudi et al. 2005), and it is possible that miRNAs could contribute to the formation and maintenance of a similar capillary pattern in the MEC. The two miRNAs with the lowest p value up-regulated in LDeep (miR-219 and miR-338) are involved in oligodendrocyte differentiation (Barca-Mayo and Lu 2012). The increased need for oligodendrocyte regulation in the deeper layer can be expected because there are higher levels of myelination in deeper cortical layers (Lodato et al. 2015). Several of the differentially expressed miRNAs regulate neuron differentiation, including miR-126 and miR-26b in LII, and miR-7a/b in LDeep. Interestingly, the LII up-regulated miR-26b and miR-126 are implicated in Alzheimer's disease (Absalon et al. 2013; Kim et al. 2014), while the LDeep up-regulated miR-219 and miR-7a/b are implicated in schizophrenia (Beveridge and Cairns 2012), diseases which both show pathologies in LII.

In summary, the known functions of the miRNAs we identified as differentially expressed in MEC, indicate that these miRNAs regulate laminar differences in MEC vascular structure and oligodendrocyte density and could contribute to laminar differences in neuron subtype specification and disease susceptibility.

Possible functions of MEC miRNA co-expression modules

By clustering the differentially expressed miRNAs, we found eight distinct patterns of co-expressed miRNAs. As expected from the statistical results (Fig. 1c), the two largest such co-expression modules had opposing patterns and contained miRNAs that primarily were differentially expressed between the early (P2 and P9) and late (P23 and P45) ages (modules 2 and 6 with 53 and 64 miRNAs, respectively; Fig. 3b; Supplementary Table 4). This probably reflects the enormous strides in development that take place between and around ages P9-P23, starting with crawling and eye opening, and ending with grid cell stabilization and the development of spatial learning abilities (Langston et al. 2010; Wills and Cacucci 2014).

To determine potential functions of the co-expressed miRNAs, we identified predicted and verified target mRNAs with negatively correlated expression to all miRNAs in each module and ran GO analyses of each set of such predicted targets. This approach relies on the assumptions that co-expressed miRNAs regulate functionally related genes and that filtering predicted miRNA targets based on negative correlation will reduce false positive predictions and identify physiologically relevant targets. Supporting the first assumption, miRNAs clustered in the genome, which tend to be co-transcribed and therefore co-expressed, tend to target functionally related genes (Hausser and Zavolan 2014; Wang et al. 2016). Similarly, other co-expressed miRNAs also tend to target functionally related genes (Bryan et al. 2014).

As for using negative correlations in expression to identify relevant miRNA targets, multiple studies have shown that predicted miRNA targets tend to be down-regulated upon miRNA overexpression, and vice versa upon miRNA down-regulation [reviewed in (Bartel 2009)]. Moreover, these changes in target mRNA expression generally result in the corresponding changes in protein levels (Baek et al. 2008; Selbach et al. 2008); indeed, miRNA's effect on mRNA expression can explain most (>80%) of the changes in protein levels for predicted targets (Guo et al. 2010). Similar results have been seen for experimentally validated miRNA targets (Hendrickson et al. 2009). These studies show that experimentally altering miRNA expression generally results in inverse expression changes for predicted miRNA targets, but miRNA and predicted targets also tend to be negatively correlated in endogenous expression data (Fulci et al. 2009; Wang and Li 2009). Consistent with these previous studies, we found that the correlations between MEC miRNAs and their evolutionary conserved predicted miRNA targets are skewed towards negative values (Supplementary Fig. 4a).

Our GO analyses found that the miRNA co-expression modules had several functions in common. All modules were significantly enriched for predicted targets involved in neuron differentiation and neurogenesis (Fig. 3c). The two largest modules, representing miRNAs differentially expressed between early and late ages, shared several predicted functions, including growth, development, and cell migration. Although many of the significant GO terms appear general, our results indicate distinctions in the predicted functions of miRNAs up-regulated at P2/9 compared with miRNAs up-regulated at P23/45 (Fig. 3d). MicroRNAs up-regulated at P2/9, and thereby down-regulated at P23/45, predict that myelination, ion channel activity, learning, and synaptic plasticity are up-regulated. In contrast, cell cycle functions are predicted to be down-regulated at these later time points. Together these data indicate that the miRNAs are involved in the development of the MEC. Importantly, the miRNAs appear to be involved in regulation of maturational processes which lead to specialized cell functions that require specific ion channels. Furthermore, these data are in line with the idea that learning and synaptic plasticity may be more prominent at older ages, and indicate that miRNAs play a role in these functions.

Possible functions of miRNAs up-regulated in stellate cells

GO analyses of predicted and validated targets of miRNAs up-regulated in the FACS-sorted stellate cells identified functions related to neuronal development and differentiation (Fig. 5a). Although neurogenesis in the EC largely takes place during embryonic development (Bayer 1980), "neurogenesis" as a GO term could reflect the reuse of similar pathways in processes that are known to take place postnatally, such as morphological and functional maturation (Casanova and Casanova 2014), or that the same miRNAs target genes involved in neurogenesis during embryonic development and other genes later in development. Many of the enriched terms, such as neurogenesis, neuron differentiation, and axonogenesis, were also among the terms enriched for mRNA and miRNAs up-regulated in LII.

Enriched terms for the stellate miRNAs also included more specific functions such as "regulation of synapse structure or activity" and "membrane depolarization during action potential". Pathways enriched for the stellate miRNAs included NGF, MAPK, and PI3K-Akt, which contribute to a wide variety of both intra-and extracellular processes, including differentiation of neurons (Berry et al. 2012; Correa and Eales 2012; Peltier et al. 2007). Fine-tuning of these pathways by miRNAs could potentially contribute to the stellate phenotype.

Likely targets of miR-143 and miR-219-5p

The top predicted target genes of miR-143, Lmo4, Tpm3, and Cachd1, indicate that miR-143 contributes to laminar and subcellular phenotypes of MEC. The Lmo4 gene, whose expression is enriched in glutamatergic populations, is an activity-dependent calcium-responsive cofactor that binds to several signaling molecules and transcription factors (Qin et al. 2012). Lmo4 is involved in the establishment of neuronal subtypes in the rostral motor cortex and in LV cortical neuron populations (Azim et al. 2009; Cederquist et al. 2013) and is implicated in hippocampus-dependent spatial learning (Qin et al. 2012). In addition, Lmo4 is strongly expressed in MEC during embryonic development, and has been implicated in characterizing this region (Abellan et al. 2014). It is therefore possible that the lower concentration of Lmo4 gene expression in LII is important for the specialization of LII. The Tpm3 protein is a component of actin microfilaments, and certain isoforms have been implicated in influencing the size and shapes of neurons (Schevzov et al. 2005). The function of Cachd1 has not been investigated, but it may be a calcium channel regulatory membrane protein as inferred from gene ontology inferred electronic annotation (Gene Ontology Consortium).

The top predicted gene targets of miR-219-5p, Fads2, Pdgfra, and Ubash3b, indicate a role for this miRNA in regulation of myelination. The Pdgfra gene is a known target of miR-219-5p involved in differentiation of oligodendrocyte precursor cells (OPCs) into mature oligodendrocytes (Barca-Mayo and Lu 2012), which corresponds well

with the *in situ* labeling of miR-219-5p in oligodendrocytes presented here. Oligodendrocytes are the main cell types involved in myelination, and the Fads2 gene, a second target of miR-219-5p, is also involved in myelination (Peters et al. 2014). Further support for the role of miR-219-5p in myelination is that Ubash3b (alias Sts-1) inhibits endocytosis of EGFR (Raguz et al. 2007) and therefore possibly plays an indirect role in oligodendrocyte development, which involves EGFR signaling (Palazuelos et al. 2014). Thus, miR-219-5p likely regulates oligodendrocyte differentiation in the MEC in a layer-specific fashion, a role which is similar to its known function in other brain areas.

Conclusions

We have presented the first analysis of miRNA expression in LII and LDeep of the developing MEC, with a special focus on stellate neurons. We have profiled miRNAs and mRNAs in MEC LII and LDeep at four time points during postnatal development—neonatal (P2), infant (P9), juvenile (P23) and young adult (P45)—and compared miRNA expression in labeled stellate cells to that in other MEC cells. Through in situ hybridizations, we confirmed the layer and cell-type expression of miR-143, which is up-regulated in LII stellate cells but also expressed in smaller cells in LII and LIII and LV pyramidal cells, and miR-219-5p, which is expressed in ependymal cells, oligodendrocytes, and glia—primarily in LV and LVI. Our analysis showed that both miRNAs and mRNAs were more dynamic across development than they were between layers. However, we did find laminar differences in miRNA expression at all postnatal ages tested. Moreover, our bioinformatics analyses of conserved, predicted target mRNAs with negatively correlated expression patterns indicate that these miRNAs could participate in regulating the laminar differences in electrophysiology, neuron morphology and disease susceptibility seen in the MEC.

The miRNA most significantly up-regulated in LDeep, miR-219-5p, plays an important role in oligodendrocyte differentiation and myelination, which generally begins around P10. The most significantly up-regulated miRNA in LII, miR-143, was found to be up-regulated particularly in stellate neurons. Our analysis revealed that a likely target of this miRNA is the Lmo4 gene, which is important for neuronal subtype specification and hippocampus-dependent spatial learning. The exact role of miR-143 in Lmo4 gene regulation and its potential importance for stellate or grid cell function remains to be determined.

Compliance with ethical standards

References

Abellan A, Desfilis E, Medina L (2014) Combinatorial expression of Lef1, Lhx2, Lhx5, Lhx9, Lmo3, Lmo4, and Prox1 helps to identify comparable subdivisions in the developing hippocampal formation of mouse and chicken. Front Neuroanat 8:59. doi:10.3389/fnana.2014.00059

Absalon S, Kochanek DM, Raghavan V, Krichevsky AM (2013) MiR-26b, upregulated in Alzheimer's disease, activates cell cycle entry, tau-phosphorylation, and apoptosis in postmitotic neurons. J Neurosci 33:14645–14659. doi:10.1523/JNEUROSCI.1327-13.2013

Ambros V (2011) MicroRNAs and developmental timing. Curr Opin Genet Dev 21:511–517. doi:10.1016/j.gde.2011.04.003

Anders S, Pyl PT, Huber W (2015) HTSeq–a Python framework to work with high-throughput sequencing data. Bioinformatics 31:166–169. doi:10.1093/bioinformatics/btu638

Arnold SE (2000) Cellular and molecular neuropathology of the parahippocampal region in schizophrenia. Ann N Y Acad Sci 911:275–292

Attar M et al (2012) MicroRNA 17–92 expressed by a transposone-based vector changes expression level of cell-cycle-related genes. Cell Biol Int 36:1005–1012. doi:10.1042/CBI20110089

Azim E, Shnider SJ, Cederquist GY, Sohur US, Macklis JD (2009) Lmo4 and Clim1 progressively delineate cortical projection neuron subtypes during development. Cereb Cortex 19(Suppl 1):i62–i69. doi:10.1093/cercor/bhp030

Baek D, Villen J, Shin C, Camargo FD, Gygi SP, Bartel DP (2008) The impact of microRNAs on protein output. Nature 455:64–71. doi:10.1038/nature07242

Barca-Mayo O, Lu QR (2012) Fine-Tuning Oligodendrocyte Development by microRNAs. Front Neurosci 6:13. doi:10.3389/fnins.2012.00013

Bartel DP (2009) MicroRNAs: target recognition and regulatory functions. Cell 136:215–233. doi:10.1016/j.cell.2009.01.002

Baskerville S, Bartel DP (2005) Microarray profiling of microRNAs reveals frequent coexpression with neighboring miRNAs and host genes. RNA 11:241–247. doi:10.1261/rna.7240905

Bayer SA (1980) Development of the hippocampal region in the rat I. Neurogenesis examined with 3 H-thymidine autoradiography. J Comp Neurol 190:87–114. doi:10.1002/cne.901900107

Berry A, Bindocci E, Alleva E (2012) NGF, brain and behavioral plasticity. Neural Plast 2012:784040. doi:10.1155/2012/784040

Beveridge NJ, Cairns MJ (2012) MicroRNA dysregulation in schizophrenia. Neurobiol Dis 46:263–271. doi:10.1016/j.nbd.2011.12.029

Bjerknes TL, Moser EI, Moser MB (2014) Representation of geometric borders in the developing rat. Neuron 82:71–78. doi:10.1016/j.neuron.2014.02.014

Boccara CN, Kjonigsen LJ, Hammer IM, Bjaalie JG, Leergaard TB, Witter MP (2015) A three-plane architectonic atlas of the rat hippocampal region. Hippocampus 25:838–857. doi:10.1002/hipo.22407

Boissonneault V, Plante I, Rivest S, Provost P (2009) MicroRNA-298 and microRNA-328 regulate expression of mouse beta-amyloid precursor protein-converting enzyme 1. J Biol Chem 284:1971–1981. doi:10.1074/jbc.M807530200

Bolger AM, Lohse M, Usadel B (2014) Trimmomatic: a flexible trimmer for Illumina sequence data. Bioinformatics 30:2114–2120. doi:10.1093/bioinformatics/btu170

Bolstad BM, Irizarry RA, Astrand M, Speed TP (2003) A comparison of normalization methods for high density oligonucleotide array data based on variance and bias. Bioinformatics 19:185–193

Borrell V et al (1999) Reelin regulates the development and synaptogenesis of the layer-specific entorhino-hippocampal connections. J Neurosci 19:1345–1358

Brewer GJ (1997) Isolation and culture of adult rat hippocampal neurons. J Neurosci Methods 71:143–155

Brewer GJ, Torricelli JR (2007) Isolation and culture of adult neurons and neurospheres. Nat Protoc 2:1490–1498. doi:10.1038/nprot.2007.207

Bryan K et al (2014) Discovery and visualization of miRNA-mRNA functional modules within integrated data using bicluster analysis. Nucleic Acids Res 42:e17. doi:10.1093/nar/gkt1318

Burton BG, Economo MN, Lee GJ, White JA (2008) Development of theta rhythmicity in entorhinal stellate cells of the juvenile rat. J Neurophysiol 100:3144–3157. doi:10.1152/jn.90424.2008

Canto CB, Witter MP (2012) Cellular properties of principal neurons in the rat entorhinal cortex II. The medial entorhinal cortex. Hippocampus 22:1277–1299. doi:10.1002/hipo.20993

Casanova EL, Casanova MF (2014) Genetics studies indicate that neural induction and early neuronal maturation are disturbed in autism. Front Cell Neurosci 8:397. doi:10.3389/fncel.2014.00397

Cederquist GY, Azim E, Shnider SJ, Padmanabhan H, Macklis JD (2013) Lmo4 establishes rostral motor cortex projection neuron subtype diversity. J Neurosci 33:6321–6332. doi:10.1523/JNEUROSCI.5140-12.2013

Chavali S et al (2013) MicroRNAs act complementarily to regulate disease-related mRNA modules in human diseases. RNA 19:1552–1562. doi:10.1261/rna.038414.113

Climent M, Quintavalle M, Miragoli M, Chen J, Condorelli G, Elia L (2015) TGFbeta triggers miR-143/145 transfer from smooth muscle cells to endothelial cells, thereby modulating vessel stabilization. Circ Res 116:1753–1764. doi:10.1161/CIRCRESAHA.116.305178

Correa SA, Eales KL (2012) The role of p38 MAPK and its substrates in neuronal plasticity and neurodegenerative disease. J Signal Transduct 2012:649079. doi:10.1155/2012/649079

Davis GM, Haas MA, Pocock R (2015) MicroRNAs: not "fine-tuners" but key regulators of neuronal development and function. Front Neurol 6:245. doi:10.3389/fneur.2015.00245

Deng JB, Yu DM, Wu P, Li MS (2007) The tracing study of developing entorhino-hippocampal pathway. Int J Dev Neurosci 25:251–258. doi:10.1016/j.ijdevneu.2007.03.002

Derdikman D, Moser EI (2010) A manifold of spatial maps in the brain. Trends Cogn Sci 14:561–569. doi:10.1016/j.tics.2010.09.004

Dobin A et al (2013) STAR: ultrafast universal RNA-seq aligner. Bioinformatics 29:15–21. doi:10.1093/bioinformatics/bts635

Domnisoru C, Kinkhabwala AA, Tank DW (2013) Membrane potential dynamics of grid cells. Nature 495:199–204. doi:10.1038/nature11973

Downes N, Mullins P (2014) The development of myelin in the brain of the juvenile rat. Toxicol Pathol 42:913–922. doi:10.1177/0192623313503518

Dvinge H, Bertone P (2009) HTqPCR: high-throughput analysis and visualization of quantitative real-time PCR data in R. Bioinformatics 25:3325–3326. doi:10.1093/bioinformatics/btp578

Eichenbaum H, Sauvage M, Fortin N, Komorowski R, Lipton P (2012) Towards a functional organization of episodic memory in the medial temporal lobe. Neurosci Biobehav Rev 36:1597–1608. doi:10.1016/j.neubiorev.2011.07.006

Fabian MR, Sundermeier TR, Sonenberg N (2010) Understanding how miRNAs post-transcriptionally regulate gene expression. Prog Mol Subcell Biol 50:1–20. doi:10.1007/978-3-642-03103-8_1

Fertuzinhos S et al (2014) Laminar and temporal expression dynamics of coding and noncoding RNAs in the mouse neocortex. Cell Rep 6:938–950. doi:10.1016/j.celrep.2014.01.036

Fulci V et al (2009) Characterization of B- and T-lineage acute lymphoblastic leukemia by integrated analysis of MicroRNA and mRNA expression profiles. Genes Chromosom Cancer 48:1069–1082. doi:10.1002/gcc.20709

Funamizu N, Lacy CR, Parpart ST, Takai A, Hiyoshi Y, Yanaga K (2014) MicroRNA-301b promotes cell invasiveness through targeting TP63 in pancreatic carcinoma cells. Int J Oncol 44:725–734. doi:10.3892/ijo.2014.2243

Gatome CW, Slomianka L, Lipp HP, Amrein I (2010) Number estimates of neuronal phenotypes in layer II of the medial entorhinal cortex of rat and mouse. Neuroscience 170:156–165. doi:10.1016/j.neuroscience.2010.06.048

Gennarino VA et al (2012) Identification of microRNA-regulated gene networks by expression analysis of target genes. Genome Res 22:1163–1172. doi:10.1101/gr.130435.111

Giocomo LM, Hussaini SA, Zheng F, Kandel ER, Moser MB, Moser EI (2011) Grid cells use HCN1 channels for spatial scaling. Cell 147:1159–1170. doi:10.1016/j.cell.2011.08.051

Gomez-Isla T, Price JL, McKeel DW Jr, Morris JC, Growdon JH, Hyman BT (1996) Profound loss of layer II entorhinal cortex neurons occurs in very mild Alzheimer's disease. J Neurosci 16:4491–4500

Greenhill SD, Chamberlain SE, Lench A, Massey PV, Yuill KH, Woodhall GL, Jones RS (2014) Background synaptic activity in rat entorhinal cortex shows a progressively greater dominance of inhibition over excitation from deep to superficial layers. PLoS One 9:e85125. doi:10.1371/journal.pone.0085125

Grimson A, Farh KK, Johnston WK, Garrett-Engele P, Lim LP, Bartel DP (2007) MicroRNA targeting specificity in mammals: determinants beyond seed pairing. Mol Cell 27:91–105. doi:10.1016/j.molcel.2007.06.017

Guo H, Ingolia NT, Weissman JS, Bartel DP (2010) Mammalian microRNAs predominantly act to decrease target mRNA levels. Nature 466:835–840. doi:10.1038/nature09267

Guo Y, Alexander K, Clark AG, Grimson A, Yu H (2016) Integrated network analysis reveals distinct regulatory roles of transcription factors and microRNAs. RNA 22:1663–1672. doi:10.1261/rna.048025.114

Hausser J, Zavolan M (2014) Identification and consequences of miRNA-target interactions–beyond repression of gene expression. Nat Rev Genet 15:599–612. doi:10.1038/nrg3765

Hebert SS et al (2008) Loss of microRNA cluster miR-29a/b-1 in sporadic Alzheimer's disease correlates with increased BACE1/beta-secretase expression. Proc Natl Acad Sci USA 105:6415–6420. doi:10.1073/pnas.0710263105

Hendrickson DG, Hogan DJ, McCullough HL, Myers JW, Herschlag D, Ferrell JE, Brown PO (2009) Concordant regulation of translation and mRNA abundance for hundreds of targets of a human microRNA. PLoS Biol 7:e1000238. doi:10.1371/journal.pbio.1000238

Hsu SD et al (2014) miRTarBase update 2014: an information resource for experimentally validated miRNA-target interactions. Nucleic Acids Res 42:D78–D85. doi:10.1093/nar/gkt1266

Kim DH et al (2014) Genetic markers for diagnosis and pathogenesis of Alzheimer's disease. Gene 545:185–193. doi:10.1016/j.gene.2014.05.031

Kole AJ, Swahari V, Hammond SM, Deshmukh M (2011) miR-29b is activated during neuronal maturation and targets BH3-only genes to restrict apoptosis. Genes Dev 25:125–130. doi:10.1101/gad.1975411

Kriegel AJ, Liu Y, Fang Y, Ding X, Liang M (2012) The miR-29 family: genomics, cell biology, and relevance to renal and cardiovascular injury. Physiol Genom 44:237–244. doi:10.1152/physiolgenomics.00141.2011

Langmead B, Trapnell C, Pop M, Salzberg SL (2009) Ultrafast and memory-efficient alignment of short DNA sequences to the human genome. Genome Biol 10:R25. doi:10.1186/gb-2009-10-3-r25

Langston RF et al (2010) Development of the spatial representation system in the rat. Science 328:1576–1580. doi:10.1126/science.1188210

Law CW, Chen Y, Shi W, Smyth GK (2014) voom: Precision weights unlock linear model analysis tools for RNA-seq read counts. Genome Biol 15:R29. doi:10.1186/gb-2014-15-2-r29

Liao Y, Smyth GK, Shi W (2014) featureCounts: an efficient general purpose program for assigning sequence reads to genomic features. Bioinformatics 30:923–930. doi:10.1093/bioinformatics/btt656

Lippi G et al (2011) Targeting of the Arpc3 actin nucleation factor by miR-29a/b regulates dendritic spine morphology. J Cell Biol 194:889–904. doi:10.1083/jcb.201103006

Lodato S, Shetty AS, Arlotta P (2015) Cerebral cortex assembly: generating and reprogramming projection neuron diversity. Trends Neurosci 38:117–125. doi:10.1016/j.tins.2014.11.003

Lopez-Romero P (2011) Pre-processing and differential expression analysis of Agilent microRNA arrays using the AgiMicroRna Bioconductor library. BMC Genom 12:64. doi:10.1186/1471-2164-12-64

Martin M (2011) Cutadapt removes adapter sequences from high-throughput sequencing reads. EMBnet J 17:10–12

Michaloudi H, Grivas I, Batzios C, Chiotelli M, Papadopoulos GC (2005) Areal and laminar variations in the vascularity of the visual, auditory, and entorhinal cortices of the developing rat brain. Dev Brain Res 155:60–70. doi:10.1016/j.devbrainres.2004.11.007

Moser EI, Moser MB (2013) Grid cells and neural coding in high-end cortices. Neuron 80:765–774. doi:10.1016/j.neuron.2013.09.043

Nilsen G, Borgan O, Liestol K, Lingjaerde OC (2013) Identifying clusters in genomics data by recursive partitioning. Stat Appl Genet Mol Biol 12:637–652. doi:10.1515/sagmb-2013-0016

O'Donnell KA, Wentzel EA, Zeller KI, Dang CV, Mendell JT (2005) c-Myc-regulated microRNAs modulate E2F1 expression. Nature 435:839–843. doi:10.1038/nature03677

O'Reilly KC, Flatberg A, Islam S, Olsen LC, Kruge IU, Witter MP (2015) Identification of dorsal-ventral hippocampal differentiation in neonatal rats. Brain Struct Funct 220:2873–2893. doi:10.1007/s00429-014-0831-8

Ohtaka-Maruyama C, Okado H (2015) Molecular pathways underlying projection neuron production and migration during cerebral cortical development. Front Neurosci 9:447. doi:10.3389/fnins.2015.00447

Olde Loohuis NF, Kos A, Martens GJ, Van Bokhoven H, Nadif Kasri N, Aschrafi A (2012) MicroRNA networks direct neuronal development and plasticity. Cell Mol Life Sci 69:89–102. doi:10.1007/s00018-011-0788-1

Olsen L, Klausen M, Helboe L, Nielsen FC, Werge T (2009) MicroRNAs show mutually exclusive expression patterns in the brain of adult male rats. PLoS One 4:e7225. doi:10.1371/journal.pone.0007225

Palazuelos J, Crawford HC, Klingener M, Sun B, Karelis J, Raines EW, Aguirre A (2014) TACE/ADAM17 is essential for oligodendrocyte development and CNS myelination. J Neurosci 34:11884–11896. doi:10.1523/JNEUROSCI.1220-14.2014

Paxinos G, Watson C (2007) The rat brain in stereotaxic coordinates., 6th edn. Academic Press/Elsevier, Amsterdam, Boston

Peltier J, O'Neill A, Schaffer DV (2007) PI3K/Akt and CREB regulate adult neural hippocampal progenitor proliferation and differentiation. Dev Neurobiol 67:1348–1361. doi:10.1002/dneu.20506

Peters BD et al (2014) Brain white matter development is associated with a human-specific haplotype increasing the synthesis of long chain fatty acids. J Neurosci 34:6367–6376. doi:10.1523/JNEUROSCI.2818-13.2014

Popken GJ, Dechert-Zeger M, Ye P, D'Ercole AJ (2005) Brain development. Adv Exp Med Biol 567:187–220. doi:10.1007/0-387-26274-1_8

Qin Z et al (2012) LIM domain only 4 (LMO4) regulates calcium-induced calcium release and synaptic plasticity in the hippocampus. J Neurosci 32:4271–4283. doi:10.1523/JNEUROSCI.6271-11.2012

Raguz J, Wagner S, Dikic I, Hoeller D (2007) Suppressor of T-cell receptor signalling 1 and 2 differentially regulate endocytosis and signalling of receptor tyrosine kinases. FEBS Lett 581:4767–4772. doi:10.1016/j.febslet.2007.08.077

Ramsden HL, Surmeli G, McDonagh SG, Nolan MF (2015) Laminar and dorsoventral molecular organization of the medial entorhinal cortex revealed by large-scale anatomical analysis of gene expression. PLoS Comput Biol 11:e1004032. doi:10.1371/journal.pcbi.1004032

Rangrez AY, Massy ZA, Metzinger-Le Meuth V, Metzinger L (2011) miR-143 and miR-145: molecular keys to switch the phenotype of vascular smooth muscle cells. Circ Cardiovasc Genet 4:197–205. doi:10.1161/CIRCGENETICS.110.958702

Reimand J, Kull M, Peterson H, Hansen J, Vilo J (2007) g:Profiler–a web-based toolset for functional profiling of gene lists from large-scale experiments. Nucleic Acids Res 35:W193–W200. doi:10.1093/nar/gkm226

Ritchie ME, Phipson B, Wu D, Hu Y, Law CW, Shi W, Smyth GK (2015) limma powers differential expression analyses for

RNA-sequencing and microarray studies. Nucleic Acids Res 43:e47. doi:10.1093/nar/gkv007

Robinson MD, Oshlack A (2010) A scaling normalization method for differential expression analysis of RNA-seq data. Genome Biol 11:R25. doi:10.1186/gb-2010-11-3-r25

Rowland DC, Roudi Y, Moser MB, Moser EI (2016) Ten years of grid cells. Annu Rev Neurosci 39:19–40. doi:10.1146/annurev-neuro-070815-013824

Sargolini F, Fyhn M, Hafting T, McNaughton BL, Witter MP, Moser MB, Moser EI (2006) Conjunctive representation of position, direction, and velocity in entorhinal cortex. Science 312:758–762. doi:10.1126/science.1125572

Schevzov G et al (2005) Specific features of neuronal size and shape are regulated by tropomyosin isoforms. Mol Biol Cell 16:3425–3437. doi:10.1091/mbc.E04-10-0951

Schratt G (2009) Fine-tuning neural gene expression with micro-RNAs. Curr Opin Neurobiol 19:213–219. doi:10.1016/j.conb.2009.05.015

Schwarcz R, Eid T, Du F (2000) Neurons in layer III of the entorhinal cortex. A role in epileptogenesis and epilepsy? Ann N Y Acad Sci 911:328–342

Selbach M, Schwanhausser B, Thierfelder N, Fang Z, Khanin R, Rajewsky N (2008) Widespread changes in protein synthesis induced by microRNAs. Nature 455:58–63. doi:10.1038/nature07228

Semple BD, Blomgren K, Gimlin K, Ferriero DM, Noble-Haeusslein LJ (2013) Brain development in rodents and humans: Identifying benchmarks of maturation and vulnerability to injury across species. Prog Neurobiol 106–107:1–16. doi:10.1016/j.pneurobio.2013.04.001

Smyth GK (2004) Linear models and empirical bayes methods for assessing differential expression in microarray experiments. Stat Appl Genet Mol Biol 3:3. doi:10.2202/1544-6115.1027

Sonntag KC, Woo TU, Krichevsky AM (2012) Converging miRNA functions in diverse brain disorders: a case for miR-124 and miR-126. Exp Neurol 235:427–435. doi:10.1016/j.expneurol.2011.11.035

Stappert L, Roese-Koerner B, Brustle O (2015) The role of micro-RNAs in human neural stem cells, neuronal differentiation and subtype specification. Cell Tissue Res 359:47–64. doi:10.1007/s00441-014-1981-y

Stranahan AM, Erion JR, Wosiski-Kuhn M (2013) Reelin signaling in development, maintenance, and plasticity of neural networks. Ageing Res Rev 12:815–822. doi:10.1016/j.arr.2013.01.005

Tamamaki N, Nojyo Y (1993) Projection of the entorhinal layer II neurons in the rat as revealed by intracellular pressure-injection of neurobiotin. Hippocampus 3:471–480. doi:10.1002/hipo.450030408

Tang Q et al (2014) Pyramidal and stellate cell specificity of grid and border representations in layer 2 of medial entorhinal cortex. Neuron 84:1191–1197. doi:10.1016/j.neuron.2014.11.009

Van Peer G et al (2014) miRBase Tracker: keeping track of micro-RNA annotation changes. Database (Oxford) 2014:bau080. doi:10.1093/database/bau080

Wang YP, Li KB (2009) Correlation of expression profiles between microRNAs and mRNA targets using NCI-60 data. BMC Genomics 10:218. doi:10.1186/1471-2164-10-218

Wang Y, Li X, Hu H (2011) Transcriptional regulation of co-expressed microRNA target genes. Genomics 98:445–452. doi:10.1016/j.ygeno.2011.09.004

Wang Y, Luo J, Zhang H, Lu J (2016) microRNAs in the same clusters evolve to coordinately regulate functionally related genes. Mol Biol Evol 33:2232–2247. doi:10.1093/molbev/msw089

Wills TJ, Cacucci F (2014) The development of the hippocampal neural representation of space. Curr Opin Neurobiol 24:111–119. doi:10.1016/j.conb.2013.09.006

Woodworth MB, Custo Greig L, Kriegstein AR, Macklis JD (2012) SnapShot: cortical development. Cell 151(918–918):e911. doi:10.1016/j.cell.2012.10.004

Zhao X et al (2010) MicroRNA-mediated control of oligodendrocyte differentiation. Neuron 65:612–626. doi:10.1016/j.neuron.2010.02.018

Zhu G, Wang Y, Mijiti M, Wang Z, Wu PF, Jiafu D (2015) Upregulation of miR-130b enhances stem cell-like phenotype in glioblastoma by inactivating the Hippo signaling pathway. Biochem Biophys Res Commun 465:194–199. doi:10.1016/j.bbrc.2015.07.149

MicroRNAs contribute to postnatal development of laminar differences and neuronal subtypes in the rat medial entorhinal cortex

Lene C. Olsen[1], Kally C. O'Reilly[2], Nina B. Liabakk[1], Menno Witter[2], and Pål Sætrom[1,3,4,*]

1) Department of Cancer Research and Molecular Medicine, Norwegian University of Science and Technology, Trondheim, Norway.
2) Kavli Institute for Systems Neuroscience and Centre for Neural Computation, Norwegian University for Science and Technology, Trondheim, Norway.
3) Department of Computer and Information Science, Norwegian University for Science and Technology, Trondheim, Norway.
4) Bioinformatics core facility - BioCore, Norwegian University of Science and Technology, Trondheim, Norway.

*)Correspondence and request for materials should be addressed to P.S. (e-mail: pal.satrom@ntnu.no)

Supplementary Materials
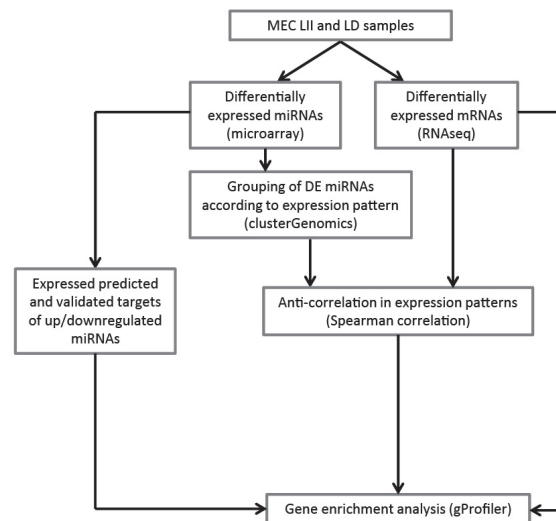
Supplementary Fig. 1: Summary of workflow for analysis of laminar samples. The samples were analyzed for differential miRNA and mRNA expression. Differentially expressed miRNAs were grouped according to correlating expression pattern, and the predicted target genes for the miRNAs in each group were analyzed for anti-correlative expression patterns. Anti-correlated targets, along with differentially expressed genes and all predicted and validated expressed targets of differentially expressed miRNAs were analyzed for enriched gene ontology terms.
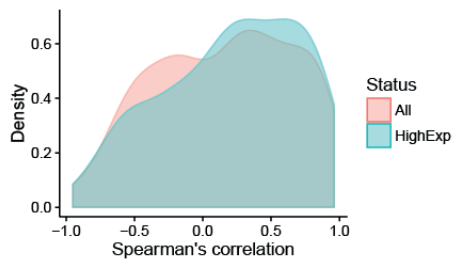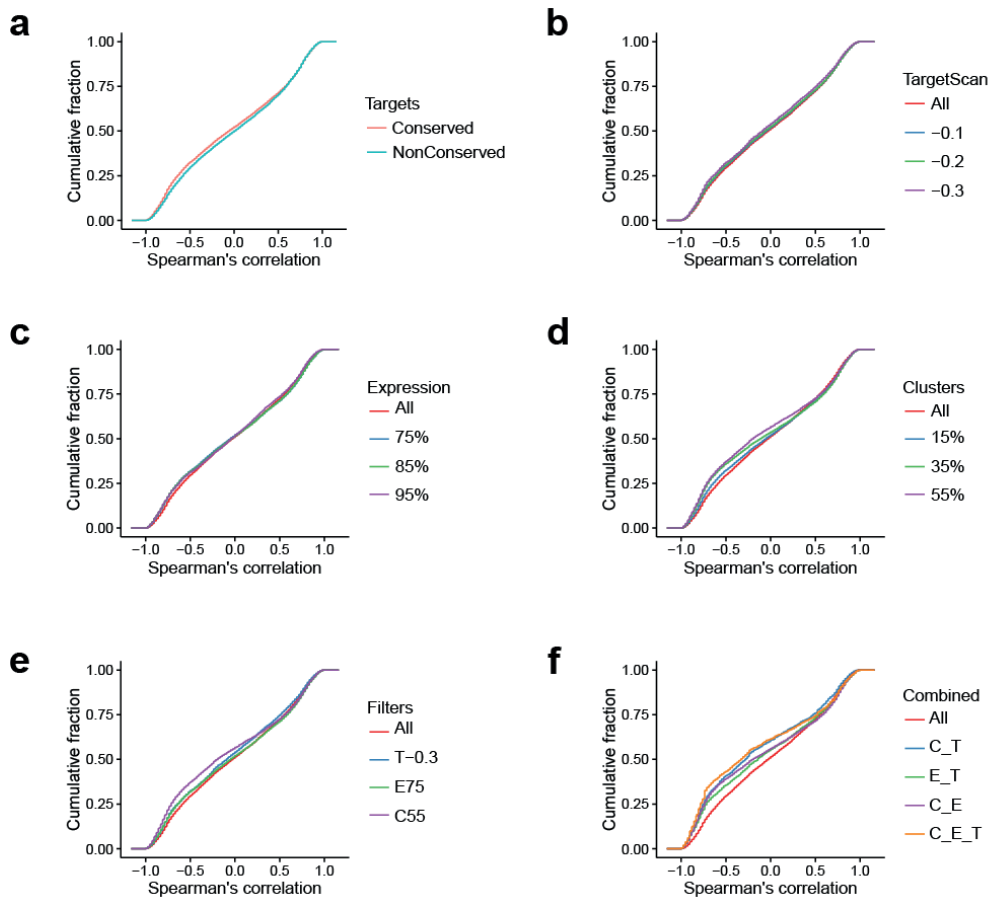
Supplementary Fig. 2: Correlation between the expression patterns across layers and development of the mature miRNAs as measured by microarray and the expression patterns of the pre-mirs as measured by deep sequencing. The correlation of all miRNA-pre-mirs in red, and of the miRNAs that are expressed with a minimum median normalized expression level of 5 (as determined by microarrays) in turquoise.
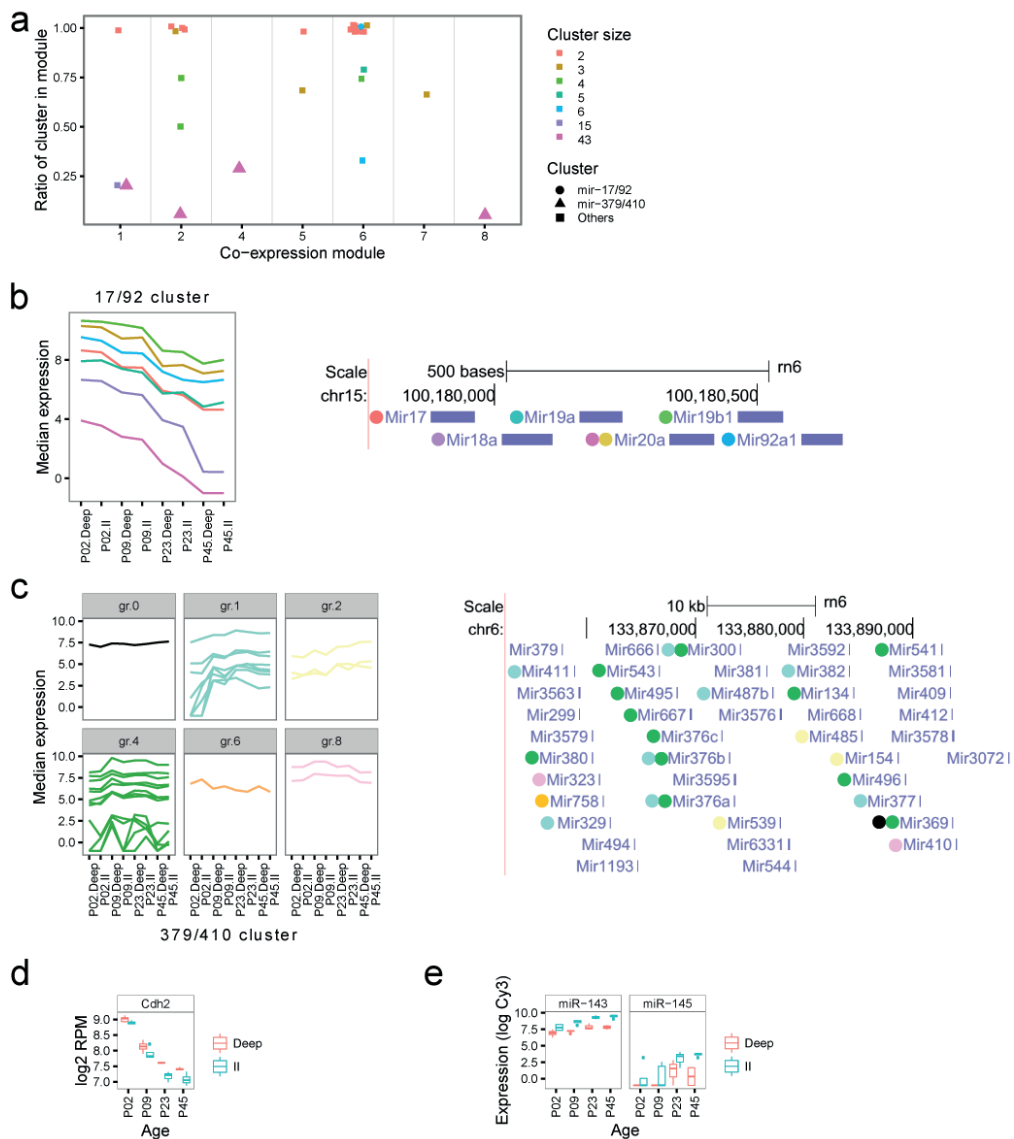
Supplementary Fig. 3: a) Co-expression patterns of miRNAs clustered in the genome. Each point represents miRNAs from a genomic miRNA cluster, grouped by their co-expression patterns and color coded by the number of miRNA hairpins in the genomic cluster. Module 3 is not presented because it did not contain any miRNA genomic clusters. The y-axis gives the proportion of miRNAs from the cluster that is present in the given module. All six members of the mir-17/92 cluster are present in module 6 (circle; see D), yielding a ratio of 1; members of the mir-379/410 cluster are present in four different modules (triangle; see E). **b)** Genomic organization of the members of the mir-17/92 cluster in the rat genome (rn6), along with median expression levels for each member of the cluster. The identity of each pre-mir is color coded. Pre-mir-20a is represented with two colors, with the yellow depicting the expression of the mature miR-20a and the magenta the mature miR-20a*. **c)** Genomic organization of the members of the mir-379/410 cluster in the rat genome (rn6), along with median

expression levels for the members of the cluster present in each co-expression module. The color coding is according to co-expression module, gr.0 being the outlier group. **d)** The expression of the Cdh2 gene across time points. Laminar samples are colored as in Fig. 1. **e)** Comparison of expression patterns for miR-143 and miR-145, which belong to the same miRNA cluster.
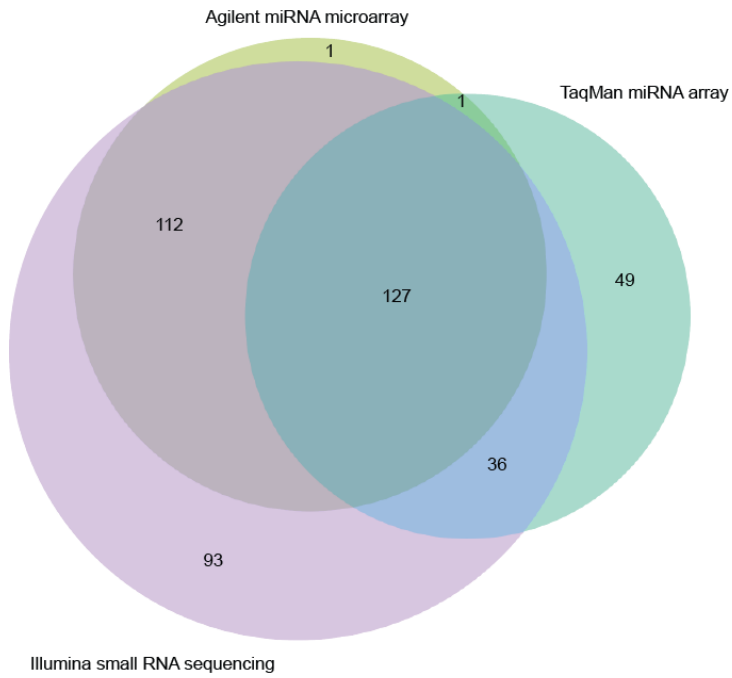
Supplementary Fig. 4: Cumulative distribution of the correlation between miRNA expression and the expression of predicted target genes. **a)** Curves show correlations for predicted conserved (red) and non-conserved (turquoise) target genes. The predicted conserved miRNA target genes are more skewed towards negative correlation values than those for non-conserved miRNA target genes. **b)** Curves show correlations for all predicted targets (red) and predicted targets with context scores of <-0.1 (blue), <-0.2 (green), and <-0.3 (purple). There is a shift towards more negative correlation when the context score threshold is decreased (corresponding to more stringent predictions). **c)** Curves show correlations for all predicted targets (red) and for the pairs where the miRNAs with the 75% (blue), 85% (green), and 95% (purple) lowest expression levels have been filtered out. The higher the expression of the miRNAs, the higher the tendency towards negative correlation. **d)** Curves show correlations for all predicted targets (red) compared to when at least 15% (blue), 35% (green), and 55% (purple) of the target sites in the predicted target genes are present in the same co-expression module. The higher the percentage of target sites targeted by miRNAs in the same co-expression module, the greater the shift towards negative correlation. **e)** Curves show correlations for all predicted targets (red) compared with the cumulative correlation when using the different kinds of filters (TargetScan context score < -0.3 in blue, miRNAs with expression levels above the 75th percentile in green, and >55% of target sites covered by the same co-expression module in purple). **f)** Curves show correlations when using varying criteria for miRNA expression level, TargetScan context

score, and coverage of predicted target sites by the miRNAs in the same co-expression module. All target gene – miRNA pairs (red) are compared to the pairs with the following combination of criteria: C_T (blue) are pairs where the target site has a context score <= -0.3 in TargetScan v. 6.0 and where >55% of the target sites are covered by the miRNAs in the same co-expression module (blue), pairs where the only miRNAs that have expression levels in the upper quartile are included (green), and pairs where the target site has a context score of <-0.3 in TargetScan v. 6.0 (purple). Pairs fulfilling all three criteria are shown in orange. All filters lead to a shift towards negative correlation, with the combination of all the filters displaying the highest degree of negative correlation.
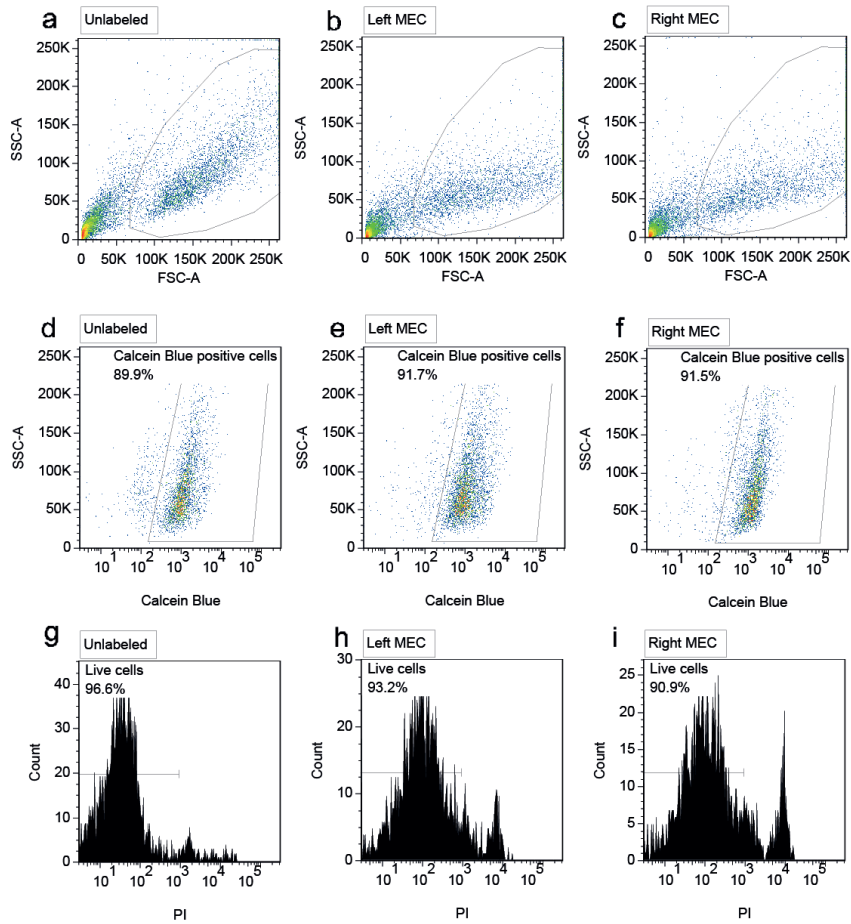
Supplementary Fig. 5: FACS gating. Forward and side scatter plot of a representative population of dissociated, unlabeled MEC showing gating of selected population for dissociated **a)** unlabeled MEC, **b)** labeled MEC from the left hemisphere, and **c)** labeled MEC from the right hemisphere. The gated population in A-C showed a high percentage of live cells as indicated by Calcein Blue staining in **d)** unlabeled MEC, **e)** labeled MEC from the left hemisphere, and **f)** labeled MEC from the right hemisphere. The bottom panel shows gating of PI negative cells for **g)** unlabeled MEC, **h)** labeled MEC from the left hemisphere, and **i)** labeled MEC from the right hemisphere. The FSC/SSC and PI gating were used for the sort.

Agilent miRNA microarray

1

TaqMan miRNA array

1

112

127

49

36

93

Illumina small RNA sequencing

Supplementary Fig. 6: Venn diagram showing overlap of detected miRNAs in P23 MEC samples between the two array platforms used in this paper (Agilent miRNA microarray and TaqMan miRNA array) and Illumina small RNA sequencing of P23 MEC.
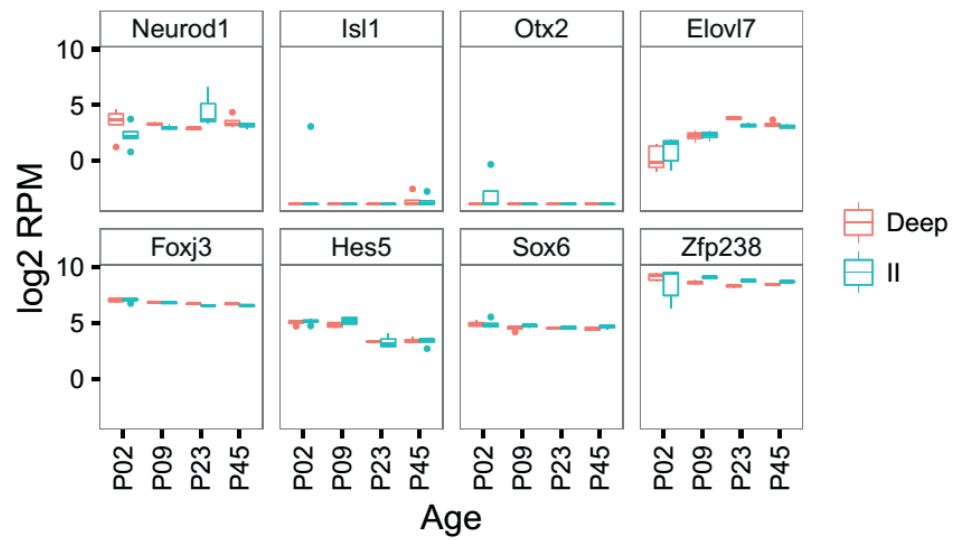
Supplementary Figure 7: Expression patterns of known miR-219-5p target genes important for oligodendrocyte differentiation.

Supplementary Analyses

SA1: Correlation of precursor miRNA expression with mature miRNA expression

As the library preparation in our study included all RNA molecules, but with depletion of ribosomal RNAs, we were able to also identify a few precursor miRNAs (pre-mirs). Pre-mir-143 was upregulated in LII (LFC 1.17, BH p=0.01), providing further verification of its differential expression between MEC layers. The adjacent mir-145 was also detected by the RNA-seq, and showed the same trend in expression, but did not reach significance levels due to higher variation (Supplementary Fig. 3e). In general, the mature miRNA expression from the microarray experiment correlated positively with the pre-mir expression from the RNA-seq experiment (Supplementary Fig. 2). The shift was further pronounced when we only examined highly expressed miRNAs (mature miRNAs with median normalized expression level > 5). Thus overall, RNA-seq reads mapping to pre-mirs appear to be representative for miRNA expression in postnatal rat EC.

SA2: Genomically clustered miRNAs in co-expression modules

As miRNAs encoded close together in the genome (genomic clusters) tend to share expression profiles (Thapa et al. 2015), we expected that such clustered miRNAs would be grouped in the same or similar co-expression modules. To test whether the grouping of miRNAs in our modules was consistent with known miRNA clusters, we examined the chromosomal locations of each miRNA within each module for clustering of miRNAs in the genome. Most modules contained at least one pair of genomically clustered miRNAs, except the outlier module and module 3 which contained no clustered miRNAs (Supplementary Fig. 3a).

The modules displaying the clearest developmental profiles (modules 2 and 6) contained several oncomiR and anti-oncomiR clusters, such as the miR-125a/let-7c/99b and miR-23b/27b/24-1 clusters. Module 6 contained all members of the miR-17/92 oncomiR cluster (Supplementary Fig. 3b) that is known to regulate the cell cycle and apoptosis, and has been implicated in neurodegenerative diseases (Jovicic et al. 2013; Mogilyansky and Rigoutsos 2013). This cluster is also of particular importance for oligodendrocyte proliferation (Petri et al. 2014). Thus, cell cycle, apoptosis, and oligodendrocyte proliferation is highly regulated by the miR-17/92 early in development, and this regulation decreases by P23 to adulthood.

Twelve of the 23 miRNAs in module 4 are members of the neuron-specific miR-379/410 cluster (Supplementary Fig. 3c), although other members of this large cluster of 42 miRNAs could also be found in module 1 (8 members), module 2 (3 members) and module 8 (2 members). There is little laminar difference for the miRNAs in the modules enriched in this cluster, apart from a downregulation in LII at P9 for some miRNAs. This cluster has been found to fine-tune the expression of N-cadherin (Rago et al. 2014), thereby regulating neuronal differentiation and migration. N-cadherin (Cdh2) shows slight laminar differences (LFC -0.28, BH = 0.00016), but is strongly down-regulated in all layers from P9 (Supplementary Fig. 3d). The general expression pattern of the miR-379/410 cluster members is consistent with the majority of the miRNAs being up-regulated or having peak activity at P9 (modules 2 and 4), or being progressively turned on through development (module 2). The high expression at P9 is negatively correlated with the downregulation of the Cdh2 gene at the same age, which can indicate the regulation of this gene by the miR-379/410 cluster also in the MEC.

The miRNA with the most significant laminar difference, miR-143, was upregulated in LII. It is encoded in an intergenic region of the genome, close to miR-145. The expression of miR-145 followed a similar pattern to miR-143 (LFC=1.88, BH p=0.005), although at a much lower level (Supplementary Fig. 3e). According to miRBase, these miRNAs have similar expression levels in humans, but in mice miR-143 is expressed at a much higher level than miR-145, so this pattern seems common for rodents. These two miRNAs are commonly found at high levels in vascular smooth muscle cells in other tissues, where they play a role in angiogenesis and blood vessel stabilization (Climent et al. 2015). The laminar expression difference for these miRNAs could therefore suggest laminar differences in MEC vascular structure, but could also indicate that these miRNAs have hitherto unrecognized brain-specific functions.

SA3: Comparison of miRNA detection between platforms

We used two different technologies for the miRNA expression studies, microarray for the layer samples, and TaqMan array for the stellate subtype samples. To investigate the technical issues of using different technologies, we compared detected miRNAs in the microarray layer experiment (P23 median miRNA expression across MEC layers) and the TaqMan array study (miRNA expression of total RNA from whole MEC P23) with Illumina small RNA sequencing data of total RNA from whole MEC at P23.

All of the three technologies have their own biases. Both Illumina sequencing and the TaqMan array use PCR, which can differ in amplification efficiency depending on the GC content of the cDNA (Meyer and Liu 2014; Polz and Cavanaugh 1998). For the TaqMan array protocol we also used pre-amplification, which could potentially introduce more bias, although this technology has high sensitivity and accuracy for samples of low concentration (Mestdagh et al. 2014). Another difference with the samples used for the TaqMan array is that they came from dissociated, FACS sorted cells. This process can be very stressful to the cells, which in turn could potentially alter the miRNA expression. However, results from Okaty *et al.* (2011) (Okaty et al. 2011) showed no significant difference in the expression of stress, apoptosis, and immediate early genes between FACS and laser capture microdissection, indicating that FACS is not much more stressful for the cells than other technologies. As for the microarray technology, it has a more limited range than the other two technologies, and we could therefore have missed some differentially expressed miRNAs. Also, as with the TaqMan array, the microarray can only measure the concentration of miRNAs for which it has appropriate probes.

When comparing the platforms, we found 127 miRNAs to be detected by all three technologies (Supplementary Fig. 6). All but two of the miRNAs detected in the microarray experiment were detected with deep sequencing, of which one was also detected by TaqMan array. Four additional miRNAs were not detected in the deep sequencing analysis pipeline as they did not align to the genome (see Methods), but they were detected with reads in the raw data. Fourty-nine miRNAs were detected by the TaqMan array and not by deep sequencing or microarray. Only ten of these are found in v.21 of miRBase. The rest were putative miRNAs at the time of the design of the qPCR array, and are likely not real miRNAs. Five miRNAs detected by the TaqMan array did not align to the genome, but were detected in the raw reads.

The correlation between the different technologies was highest for small RNA sequencing and the TaqMan array (rho = -0.70, BH <2.2e-16), and lowest for the TaqMan array and microarray (rho = -

0.61, BH 3.5e-14). This latter figure is higher than what Chen *et al.* (Chen et al. 2009) found when comparing TaqMan array and microarrays. The correlation between microarray and small RNA sequencing was 0.64 (Spearman's rho, BH <2.2e-16), which is slightly lower than what Tam *et al.* (Tam et al. 2014) found when correlating Illumina small RNA sequencing and Illumina miRNA microarray (0.69). This slightly lower correlation could be due to differences in technologies, but could also be because of differences between the samples we used for sequencing and microarray analyses. The sample used for sequencing came from whole MEC, whereas the microarray samples were MEC layers from other rats than that used for sequencing. Despite these sample differences, correlations between technologies were similar to what has previously been found by others.

SA4: Analysis of known targets of miR-219-5p

miR-219-5p has several known targets involved in the differentiation of oligodendrocytes. Of the three target genes involved in early development from neural stem cells to OPCs (NeuroD1, Isl1, and Otx2), only NeuroD1 showed expression, and this was fairly stable across time (Supplementary Fig. 7). This result indicates that the OPC developmental stage is largely finished by the P2. The six known target genes involved in development from OPCs to myelinating oligodendrocytes (Elovl7, Foxj3, Hes5, Pdgfra, Sox6, Zfp238) were all expressed (Figure 5e, Supplementary Fig. 7), which was expected as myelination occurs during the age range tested (from P10, (Downes and Mullins 2014)). Expression of all of these genes, except for Elovl7, was negatively correlated with miR-219-5p expression, but only Pdgfra and Zfp238 displayed the opposite laminar pattern to the miRNA. The Hes5 gene, a powerful repressor of myelin gene expression (Liu et al. 2006), showed a sharp downregulation in its expression between P9 and P23, which is when myelination begins.

Supplementary References

Chen Y, Gelfond JA, McManus LM, Shireman PK (2009) Reproducibility of quantitative RT-PCR array in miRNA expression profiling and comparison with microarray analysis BMC Genomics 10:407 doi:10.1186/1471-2164-10-407

Climent M, Quintavalle M, Miragoli M, Chen J, Condorelli G, Elia L (2015) TGFbeta Triggers miR-143/145 Transfer From Smooth Muscle Cells to Endothelial Cells, Thereby Modulating Vessel Stabilization Circ Res 116:1753-1764 doi:10.1161/CIRCRESAHA.116.305178

Downes N, Mullins P (2014) The development of myelin in the brain of the juvenile rat Toxicol Pathol 42:913-922 doi:10.1177/0192623313503518

Jovicic A, Roshan R, Moisoi N, Pradervand S, Moser R, Pillai B, Luthi-Carter R (2013) Comprehensive expression analyses of neural cell-type-specific miRNAs identify new determinants of the specification and maintenance of neuronal phenotypes J Neurosci 33:5127-5137 doi:10.1523/JNEUROSCI.0600-12.2013

Liu A, Li J, Marin-Husstege M, Kageyama R, Fan Y, Gelinas C, Casaccia-Bonnefil P (2006) A molecular insight of Hes5-dependent inhibition of myelin gene expression: old partners and new players EMBO J 25:4833-4842 doi:10.1038/sj.emboj.7601352

Mestdagh P et al. (2014) Evaluation of quantitative miRNA expression platforms in the microRNA quality control (miRQC) study Nat Methods 11:809-815 doi:10.1038/nmeth.3014

Meyer CA, Liu XS (2014) Identifying and mitigating bias in next-generation sequencing methods for chromatin biology Nat Rev Genet 15:709-721 doi:10.1038/nrg3788

Mogilyansky E, Rigoutsos I (2013) The miR-17/92 cluster: a comprehensive update on its genomics, genetics, functions and increasingly important and numerous roles in health and disease Cell Death Differ 20:1603-1614 doi:10.1038/cdd.2013.125

Okaty BW, Sugino K, Nelson SB (2011) A quantitative comparison of cell-type-specific microarray gene expression profiling methods in the mouse brain PLoS One 6:e16493 doi:10.1371/journal.pone.0016493

Petri R, Malmevik J, Fasching L, Akerblom M, Jakobsson J (2014) miRNAs in brain development Exp Cell Res 321:84-89 doi:10.1016/j.yexcr.2013.09.022

Polz MF, Cavanaugh CM (1998) Bias in template-to-product ratios in multitemplate PCR Appl Environ Microbiol 64:3724-3730

Rago L, Beattie R, Taylor V, Winter J (2014) miR379-410 cluster miRNAs regulate neurogenesis and neuronal migration by fine-tuning N-cadherin EMBO J 33:906-920 doi:10.1002/embj.201386591

Tam S, de Borja R, Tsao MS, McPherson JD (2014) Robust global microRNA expression profiling using next-generation sequencing technologies Lab Invest 94:350-358 doi:10.1038/labinvest.2013.157

Thapa I, Fox HS, Bastola D (2015) Coexpression Network Analysis of miRNA-142 Overexpression in Neuronal Cells Biomed Res Int 2015:921517 doi:10.1155/2015/921517

PAPER III